ELECTROCHEMICALLY DEPOSITED CONDUCTING POLYMERS FOR RELIABLE BIOMEDICAL INTERFACING MATERIALS: FORMULATION, MECHANICAL CHARACTERIZATION, AND FAILURE ANALYSIS

by

Jing Qu

A dissertation submitted to the Faculty of the University of Delaware
in partial fulfillment of the requirements for the degree of
Doctor of Philosophy in Materials Science and Engineering

Winter 2017

ELECTROCHEMICALLY DEPOSITED CONDUCTING POLYMERS FOR RELIABLE BIOMEDICAL INTERFACING MATERIALS: FORMULATION, MECHANICAL CHARACTERIZATION, AND FAILURE ANALYSIS

by

Jing Qu

Approved: _____
Darrin J. Pochan, Ph.D.
Chair of the Department of Materials Science and Engineering

Approved: _____
Babatunde A. Ogunnaike, Ph.D.
Dean of the College of Engineering

Approved: _____
Ann L. Ardis, Ph.D.
Senior Vice Provost for Graduate and Professional Education

I certify that I have read this dissertation and that in my opinion it meets the academic and professional standard required by the University as a dissertation for the degree of Doctor of Philosophy.

Signed: _____

David C. Martin, Ph.D.
Professor in charge of dissertation

I certify that I have read this dissertation and that in my opinion it meets the academic and professional standard required by the University as a dissertation for the degree of Doctor of Philosophy.

Signed: _____

Joshua M. O. Zide, Ph.D.
Member of dissertation committee

I certify that I have read this dissertation and that in my opinion it meets the academic and professional standard required by the University as a dissertation for the degree of Doctor of Philosophy.

Signed: _____

Xinqiao Jia, Ph.D.
Member of dissertation committee

I certify that I have read this dissertation and that in my opinion it meets the academic and professional standard required by the University as a dissertation for the degree of Doctor of Philosophy.

Signed: _____

David L. Burris, Ph.D.
Member of dissertation committee

ACKNOWLEDGMENTS

This thesis would not have been possible without the support, guidance, and encourage from Dr. Martin. His door is always open, while I have questions and need help from him. His unpretending and dedicated attitude towards pursuing the knowledge has pushed me to set higher standards for myself. He teaches me how to think, a capability that I value the most in my life.

I am especially grateful to the members of my doctoral committee. I have always admired the earnest and serious attitude of Dr. Xinqiao Jia towards the research, which is a model for my future career. Without Dr. Burris's help and guidance, it would be much more difficult to move on in the later period of my Ph.D. research. The valuable suggestions and advice from Dr. Zide has led me to a higher level to evaluate my research with a logical and comprehensive vision.

This interdisciplinary research would have not been possible without the help of our collaborators. My sincere thanks to Dr. Melanie Urbancheck, Dr. Paul Cederna, in the University of Michigan for the opportunity of learning how the biomedical electronics interact with animal bodies. Thanks to Nikolay Garabedian for his collaboration and friendship throughout our project.

I would also like to thank the colleagues in Keck lab at UD, and in particular Dr. Chaoying Ni, Frank Kriss, and Dr. Fei Deng. I am especially grateful to Gerald Poirier in the Advanced Materials Characterization Lab at UD for his great generosity, friendship and mentoring through this journey.

My thanks go to the entire Martin research group, including past and current members, for creating a supportive and stimulating environment to work in. I have learned a lot from each and every one of them.

I would like to express my gratefulness to all my friends, especially to Chuan Qin, Yao Yao, and Zi Tong. Thanks for always being there for me. It would be much more difficult for me during this journey without your support.

Last, but certainly not least, I'm grateful to have my awesome parents, Guiqian Qu and Shaolin Feng. I'm immensely appreciative of your understanding, encouragement, and sacrifices. Without your endless love and unconditional support, I would never have reached this point.

This work was financially supported by the Defense Advanced Research Projects Agency (DARPA), National Institute of Health (NIH), and University of Delaware.

TABLE OF CONTENTS

LIST OF TABLES

LIST OF FIGURES

ABSTRACT

Conjugated polymers such as poly(3,4-ethylenedioxythiophene) (PEDOT) are of interest for a variety of applications including interfaces between electronic biomedical devices and living tissue. These polymers provide an improved interface compared to metal and semiconducting electrodes because of their ionic conductivity, relatively lower stiffness, and ability to incorporate biological molecules. Even though the signal transfer and biocompatibility of conjugated polymers are superior as the biointerfacing materials, the durability has been the weakest part for the long-term applications. Some efforts have been made to improve the durability of conjugated polymers, however, little quantitative information of the improved cohesion, adhesion and durability has been reported.

In this thesis, the methods of improving the durability of conjugated polymer films, especially PEDOT, were investigated, including alternating the processing methods and components in synthesis. The 7-month in vivo testing showed a superior neural signal recording performance, however the durability of PEDOT films still needed to be improved.

As a coating for biosignal transfer, the cohesion, adhesion and electrochemical stability of PEDOT are vital to determine the long-term performance. By far, not much information of cohesion and adhesion of conjugated polymer coatings has been

dug out. In this thesis, a thin film cracking method was developed to measure the stiffness, strength and the interfacial shear strength (adhesion) of electrochemically deposited PEDOT. The estimated Young's modulus of the PEDOT films was 2.6 ± 1.4 GPa, and the strain to failure was around 2%. The tensile strength was measured to be 56 ± 27 MPa. The effectiveness of crosslinker and adhesion promoter was demonstrated by this method. It was shown that 5 mole% addition of a tri-functional EDOT crosslinker increased the tensile strength of the films to 283 ± 67 MPa, while the strain to failure remained about the same (2%). With the modification of EDOT-acid to the surface of stainless steel substrate, the interfacial shear strength was improved from 11.8 MPa to 32.5 MPa.

To correlate the adhesion with the durability of PEDOT coatings, a tribology test was introduced. It was found that the durability of PEDOT on Au electrode was exceptionally good, and even better than the adhesion promoted coatings with EDOT-acid on stainless steel and ITO substrates. The characterization method developed in this thesis made a critical difference in systematically comparing different materials, and provided valuable information for materials development and selection.

Chapter 1

INTRODUCTION: CONJUGATED POLYMERS FOR BIOMEDICAL INTERFACES

1.1 Background and overview

1.1.1 Demands for biomedical electronics

Statistics estimate there are about 2 million people in the US alone suffering from traumatic brain injury (Hyder et al. 2007) and about 1.7 million people living with limb loss (Ziegler-Graham et al. 2008). Each year, 610,000 people die (corresponding to 1 of every 4 deaths) because of heart disease (Graham 2014). At the same time, 7 million American people suffer from visual disabilities (Brault 2012). These numbers are growing. The emergence of biomedical electronics, such as deep brain stimulators (Cogan 2008), neural interface devices for prosthetic limbs (Kung et al. 2014), cardiac electrodes (Viventi et al. 2010), and retinal prostheses (Weiland et al. 2011), provides potential solutions for research and treatment of diverse organs and tissues. Currently, there are great demands in the science and technology for developing biomedical electronics to improve people's quality of life.

1.1.2 Current technologies of biomedical electrodes

Bioelectronic medicine has been described as the general concept of integrating various types of engineered electronic components with living systems to achieve desirable therapeutic outcomes (Birmingham et al. 2014). In all of these applications, a biomedical interface has to be involved. The term "biomedical

interface" refers to the region of contact between a cell, biological tissue or living organism with external components for biosignal transmission purposes. Currently, the biomedical interfaces normally refer to biomedical electrodes implanted *in vivo*, which serve as the direct contact between the targeted tissue and the machine, and transfer both recording and stimulating signals (Cogan 2008).

In general, according to the functioning locations, there are mainly two types of *in-vivo* biomedical electrodes: surface-mounted electrodes, and penetrating electrodes (Cogan 2008). For the penetrating electrodes, there are 2 typical geometry designs of interfacing spots: flat and pointed (Figure 1.1).

Even though there are several designs for the biomedical electrodes, similar performance criteria have to be met. First, they should be biocompatible in long-term applications (Simon et al. 2016). Second, they should be sensitive to the biosignals (Hochberg et al., 2012), which in turn requires good conductivities in the electrolytic environment. Third, they should have long durability, which means the electrodes must be chemically, mechanically and electrically stable (Martin 2015). It is a big challenge to meet all these qualifications (Green et al. 2008). Each requirement puts certain constraints on the microelectrode designs and material selections. This thesis will cut into those huge and broad topics through a small subject: the most critical component of biomedical electrodes—interfacing materials. The following part of this chapter will describe the challenges for the interfacing material selections.

1.2 Challenges for interfacing material selections

1.2.1 Bridging the abiotic and biotic

The most common interfacing materials for biomedical electrodes currently being used are inorganic conductors and semiconductors, such as platinum/platinum iridium, gold, titanium oxide, and iridium oxide (Merrill et al. 2005). However, the big differences in chemistry and mechanics of those hard materials and the soft tissues can cause critical problems.

1.2.1.1 The superior conjugated polymers

First, the typical stiffnesses of the inorganic interfacing materials are in the range of 100-1000 GPa (Table 1.1), which is much higher than the 10^{-6}-10^{-4} GPa characteristic of living tissues (Subbaroyan et al. 2005). One hypothesis that has been discussed in the neuroscience field is that the immune response and neural degeneration surrounding the cortical electrodes are made worse from the huge mechanical mismatch between the hard material and soft tissue (Lee et al. 2005) (Subbaroyan et al. 2005). With intermediate stiffnesses of 0.5-5 GPa (Qu et al. 2015)(Lang et al. 2009), conjugated polymers show great advantages as the interfacing material to bridge the mechanical gap.

Second, the inorganic conductors or semiconductors are electron or hole conductors, which are not that efficient when interfacing with the living tissues, where the signals transfer in ionic solutions. For example, an obvious lag was observed during the neural signal recording (Kung et al. 2014). The inefficient signal transfer of inorganic materials can also bring troubles for battery life and device accuracy. The gap between the hard electron conducting materials and the soft ion-conductive tissues can be bridged by conjugated polymers. The π-conjugated backbones can facilitate the

movement of electrons or holes when the polymers are doped, resulting in conductivity. The ionic dopants also contribute to the ion conductivity while applied in electrolytic solutions. Repeated experimental results have shown that the impedance of the conjugated polymers in an electrolytic environment is much lower than that of metallic conductors, especially at the biologically significant frequencies of 1 kHz and less (Fig 1.2a&b). That means as the biomedical interfacing materials, conjugated polymers are more efficient and sensitive (Fig 1.2c). Further, with the potential of chemical modification for drug delivery, the conjugated polymers are promising to reduce the immune response and improve the biocompatibility.

These superior properties make conjugated polymers promising materials in the biomedical interfacing applications. A number of excellent reviews have given a thorough evaluation of conjugated polymers in bioelectronic devices (Chen et al. 2000)(Berggren & Richter-Dahlfors 2007)(Rivnay et al. 2014) (Martin 2015)(Simon et al. 2016)(Green & Abidian 2015).

1.2.1.2 From PPy to PEDOT

In general, the types of conjugated polymers used for electrode coatings have monomers with low oxidation potentials including polyaniline (PANI), polypyrrole (PPy), polythiophenes (PTh), and derivatives of these polymers (Skotheim & Reynolds 2006). The chemical structures of related conjugated monomers and polymers are listed in Fig 1.3. However, the application of PANI in biomedical systems is limited as a consequence of the lost activity at pH above 4 (Karyakin et al. 1994)(Mu 2011)(Milica et al. 2011).

Studies applying PPy as the biomedical interface were pioneered by Schmidt group (Schmidt et al. 1997), and then developed by many others as well (Smela

1998)(Lu et al. 2002)(Cui et al. 2003). PPy-coated cochlear electrodes showed decreased impedance as compared to bare Pt electrodes (Richardson et al. 2009). PPy coatings also decreased the impedance of gold neural electrodes (Cui et al. 2001). The major disadvantage of PPy as the biomedical interfacing material was their limited chemical instability. PPy can be relatively easily oxidized through the α and β positions on the pyrrole backbone, which leads to the degradation of the polymer (Schlenoff & Xu 1992). Under physiological conditions, this instability is a concern for the long-term applications (Yamato et al. 1995) (Cui et al. 2003) (Harris et al. 2013).

Later on, a derivative of polythiophene—poly (3,4-ethylenedioxythiophene) (PEDOT) emerged. The electrochemical polymerization of 3,4-ethylenedioxythiophene (EDOT) was first published in 1992 (Heywang & Jonas 1992). The polymer PEDOT quickly became of interest as an electrode coating, because of its low oxidation potential and high chemical and electrical stability (Schottland et al. 2000). Compared to PPy, PEDOT had greatly improved electrochemical stability. While PPy film lost its electroactivity after 400 CV cycling between -0.9~0.5 V, PEDOT films maintained most of its charge storage capacity (Cui & Martin 2003). Like PPy, PEDOT has a higher charge capacity and lower impedance in electrolytic solutions, compared to the metallic electrodes used for deposition. The lower impedance was mainly caused by the high surface area morphologies. Compared to ITO (Nyberg et al. 2007), IrO_x (Wilks et al. 2009), gold (Leleux et al. 2014), and Pt (Venkatraman et al. 2011) interfacing materials, the impedance of PEDOT at low frequencies (1-1000 Hz) were much lower. This meant that the PEDOT coated biomedical electrodes were safer, because much lower potentials were needed to

deliver the same amount of current for stimulation purposes. Application of PEDOT as the biomedical interfacing materials were pioneered by Martin et al (Cui & Martin 2003)(Xiao et al. 2004). Recntly, many other groups have done more inspiring work in the biomedical electronics area (Crispin et al. 2006)(Abidian et al. 2010)(Khodagholy et al. 2013) (Xu et al. 2015).

A number of in vitro toxicity and biocompatibility experiments have demonstrated that PEDOT is not cytotoxic to cells. Hep-2 human epithelial cells were shown to adhere better to PEDOT doped with perchlorate counter-ion than stainless steel electrodes and exhibited normal morphology and proliferation (del Valle et al. 2007). To further examine the cytotoxicity of EDOT and PEDOT and to create hybrid conducting polymer-live cell electrodes, Richardson-Burns et al. polymerized EDOT around living SH-SY5Y neuroblastoma cells (Richardson-Burns et al. 2007). EDOT monomer was not significantly toxic to the cells over the time periods needed for polymerization and the cells were able to survive the polymerization process. This finding even led to a pioneering *in vivo* polymerization of EDOT (Ouyang et al. 2014).

Recently, in order to improve the processability of conjugated polymers, a number of studies were conducted to functionalize the conjugated polymers. Luo et al. used hydroxymethyl-functionalized EDOT (EDOT-OH) to create pendant carboxylic acid (EDOT-COOH) (Povlich et al. 2013), azide (EDOT-N3) on the EDOT monomers (Povlich et al. 2011). Another thiophene derivative—3,4-propylenedioxythiophene (ProDOT) was also developed (Skotheim & Reynolds 2006) for functionalization, PProDot-Me_2 (Liu & Reynolds 2010), PProDOT-ene (Feldman & Martin 2012), and PProDOT-diene (Wei et al. 2015) were reported. Those functional groups also brought the possibility for further drug delivery and protein attachment.

1.2.2 Achieving the expectant durability

The lack of chemical and mechanical durability remains a big problem for all current interfacing materials (Fig 1.4). Although PEDOT is more stable than other current conjugated polymers, the durability of PEDOT coatings is not superior to inorganic interfacing materials.

The external stress, repeated charge and mass transport, and gradual corrosion can cause materials failure. Two common failure modes observed in interfacing materials are cracking and delamination (Cui & Zhou 2007)(Abidian et al. 2010)(Campbell et al. 2011)(Gilgunn et al. 2013).

The delamination often comes from the lack of adhesion to the solid substrate. Cracking normally stems from the lack of cohesive strength and electrochemical stability. As a relatively brittle material (Qu et al. 2015), PEDOT is also not stable when it is over-oxidized. The delamination and cracking of PEDOT films was found after 3 cycles of CV from -0.3 V to 1.5 V (Láng et al. 2012). Sometimes material failures could happen during the sterilization process (Green et al. 2013).

Under repeated electric stimulation, PEDOT has shown issues with its durability. It was found some PEDOT coating cracked and delaminated from the electrodes after chronic electric stimulation (Cui & Zhou, 2007).

1.3 Motivations and objectives

To develop an excellent biomedical interfacing material, the goal is to improve the most essential properties: durability, conductivity and biocompatibility in living tissues. Among those, the durability is the weakest link for the long-term applications. To achieve the above goal, a full cycle of chemistry and formulation development, materials characterization (including electrochemical, chemical, mechanical

characterization and durability test), *in vitro* and in *vivo* tests should be conducted. For many years, a lot of attention has been put in developing strategies of new chemistry for conjugated polymers and dopants. However, little information was published surrounding the formulation development or the characterization of mechanical properties and durability tests. Without a quantitative analysis of the mechanical properties and durability, it is difficult to identify the effective modification methods and establish systematic studies. This thesis will cover the parts which have not been as carefully examined in previous studies, and focus on solving two important outstanding problems. The first is improving the durability of PEDOT while maintaining the superior signal conductivity and biocompatibility. The second is characterizing and confirming the improved durability.

1.4 Outline of the thesis

Methods for improving the performance of conjugated polymer films using variations in processing will be discussed in Chapter 2 and 3, using alternative methods of processing and variations in synthesis. Methods for characterizing the mechanical properties of conjugated polymers films, and identifying modes of failure, will be described in Chapter 4 and 5. The content of Chapter 5 is based on the knowledge and results in Chapter 4. The following is the outline of the thesis.

Chapter 2 describes the formulation modification for electrochemical depositions. The modification improved the conductivity and durability of PEDOT coatings. The electrodes produced were applied in the 7-month in-vivo testing of rats. With the valuable feedbacks from these in vivo tests, we realized that, at the current stage, the mechanical durability of PEDOT remains a concern for long-term applications.

Chapter 3 reviews the strategies to improve the cohesion and adhesion of conjugated polymer coatings, including new chemistry and physical treatments. This chapter is the first systematic review of methods to improve the durability of conjugated polymer coatings.

Chapter 4 describes a method to characterize the stiffness, strength and adhesion of electrochemically deposited PEDOT coatings, which is the first time of quantitative measurement of the mechanical properties other than the stiffness of electrochemical deposited conjugated polymer coatings. This chapter also paved the way for the studies in next chapter.

Chapter 5 describes new testing methods to correlate the properties (cohesive and adhesive strength, and electrochemical stability) of materials with their durability, and also illustrates the analysis of the failure modes and mechanisms of biomedical interfacing materials.

A summary of results from each chapter and suggestions for future work are presented in Chapter 6.

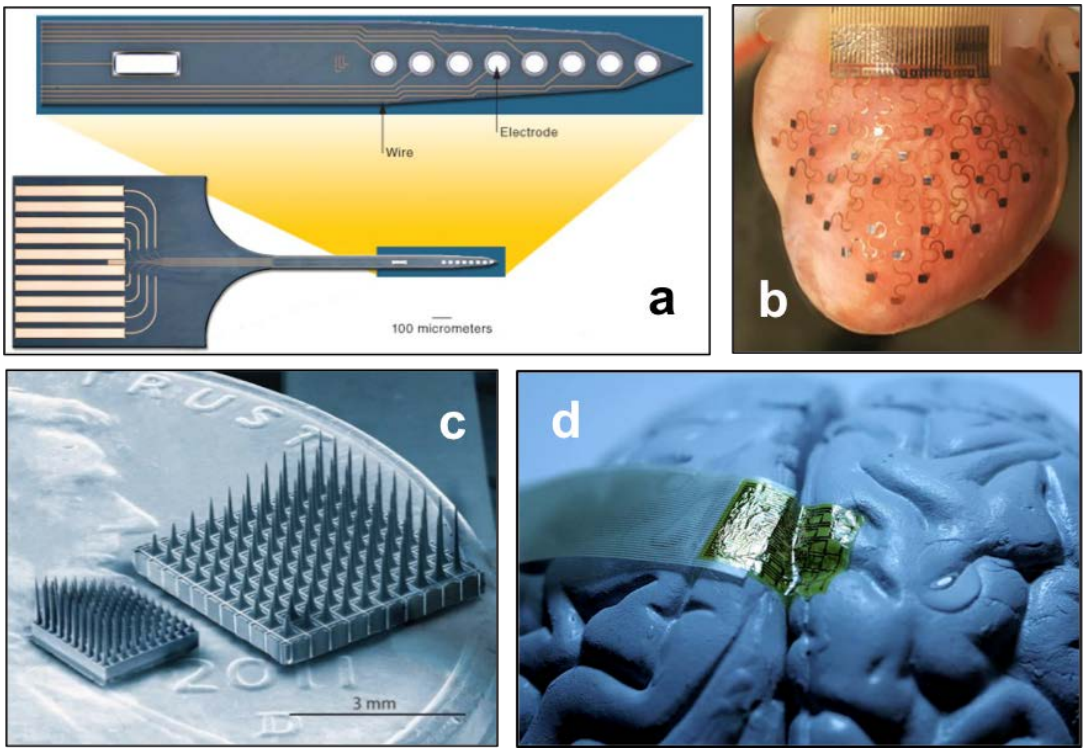

Figure 1.1 Current technologies of biomedical electrodes: (a, c) penetrating probes (image adapted from (Wark et al. 2013)), (b) surface-mounted cardiac electrode (image adapted from (Xu et al. 2015)), surface-mounted neural electrodes (image adapted from (Kim et al. 2008)).

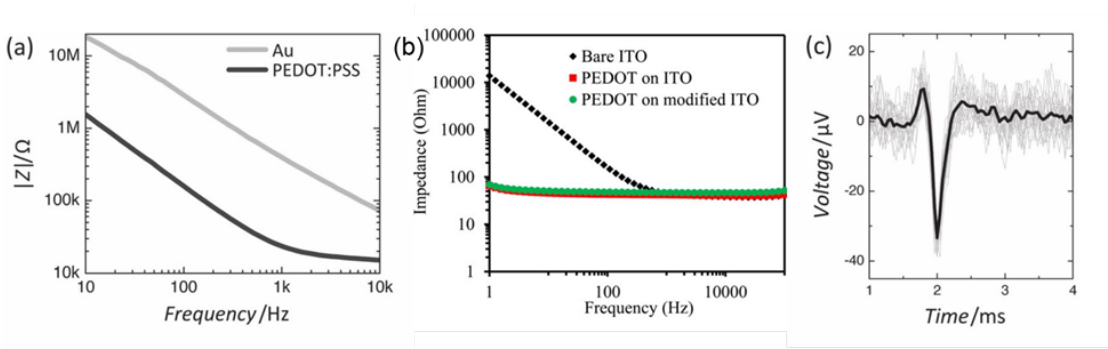

Figure 1.2 The superior electrical properties of conjugated polymers. Figure (a) & (c) compared the impedance and signal clarity obtained from Au and PEDOT:PSS (Sessolo et al. 2013), (b) compared ITO and PEDOT:$LiClO_4$ (Wei, Liu, et al. 2015)

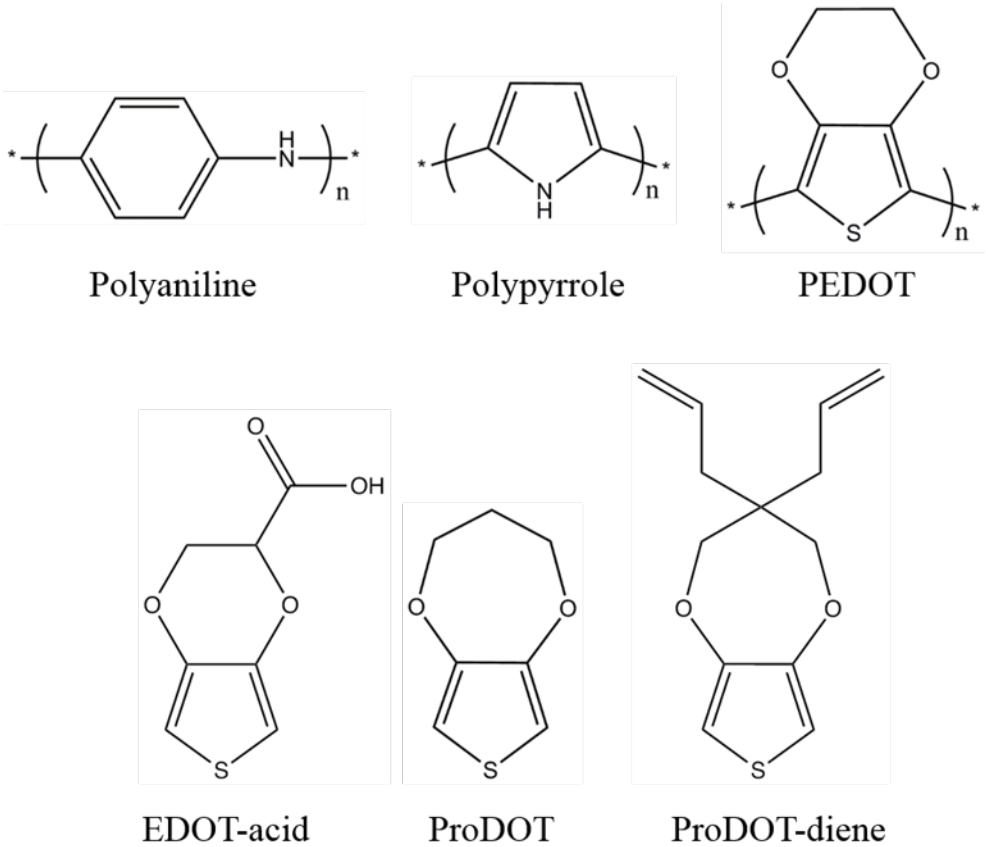

Figure 1.3 Chemical structures of polyaniline, polypyrrole, PEDOT, carboxylic-acid functionalized EDOT, ProDOT, diene functionalized ProDOT.

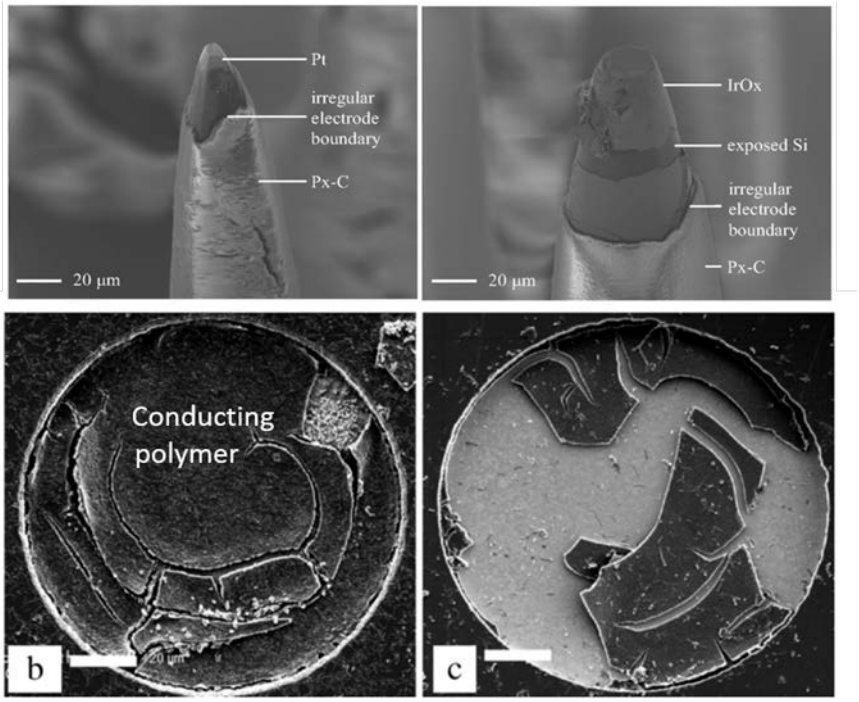

Figure 1.4 Failures of interfacing materials. The upper images are cracking of Pt and IrO_x (Gilgunn et al. 2013), and the lower images are cracking of PEDOT (Cui & Zhou 2007).

Table 1.1 The mechanical and charge carrier gap between interfacing materials and tissues.

	TiN	IrO_2	Pt/PtIr	Au	CPs	Tissues
Stiffness (GPa)	450-590	500	170	80	0.5-5	10^{-6}-10^{-4}
Charge carriers	Electrons	Electrons	Electrons	Electrons	Electrons & ions	Ions

REFERENCES

Abidian, M. et al., 2010. Conducting-polymer nanotubes improve electrical properties, mechanical adhesion, neural attachment, and neurite outgrowth of neural electrodes. *Small*, 6(3), pp.421–9.

Berggren, M. & Richter-Dahlfors, A., 2007. Organic bioelectronics. *Advanced Materials*, 19(20), pp.3201–3213.

Birmingham, K. et al., 2014. Bioelectronic medicines: A research roadmap. *Nature Reviews Drug Discovery*, 13(6), pp.399–400.

Brault, M.W., 2012. Americans With Disabilities: 2010. *Current population reports*, 423(July), pp.70–131.

Campbell, A. et al., 2011. A preliminary study of vapour-phase polymerized poly(3,4-ethylenedioxythiophene) as a transparent neural electrode. In *Proceedings of IEEE Sensors*. IEEE, pp. 1575–1578.

Chen, G.Z. et al., 2000. Carbon nanotube and polypyrrole composites: coating and doping. *Advanced Materials*, 12(7), pp.522–526.

Cogan, S.F., 2008. Neural stimulation and recording electrodes. *Annual review of biomedical engineering*, 10, pp.275–309.

Crispin, X. et al., 2006. The origin of the high conductivity of poly (3, 4-ethylenedioxythiophene)-poly (styrenesulfonate)(PEDOT-PSS) plastic electrodes. *Chemistry of Materials*, 18(July), p.4354.

Cui, X. et al., 2003. In vivo studies of polypyrrole/peptide coated neural probes. *Biomaterials*, 24(5), pp.777–787.

Cui, X. et al., 2001. Surface modification of neural recording electrodes with conducting polymer/biomolecule blends. *Journal of Biomedical Materials Research*, 56(2), pp.261–272.

Cui, X. & Martin, D.C., 2003. Electrochemical deposition and characterization of poly(3,4-ethylenedioxythiophene) on neural microelectrode arrays. *Sensors and Actuators B: Chemical*, 89(1–2), pp.92–102.

Cui, X. & Zhou, D., 2007. Poly (3,4-Ethylenedioxythiophene) for Chronic Neural Stimulation. *IEEE Transactions on Neural Systems and Rehabilitation Engineering*, 15(4), pp.502–508.

Feldman, K.E. & Martin, D.C., 2012. Functional conducting polymers via thiol-ene chemistry. *Biosensors*, 2(3), pp.305–317.

Gilgunn, P.J. et al., 2013. Structural analysis of explanted microelectrode arrays. In *International IEEE/EMBS Conference on Neural Engineering, NER*. pp. 719–722.

Graham, G., 2014. Population-based approaches to understanding disparities in cardiovascular disease risk in the United States. *International Journal of General Medicine*, 7, pp.393–400.

Green, R. et al., 2008. Conducting polymers for neural interfaces: challenges in developing an effective long-term implant. *Biomaterials*, 29(24–25), pp.3393–9.

Green, R. et al., 2013. Performance of conducting polymer electrodes for stimulating neuroprosthetics. *Journal of neural engineering*, 10, p.16009.

Green, R. & Abidian, M.R., 2015. Conducting Polymers for Neural Prosthetic and Neural Interface Applications. *Advanced Materials*, 27(46), pp.7620–7637.

Harris, A.R. et al., 2013. Conducting polymer coated neural recording electrodes. *Journal of neural engineering*, 10(1), p.16004.

Heywang, G. & Jonas, F., 1992. Poly(Alkylenedioxythiophene)s - New, Very Stable Conducting Polymers. *Advanced Materials*, 4(2), pp.116–118.

Hyder, A. et al., 2007. The impact of traumatic brain injuries: A global perspective. *NeuroRehabilitation*, 22(5), pp.34–35.

Karyakin, A.A., Strakhova, A.K. & Yatsimirsky, A.K., 1994. Self-doped polyanilines electrochemically active in neutral and basic aqueous solutions. Electropolymerization of substituted anilines. *Journal of Electroanalytical Chemistry*, 371(1–2), pp.259–265.

Khodagholy, D. et al., 2013. In vivo recordings of brain activity using organic transistors. *Nature Communications*, 4, p.1575.

Kung, T. et al., 2014. Regenerative peripheral nerve interface viability and signal transduction with an implanted electrode. *Plastic and reconstructive surgery*, 133(6), pp.1380–94.

Láng, G.G. et al., 2012. In situ monitoring of the electrochemical degradation of polymer films on metals using the bending beam method and impedance spectroscopy. In *Electrochimica Acta*. pp. 59–69.

Lang, U., Naujoks, N. & Dual, J., 2009. Mechanical characterization of PEDOT:PSS thin films. *Synthetic Metals*, 159(5–6), pp.473–479.

Lee, H. et al., 2005. Biomechanical analysis of silicon microelectrode-induced strain in the brain. *Journal of neural engineering*, 2(4), pp.81–9.

Leleux, P. et al., 2014. Conducting Polymer Electrodes for Electroencephalography. *Advanced Healthcare Materials*, 3(4), pp.490–493.

Liu, D.Y. & Reynolds, J.R., 2010. Dioxythiophene-based polymer electrodes for supercapacitor modules. *ACS Applied Materials and Interfaces*, 2(12), pp.3586–3593.

Lu, W. et al., 2002. Use of ionic liquids for pi-conjugated polymer electrochemical devices. *Science (New York, N.Y.)*, 297(5583), pp.983–987.

Martin, D.C., 2015. Molecular design, synthesis, and characterization of conjugated polymers for interfacing electronic biomedical devices with living tissue. *MRS Communications*, 5(2), pp.131–153.

Merrill, D.R., Bikson, M. & Jefferys, J.G.R., 2005. Electrical stimulation of excitable tissue: Design of efficacious and safe protocols. *Journal of Neuroscience Methods*, 141(2), pp.171–198.

Milica M. Gvozdenović, Branimir Z. Jugović, Jasmina S. Stevanović, T.L.T. and B.N.G., 2011. *Electrochemical Polymerization of Aniline, Electropolymerization*,

Mu, S., 2011. Synthesis of poly(aniline-co-5-aminosalicylic acid) and its properties. *Synthetic Metals*, 161(13–14), pp.1306–1312.

Nyberg, T., Shimada, A. & Torimitsu, K., 2007. Ion conducting polymer microelectrodes for interfacing with neural networks. *Journal of Neuroscience Methods*, 160(1), pp.16–25.

Ouyang, L. et al., 2014. *In vivo* polymerization of poly(3,4-ethylenedioxythiophene) in the living rat hippocampus does not cause a significant loss of performance in a delayed alternation task. *Journal of Neural Engineering*, 11(2), p.26005.

Povlich, L.K. et al., 2013. Synthesis, copolymerization and peptide-modification of carboxylic acid-functionalized 3,4-ethylenedioxythiophene (EDOTacid) for neural electrode interfaces. *Biochimica et biophysica acta*, 1830(9), pp.4288–93.

Povlich, L.K., Kim, J. & Martin, D.C., 2011. *Bio-functionalized and Biomimetic Conjugated Polymers for Interfacing Prosthetic Devices with Neural Tissue by*.

Qu, J. et al., 2015. Stiffness, strength and adhesion characterization of electrochemically deposited conjugated polymer films. *Acta Biomaterialia*.

Richardson, R.T. et al., 2009. Polypyrrole-coated electrodes for the delivery of charge and neurotrophins to cochlear neurons. *Biomaterials*, 30(13), pp.2614–2624.

Richardson-Burns, S.M. et al., 2007. Polymerization of the conducting polymer poly(3,4-ethylenedioxythiophene) (PEDOT) around living neural cells. *Biomaterials*, 28(8), pp.1539–52.

Rivnay, J., Owens, R.M. & Malliaras, G.G., 2014. The rise of organic bioelectronics. *Chemistry of Materials*, 26, pp.679–685.

Schlenoff, J.B. & Xu, H., 1992. Evolution of Physical and Electrochemical Properties of Polypyrrole during Extended Oxidation. *Journal of The Electrochemical Society*, 139(9), p.2397.

Schmidt, C.E. et al., 1997. Stimulation of neurite outgrowth using an electrically conducting polymer. *Proceedings of the National Academy of Sciences of the United States of America*, 94(17), pp.8948–8953.

Schottland, P. et al., 2000. Poly(3,4-alkylenedioxypyrrole)s: Highly stable electronically conducting and electrochromic polymers. *Macromolecules*, 33(19), pp.7051–7061.

Sessolo, M. et al., 2013. Easy-to-Fabricate Conducting Polymer Microelectrode Arrays. *Advanced materials (Deerfield Beach, Fla.)*, pp.2135–2139.

Simon, D.T. et al., 2016. Organic Bioelectronics: Bridging the Signaling Gap between Biology and Technology. *Chemical Reviews*.

Skotheim, T. & Reynolds, J., 2006. *Conjugated Polymers: Theory, Synthesis, Properties, and Characterization - Google Books*,

Smela, E., 1998. Thiol-Modified Pyrrole Monomers: 4. Electrochemical Deposition of Polypyrrole over 1-(2-Thioethyl)pyrrole. *Langmuir*, 14(11), pp.2996–3002.

Subbaroyan, J., Martin, D.C. & Kipke, D.R., 2005. A finite-element model of the mechanical effects of implantable microelectrodes in the cerebral cortex. *Journal of neural engineering*, 2(4), pp.103–113.

del Valle, L.J. et al., 2007. Cellular adhesion and proliferation on poly(3,4-ethylenedioxythiophene): Benefits in the electroactivity of the conducting polymer. *European Polymer Journal*, 43(6), pp.2342–2349.

Venkatraman, S. et al., 2011. In vitro and in vivo evaluation of PEDOT microelectrodes for neural stimulation and recording. *IEEE transactions on neural systems and rehabilitation engineering : a publication of the IEEE Engineering in Medicine and Biology Society*, 19(3), pp.307–16.

Viventi, J. et al., 2010. A conformal, bio-interfaced class of silicon electronics for mapping cardiac electrophysiology. *Science translational medicine*, 2(24), p.24ra22.

Wei, B., Ouyang, L., et al., 2015. Post-polymerization functionalization of poly(3,4-propylenedioxythiophene) (PProDOT) via thiol–ene “click” chemistry. *J. Mater. Chem. B*, 3, pp.5028–5034.

Wei, B., Liu, J., et al., 2015. Significant Enhancement of PEDOT Thin Film Adhesion to Inorganic Solid Substrates with EDOT-Acid. *ACS applied materials & interfaces*, 7(28), pp.15388–94.

Weiland, J.D., Cho, A.K. & Humayun, M.S., 2011. Retinal prostheses: Current clinical results and future needs. *Ophthalmology*, 118(11), pp.2227–2237.

Wilks, S.J. et al., 2009. Poly(3,4-ethylenedioxythiophene) as a Micro-Neural Interface Material for Electrostimulation. *Frontiers in neuroengineering*, 2(June), p.7.

Xiao, Y., Cui, X. & Martin, D.C., 2004. Electrochemical polymerization and properties of PEDOT/S-EDOT on neural microelectrode arrays. *Journal of Electroanalytical Chemistry*, 573(1), pp.43–48.

Xu, L. et al., 2015. Materials and fractal designs for 3D multifunctional integumentary membranes with capabilities in cardiac electrotherapy. *Advanced Materials*, 27(10), pp.1731–1737.

Yamato, H., Ohwa, M. & Wernet, W., 1995. Stability of polypyrrole and poly(3,4-ethylenedioxythiophene) for biosensor application. *Journal of Electroanalytical Chemistry*, 397(1–2), pp.163–170.

Ziegler-Graham, K. et al., 2008. Worldwide variation in the doubling time of Alzheimer's disease incidence rates. *Alzheimer's & Dementia*, 4(5), pp.316–23.

Chapter 2

DEVELOPMENT OF DURABLE PEDOT COATED ELECTRODES FOR REGENERATIVE PERIPHERAL NERVE INTERFACES (RPNI)

2.1 Introduction

Metallic electrodes used in neural prosthetics usually have poor long-term performance due to the degeneration of surrounding neurons (Grill 2008) and the development of a local immune response, manifested as glial scar formation (Polikov et al. 2005)(Donoghue 2008)(Minev et al. 2013). Modification with conducting polymers has been investigated as a promising approach to improve the tissue-electrode interactions and thus extend the effective lifetime of neural electrodes (Yang & Martin 2006)(Cui & Zhou 2007)(Kung et al. 2013). With their ionic conductivity and increased effective surface area, conducting polymer coated electrodes are more sensitive, and show faster neural signal recording performance, as compared to the bare metallic electrodes (Kung et al. 2013). The reduced mechanical mismatch between the conducting polymer coated electrode and surrounding tissues has also been hypothesized around devices implanted in neural tissue (Polikov et al. 2005) (Minev et al. 2013).

Poly(3,4-ethylenedioxythiophene) (PEDOT), a derivative of polythiophene, has been well studied. The alkoxy subsitutents on the 3 and 4 position of the thiophene ring insures that the oxidative polymerization must result in linear chains. As a more chemically stable polymer than either polythiophene and polypyrrole, PEDOT was selected to be deposited on metallic neural electrodes in this study. Generally,

conducting polymer coatings can be obtained by either chemical or electrochemical polymerization. In our case, the electrochemical polymerization is favorable, since it is not limited by the geometry of the biomedical electrode, and is easier to control the thickness of the deposited coating.

In order to insure the biocompatibility and low toxicity of the PEDOT coating, almost all previous PEDOT coated neural electrodes reported in the literature were obtained from aqueous solutions (Xiao et al. 2004)(Cui et al., 2001)(Venkatraman et al. 2011). However, PEDOT deposition from water is typically uneven and the resulting films are relatively easy to crack and may delaminate from the metal surface even before implantation into animals (Zhou et al. 2010).

To obtain more mechanically robust PEDOT coatings, alternative solvents for electrochemical polymerization were investigated. Organic solvents such as acetonitrile, propylene carbonate and dichloromethane have been used for the electrochemical polymerization of PEDOT (Noël et al. 2003)(Hillman et al. 2007). The morphology of PEDOT deposited from organic solvents is typically more porous as compared to the compact, lumpy surface of PEDOT deposited from water. This increases the surface area and thus has the potential to reduce the impedance of PEDOT. Since the PEDOT coated electrodes are targeted to be implanted into living tissue, their potential biocompatibility is a high priority. Among candidate organic solvents (Table 2.1), propylene carbonate was found to be relatively non-toxic, with a broad electrochemical window and high current efficiency.

In this chapter, the PEDOT deposition was studied from two solvents: water and propylene carbonate, and the mechanical and electrical properties of these two

kinds of PEDOT coated electrodes were compared. After that, the PEDOT coated electrodes were implanted into rats for *in vivo* tests.

2.2 Experimental procedures

2.2.1 Materials

3,4-ethylenedioxythiophene (EDOT), lithium perchlorate ($LiClO_4$), and propylene carbonate were purchased from Sigma-Aldrich. All other chemicals were of analytical grade, and deionized water from a Millipore Q water purification system was used throughout. All reagents and solvents were used without further purification, unless otherwise noted. Stainless steel pad electrodes were purchased from Plastics One.

2.2.2 Electrochemical deposition

The stainless steel (SS) pad electrodes (~1 mm x 3 mm) were ultrasonically cleaned (Kendal HB-23, 220 W) in acetone, 2-propanol, and deionized water, respectively for 10 min.

The electrochemical polymerization and characterization were performed with an Autolab PGstat12 Potentiostat/Galvanostat (EcoChemie) using the Nova 1.8 electrochemical software in a three-electrode cell. PEDOT was polymerized on SS pad electrodes under galvanostatic conditions (10 μA) for 3000 s from an aqueous solution containing 0.01 M EDOT, 0.1M $LiClO_4$, and a propylene carbonate solution containing 0.1 M EDOT, 0.1 M $LiClO_4$ respectively. $LiClO_4$ was chosen as the counter-ion due to its relatively low cytotoxicity and better ionic conductivity performance in the low frequency range as compared to other counter-ions (King et al.

2011)(Baek et al. 2014). After the deposition, the coated electrodes were immerged in 70% ethanol for 12 hours.

2.2.3 Wear test

The durability of the PEDOT coatings were tested through a wear test tailored for peripheral nerve interface applications, by stimulating the sliding friction expected between the electrode implants and the skeletal muscle tissue in the upper limbs. The PEDOT coated electrodes were inserted vertically into fresh pork loin at room temperature for 100 times. The insertion spot was changed every time to ensure an intact region of tissue for each insertion. The penetration depth was 3.2 mm (the length of pad electrode). After 1, 5, 10, 20, 30, and 100 insertions, the surface of the PEDOT-coated electrodes was examined with a Nikon Stereoscope. The extent of PEDOT layer retention (percentage of remained area) on the electrode surface was calculated by ImageJ from the stereoscopic images. After the wear test, the PEDOT coated electrodes were observed under the scanning electron microscope (SEM) to confirm the morphology and integrity of the film.

2.2.4 Electrochemical characterization

Electrochemical impedance spectroscopy (EIS) and biphasic stimulation were also conducted an Autolab PGstat12 Potentiostat/Galvanostat (EcoChemie) using the Nova 1.8 electrochemical software in a three-electrode cell containing 1x PBS solution. To obtain the EIS results, the electrodes were scanned from 10^5 Hz to 0.1 Hz

at 0.01 V. For biphasic stimulation, a -0.1 V-0.1V stage current signal was applied to the electrodes.

2.2.5 *In vivo* test

7-month *in-vivo* tests in rats were conducted by our collaborators at the University of Michigan, Ann Arbor (Kung et al., 2013). Ten rats underwent regenerative peripheral nerve interface (RPNI) fabrication whereby the left extensor digitorum longus (EDL) muscle was removed as a non-vascularized free tissue transfer and reinnervated by the divided ipsilateral common peroneal nerve. The RPNI was interfaced to either a stainless steel pad electrode (RPNISS group, n = 5) or a pad electrode coated with conductive polymer (RPNICP group, n = 5) tunneled to a head cap to allow for serial testing. The contralateral intact EDL muscle of each rat was used as control (ControlSS and ControlCP, n = 5 each). Nerve conduction studies were performed 1 month postoperatively using percutaneous stimulation. Needle electromyography (EMG) was used to evaluate reinnervation of the EDL muscle within the RPNI. After fabrication of the Micro-TMR, either a stainless steel pad electrode or a PEDOT coated pad electrode was used for the interface.

2.3 Results and discussion

2.3.1 Wear test

Almost 45% of surface area was lost on PEDOT coated electrodes from water after 100 insertions, while the surface of PEDOT coated electrodes from propylene carbonate remained nearly intact even after 100 insertions, as shown in Fig 2.2(c), the highlighted layer on the PC-PEDOT surface was the pork meat tissue. The meat test

showed that the PC-PEDOT was much more durable than the water-PEDOT, and suggests that both the cohesive and adhesive strength of PC-PEDOT on the stainless steel surface were larger.

The water-PEDOT and PC-PEDOT had substantially different morphologies according to the SEM images (Fig 2.3). There were more bumps on the hummock-like surface of water-PEDOT, with typical diameters of the hummock around 1-4 μm, while more pores existed among the propylene carbonate-PEDOT nodular structure, with the nominal diameters of clusters around 1-2 μm.

2.3.2 Electrochemical characterization

It was found that the impedance of both bare and PEDOT coated electrodes was higher at low frequencies. This was because the electrode's behavior in electrolyte solution was closer to a capacitor than a conductor at lower frequencies, and both the resistance and the capacitance was higher. As seen in Fig 2.4 b, the phase angle showed that the bare SS electrode behaved like a capacitor in the 10~1000 Hz frequency reange, while the PEDOT coated electrode behaved more as a resistor at frequencies higher than 10Hz and more like a capacitor for frequencies less than 10 Hz.

The impedance of PEDOT coated electrodes was significantly lower than that of the bare stainless steel electrode over the whole range of frequencies. For example, the magnitude of impedance was decreased from ~1000 Ω for the bare electrode to ~45 Ω for water-PEDOT coated electrode and 25 Ω for propylene carbonate-PEDOT coated electrode at 100 Hz. This frequency range is similar to that of EMG signals, with typically oscillates at 0.5 ~ 500 Hz (Boxtel 2001). One explanation for the origin

of this phenomenon is the increase of effective charge transport area after PEDOT deposition. The other reason is the ionic conductivity of PEDOT. As seen in Fig 2.4 b, the phase angle showed that the bare SS electrode behaved like a capacitor during over the whole range of frequencies, while the PEDOT-coated electrode behaved more as a resistor in frequencies higher than 40 Hz and more like a capacitor for frequencies less than 40 Hz. With both electronic and ionic conductivity, the PEDOT coated electrodes provides efficient capacitive charge transport at low frequencies.

Even though the impedances were reduced to extremely low values with the PEDOT coatings, there were still differences between water-PEDOT and propylene carbonate-PPC. For example, the impedance of PC-PEDOT at 100 Hz was around 30 Ω, which was significantly lower than the 50 Ω of water-PEDOT.

The biphasic stimulation results (Fig 2.4d) showed that the response speed of the bare pad electrodes was slow with a huge lag phase. The slope was around 50 V/s while the signal jumped from -0.1 V to 0.1 V. The performance of the PC-PEDOT coated electrodes was the best, with the corresponding potential variations sharp and much flatter. The slope was around 2 V/s, which means the signal recording is more rapid and sensitive. At the same time, the PEDOT coated electrodes had smaller voltage excursions for fixed charge injection, which means they will be safer for neural stimulation (Luo et al. 2011).

After the wear test, the electrical properties of PC-PEDOT coated electrodes remained stable after 100 insertions due to the integrity of the surface coating. However the electrical properties of the water-PEDOT coated electrodes were obviously impaired after the wear test. The impedance of the water-PEDOT increased to around 80 Ω from 50 Ω, and the phase angle jumped from 10° to 20° at 100 Hz (Fig

2.4a). The wear test and the electrochemical characterization demonstrated the superior mechanical and electrical durability of PEDOT coated electrodes deposited from propylene carbonate.

2.3.3 *In vivo* test

The results of the in-vivo testing (summarized in Fig 2.5c.) showed that the transplanted extensor digitorum longus (EDL) muscle remained healthy with PEDOT-coated electrodes. Also the PEDOT layer significantly increased the recorded signal amplitude compared to the uncoated electrodes.

It was found that an implanted RPNI can successfully transduce bioelectric signals through an implanted pad electrode and signal quality was maintained at 7 months. The addition of the conductive polymer PEDOT onto implanted pad electrodes improved the maximum compound muscle action potential (CMAP) of the recorded signal that was transduced from the RPNI.

However, a certain amount 30% of PEDOT exfoliation during 7-month animal test was observed by SEM (Fig. 2.6), even though the recorded signal was still more accurate and stronger compared to the bare ones. These results mean that the conducting polymer layer is apparently still not durable enough for long-term implantations.

Evidence for PEDOT mechanical instabilities observed from the SEM revealed that the failure of PEDOT was mainly due to the cracking and delamination (Fig. 2.6 b, c). This means there is an urgent need to improve the long-term performance of the coating by increasing the mechanical strength and the adhesion of the PEDOT to the metallic substrate.

2.4 Conclusions

The electrochemical deposition from propylene carbonate modified the electrical and mechanical properties of PEDOT coatings as compared to the aqueous solution. The coatings were more durable under the muscle-electrode contacting environment. The 7-month *in vivo* tests demonstrated the sharper and more sensitive performance brought by the PEDOT coating during the neural signal recording procedure, the amplitude of the signal of PEDOT coated electrode was around twice of that of bare SS electrode. However, some impairment of PEDOT coatings was still observed after the in vivo test, around 30% of the coating was lost. It means more research should be done to improve the mechanical and electrochemical stability of conducting polymers in the near future.

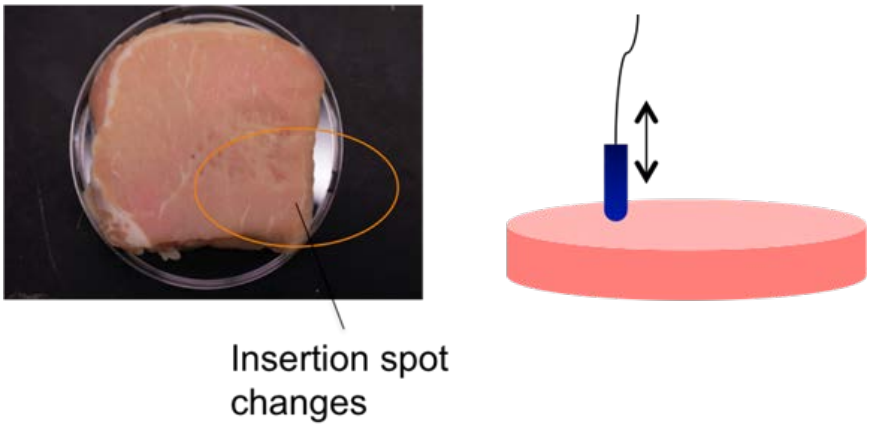

Figure 2.1 Schematic meat insertion test.

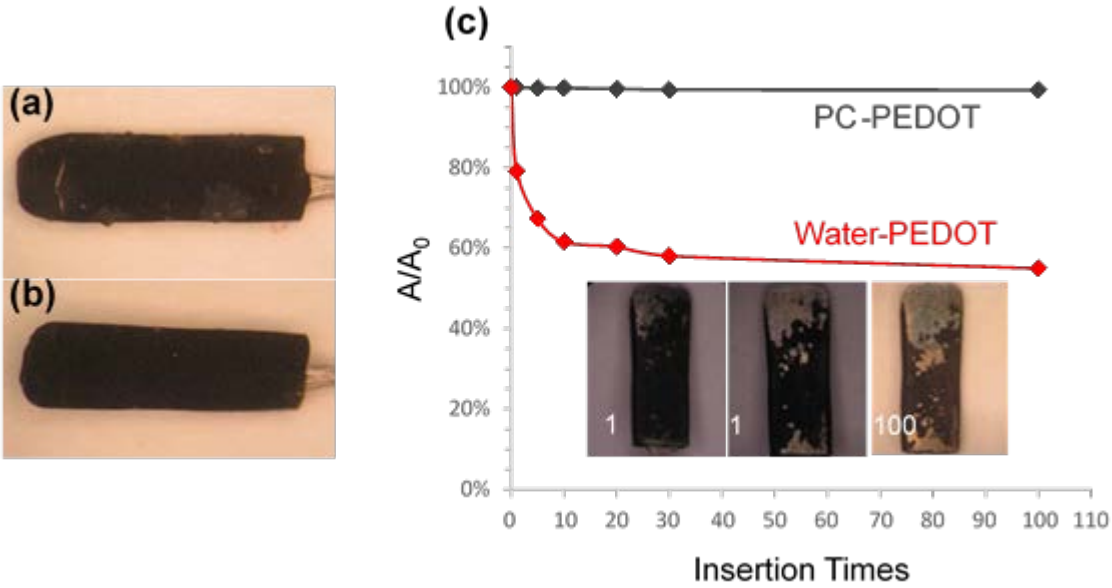

Figure 2.2 PEDOT coated electrode from deionized water (a) and propylene carbonate (b), and (c) the remained area percentage of PEDOT coated electrodes from water and propylene carbonate.

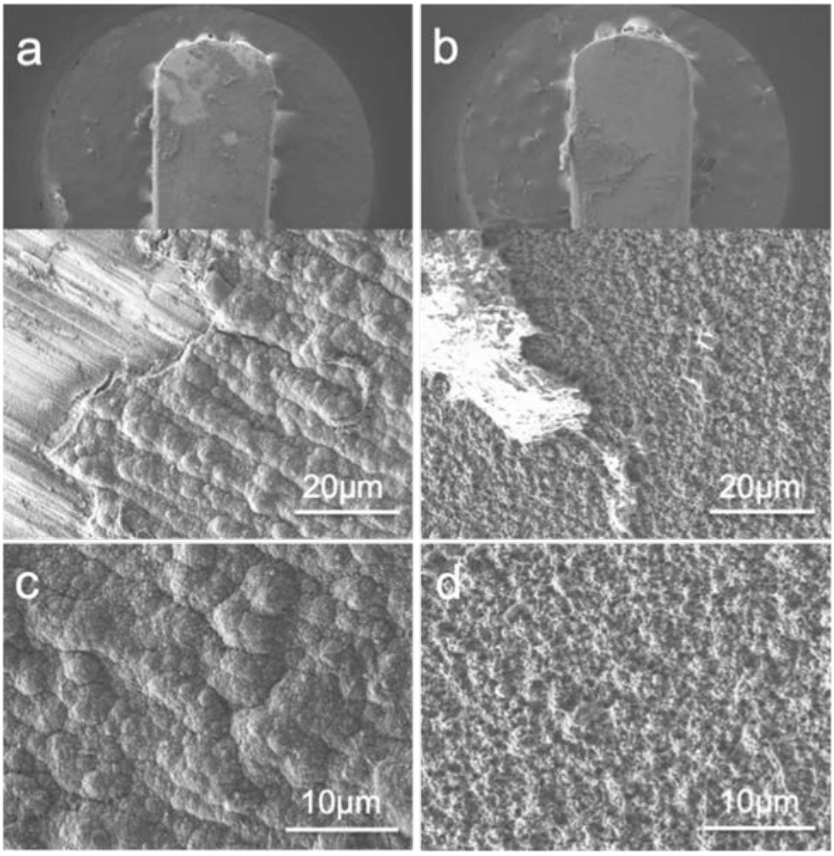

Figure 2.3 SEM images of water-PEDOT (a,c) and propylene carbonate-PEDOT (b,d) coated pad electrodes after 100-insertion meat test.

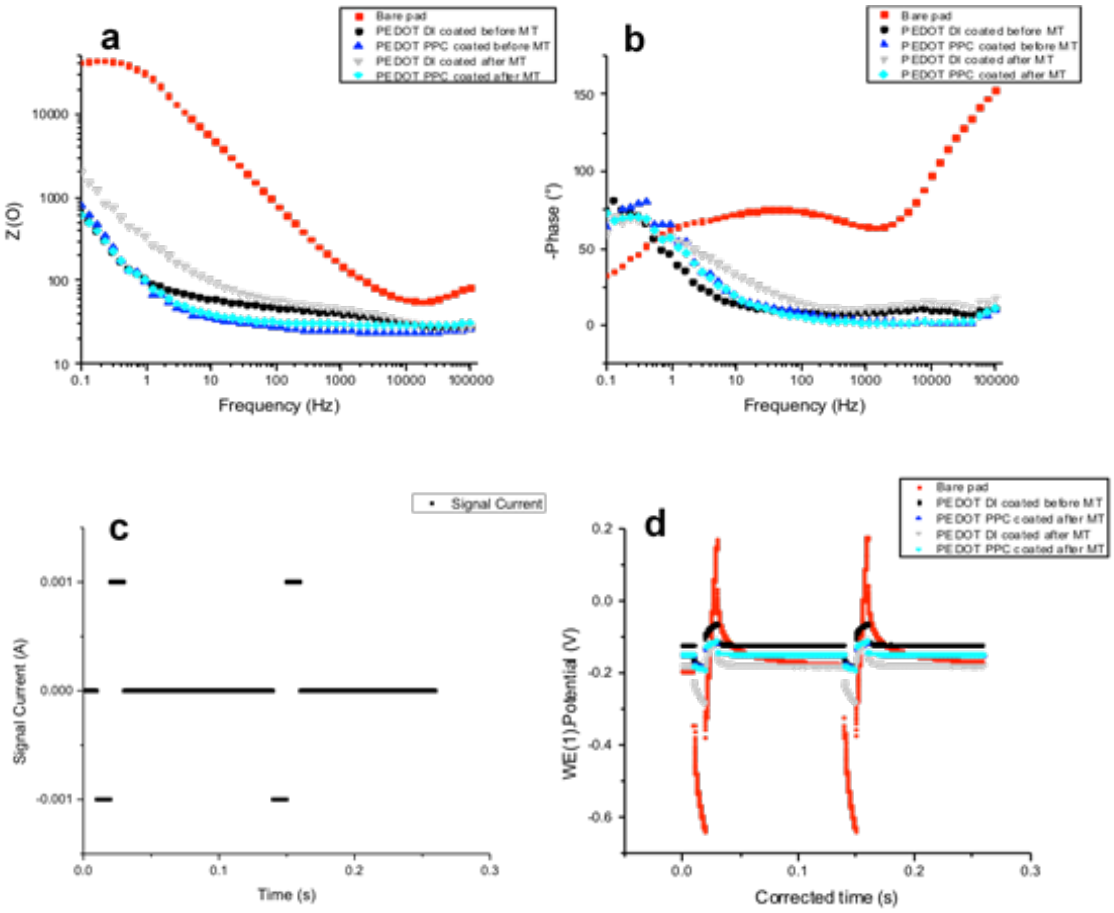

Figure 2.4 (a, b) The bode mode of EIS; (c, d) biphasic stimulation of different PEDOT coated electrodes before and after 100-insertion meat test.

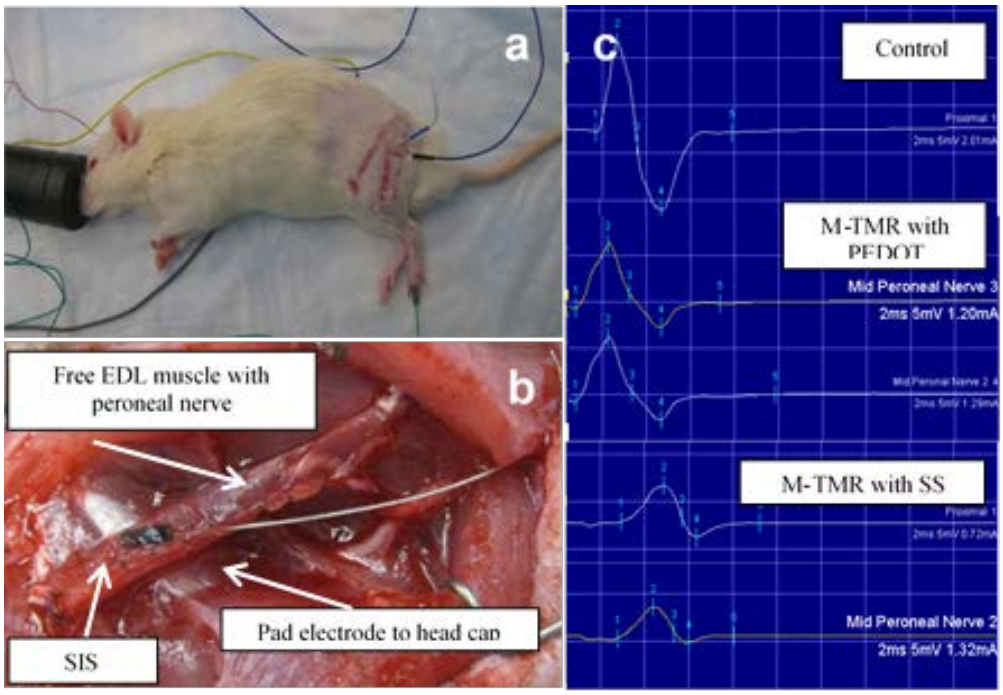

Figure 2.5 (a) Serial Nerve Conduction/EMG Testing, (b) micro-TMR with pad electrode, (c) nerve conduction recordings of compound muscle action potentials (CMAP) from the Micro-TMR via the implanted electrode for Control, Stainless Steel (SS), and PEDOT groups. (Kung, T.A. et al, 2013)

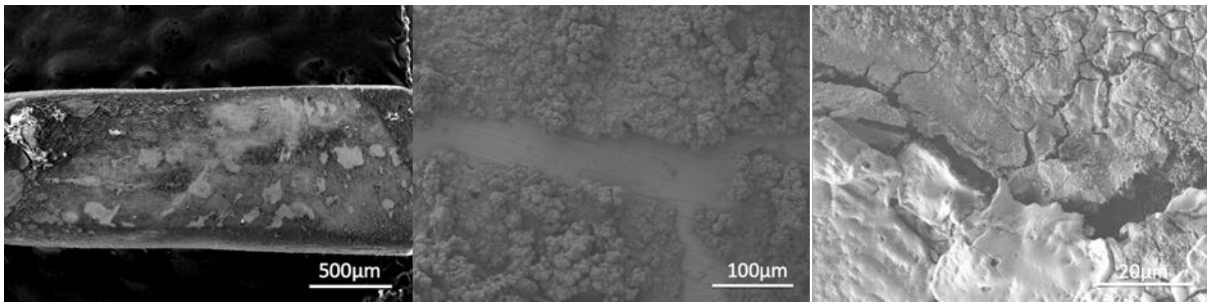

Figure 2.6 SEM images of PEDOT coated electrode after 7-month in vivo test

Table 2.1 The electrochemical properties and toxicity of solvents (Ahmed & Farooqui 1982) (National Toxicology Program (NTP 1997).

Solvent	**Boiling point (º C)**	**Oral LD_{50}, rats (mg/kg)**	**Electrochemical window (Volt)**
Acetonitrile	81.6	2460	-3.6~2.8
Propylene carbonate	242	__	-3.7~3.2
Nitromethane	66	940	-3~3.8
Dichloromethane	39.6	1250	-2.5~2.4
Water	100	__	-2.3~1.5

REFERENCES

Ahmed, A.E. & Farooqui, M.Y.H., 1982. Comparative toxicities of aliphatic nitriles. *Toxicology Letters*, 12(2–3), pp.157–163.

Baek, S., Green, R.A. & Poole-Warren, L.A., 2014. Effects of dopants on the biomechanical properties of conducting polymer films on platinum electrodes. *Journal of Biomedical Materials Research Part A*, 102(8), pp.2743–2754.

Boxtel, A., 2001. Optimal signal bandwidth for the recording of surface EMG activity of facial, jaw, oral, and neck muscles. *Psychophysiology*, 38(1), pp.22–34.

Cui, X. et al., 2001. Surface modification of neural recording electrodes with conducting polymer/biomolecule blends. *Journal of Biomedical Materials Research*, 56(2), pp.261–72.

Cui, X. & Zhou, D., 2007. Poly (3,4-Ethylenedioxythiophene) for Chronic Neural Stimulation. *IEEE Transactions on Neural Systems and Rehabilitation Engineering*, 15(4), pp.502–508.

Donoghue, J.P., 2008. Bridging the brain to the world: a perspective on neural interface systems. *Neuron*, 60(3), pp.511–21.

Grill, W., 2008. Signal considerations for chronically implanted electrodes for brain interfacing. *Indwelling Neural Implants: Strategies for Contending …*, pp.42–61.

Hillman, A.R., Daisley, S.J. & Bruckenstein, S., 2007. *Kinetics and mechanism of the electrochemical p-doping of PEDOT*.

King, Z. a et al., 2011. Structural, chemical and electrochemical characterization of poly(3,4-ethylenedioxythiophene) (PEDOT) prepared with various counter-ions and heat treatments. *Polymer*, 52(5), pp.1302–1308.

Kung, T.A. et al., 2013. Implanted electrode with conductive polymer augments signal transduction from the regenerative neuregulin-1 / erbb2 signaling regulates early axonal regeneration. *Plastic and Reconstructive Surgery*, 131(5), p.58.

Luo, X. et al., 2011. Highly stable carbon nanotube doped poly(3,4-ethylenedioxythiophene) for chronic neural stimulation. *Biomaterials*, 32(24), pp.5551–5557.

Minev, I.R. et al., 2013. Interaction of glia with a compliant, microstructured silicone surface. *Acta Biomaterialia*, 9(6), pp.6936–6942.

National Toxicology Program (NTP, 1997), 1997. *Toxicology and Carcinogenesis Studies of Nitromethane (CAS No. 72-52-5) in F344/N Rats and B6C3F Mice (Inhalation Study)*,

Noël, V., Randriamahazaka, H. & Chevrot, C., 2003. Cyclic voltammetric studies of the relaxation processes during the oxidation of poly(3,4-ethylenedioxythiophene) in propylene carbonate solution. *Journal of Electroanalytical Chemistry*, 542, pp.33–38.

Polikov, V.S., Tresco, P. a & Reichert, W.M., 2005. Response of brain tissue to chronically implanted neural electrodes. *Journal of Neuroscience Methods*, 148(1), pp.1–18.

Venkatraman, S. et al., 2011. In vitro and in vivo evaluation of PEDOT microelectrodes for neural stimulation and recording. *IEEE transactions on neural systems and rehabilitation engineering : a publication of the IEEE Engineering in Medicine and Biology Society*, 19(3), pp.307–16.

Xiao, Y., Cui, X. & Martin, D.C., 2004. Electrochemical polymerization and properties of PEDOT/S-EDOT on neural microelectrode arrays. *Journal of Electroanalytical Chemistry*, 573(1), pp.43–48.

Yang, J. & Martin, D., 2006. Impedance spectroscopy and nanoindentation of conducting poly (3, 4-ethylenedioxythiophene) coatings on microfabricated neural prosthetic devices. *Journal of Materials Research*, 21(5).

Zhou, D.D. et al., 2010. *Implantable neural prostheses 2* D. Zhou & E. Greenbaum, eds., New York, NY: Springer New York.

Chapter 3

IMPROVING THE DURABILITY OF CONJUGATED POLYMERS ON SOLID INORGANIC SUBSTRATES

3.1 Introduction

It has been shown that the failure of conjugated polymer (CP) coatings in biomedical electrodes can happen in different stages. CP failure was observed at the end of 7-month *in vivo* study in rats (Kung et al. 2013)(Kung et al. 2014). CP failure has also been observed during the repeated charge injection simulation (Cui & Zhou 2007), and even during ETO sterilization (Green et al. 2013). Material failure may not only limit the performance of the electrodes (Kozai et al. 2015), it could also leave potential hazards when implanted in living tissues. Although several studies have demonstrated that CP coatings are not cytotoxic (Asplund et al. 2009)(Baek et al. 2014)(R. Green et al. 2008), residual fragments of CP are not likely to be easily metabolized. The potential impact of residual amounts of CP in tissue has not yet been studied in any detail. To put their superior biocompatibility and signal transfer performance into use of biomedical electronics, further studies to improve the durability of conjugated polymers are urgently required to ensure their long term performance in applications.

Even though the material failures could be caused by different mechanisms—the external stress (which stems from the collision during transportation, the friction between the electrodes and tissues), the repeated charge injection during application, the oxidation during sterilization, and the chronic corrosion by the electrolytic

environment, according to the microscopic results, they all followed two basic failure modes: cracking and delamination.

In this chapter, progress in achieving superior durability of conjugated polymers will be examined from two perspectives: eliminating cracking and reducing delamination.

3.2 Eliminating cracking

It is known that when a large stress is applied to materials, fracture may happen. Failure of polymers can also occur at relatively low stress levels. In this case, as the conjugated polymers degrade along the time, low stresses can cause failure. Polymer degradation normally relates to the decrease of chain length, and leads to a change in properties, such as tensile strength and color. Hence, the strategies of eliminating cracking of CP coatings could be addressed from three perspectives: reinforcing the stiffness, improving the ductility, and preventing the polymer degradation.

The most intuitive way of reinforcing the CPs are introducing stronger materials, such as carbon nanotubes (CNTs) and graphene. Another one is crosslinking CPs. Introducing more flexible chains may improve the ductility or toughness. The details of the studies are described in the following.

3.2.1 Increasing the stiffness

3.2.1.1 Reinforcing with carbon materials

With higher strength and more stable molecular structures, carbon materials were naturally adopted to reinforce the conjugated polymers. Chen *et al* were evidently the first to use CNTs as a dopant in the electrochemical polymerization of

conjugated polymers (Chen et al. 2000). After that, a lot of attempts have been made in fabricating the CP-CNT biomedical electrodes (Zhang et al. 2004) (Lee et al. 2011) (Mousavi et al. 2009)(Luo et al. 2011)(Gerwig et al. 2012)(Chen et al. 2013)(Samba et al. 2015)(Castagnola et al. 2014)(Abidian et al. 2010). With the emergence of graphene (reference), CP-graphene coatings were also developed (Xu et al. 2009)(Alvi et al. 2011)(Zhang & Zhao 2012). However, not many mentioned the characterization of electrochemical stability, and even fewer discussed the mechanical properties.

It was demonstrated that with the addition of CNTs and graphene, the electrochemical stability of the conjugated polymer coatings was improved, which indicated the degradation caused by the repeated charge injection could be postponed. Green et al found the electro-activity of PPy/PSS after 400 cycles of CV scan was improved from 39% to 71.5% with the MWCNT doping (R. A. Green et al. 2008). The Kim group reported that charge storage capacity of PPy-CNT coated gold electrode after 500 cycles of CV scan was improved to 80% from the 30% of PPy coated electrode (Chen et al. 2011). At the same time, no area loss was observed on PPy-CNT films, while over 50% area found on PPy coating. Lu et al. and Luo et al also characterized and demonstrated the improved electrochemical stability through the CV methods on PPy-CNT (Lu et al. 2010) and PEDOT-CNT (Luo et al. 2011) coatings.

Recently, Chen et al. demonstrated that the stability of PEDOT coating was improved with the MWCNT doping in the environment with external stress. The results showed that after 5-min sonication, the impedance of PEDOT/MWCNT coated electrode at 1 kHz was not harmed, while the impedance of PEDOT/PSS coated

electrode increased by 3.4%. However, the sonication does not really represent the external stress environment in reality (Chen et al. 2013).

Gerwig *et al.* adopted the tape test to simulate the stress test, and measured the impedance of PEDOT coated and PEDOT-CNT coated gold electrodes before and after the tape test. It was reported that the impedance of both remained intact (Gerwig et al. 2012). However, not much detail of the tape test was shown in the paper. It is worth noting that the tape test was not really the appropriate method to either simulate the external stress or characterize the mechanical properties.

The hypothesis of improving the strength and stability of conjugated polymer coatings was based on that the carbon materials could share both the stress and charge loads with CPs. Due to the lack of appropriate characterization methods, only the improved electrochemical stability was confirmed.

3.2.1.2 Crosslinking CPs

To prevent the cracking, another approach is to crosslink the polymers. A few crosslinkers have been developed, and will be described in the following.

In order to maintain the conjugated structures, Cherioux et al. and Zhu et al. synthesized a series of phenyl-core branched conjugated thiophene monomers (Cherioux et al. 1998) (Zhu & Swager 1997), as shown in Fig 3.1a. Those branched monomers were found to be electroactive and capable of forming thin films during electrochemical deposition (Köse & Mitchell 2007). However, the EIS and CV characterization didn't show enhanced electrical properties, such as lower impedance, when those branched monomers polymerized only with themselves. No further studies of mechanical properties were made.

Recently,1,3,5-tris[2-(3,4-ethylenedioxy-thienyl)]-benzene (EPh) was synthesized in our lab (Ouyang et al. 2015), following methods reported previously (Zhu & Swager 1997)(Idzik et al. 2010). It was found that the three-armed EDOT crosslinker with a benzene core, EPh, could be electrochemically copolymerized with EDOT in mixed monomer solutions to form crosslinked PEDOT-co-EPh copolymer coatings on metal electrodes. EIS showed that the copolymerization had a negative effect on the impedance of the coatings. With low EPh feeds (less than 0.02%), the PEDOT-co-EPh films had comparable impedances to neat PEDOT coatings. However, the impedance quickly increased with higher EPh feed ratios. The response speeds of the cross-linked PEDOT coated electrode (Fig 3.2c.) were also slower with higher voltage excursions than the PEDOT films, which was expected from the impedance spectroscopy results.

However, EPh proved to be efficient to improve the stiffness of PEDOT coatings. The stiffness was estimated by AFM nanoindentation tests. The results showed that with 0.5% EPh, the DMT modulus improved from 0.75 ± 0.16 GPa to 4.9 ± 2.1 GPa (Ouyang et al. 2015). Even though the conjugated crosslinkers have the potential to improve the stiffness of coatings, the crosslinking also shortened the effective conjugation length.

Some crosslinkers with non-conjugated, flexible chains have also been introduced to the conjugated polymers. This actually reduces the stiffness of CPs, and increases the ductility, as will be described in the next section.

Besides crosslinking the conjugated polymer backbones, another approach is to modify the molecular structure of their dopants. Physical and chemical crosslinking the macromolecular dopant—polystyrene sulfonate (PSS) was tried by a few groups

(Ghosh & Inganäs 1999b)(Ghosh & Inganäs 1999a). The cathodic and anodic peaks appeared at the same position when the scan rate of CV was lower than 50 mV/s, which showed ideally reversible redox cycles, and indicated improved electrochemical stability. Similarly, no mechanical characterization was reported.

3.2.2 Improving the ductility

The fracture strain of PEDOT is around 2% (Lang et al. 2009)(Qu et al. 2015). The lack of ductility of conjugated polymers is caused by their rigid backbones. Introducing flexible chains may be an effective way to improve their ductility. The improvement of ductility or flexibility should not only improve the resistance to the loaded strain, but would also promote the electrochemical stability by increase the endurance of repeated swelling and shrinking during the redox switching.

With high solubility, flexibility and excellent biocompatibility, polyethylene glycol (PEG) has been widely considered to introduce to the conjugated polymers. To replace platinum as an electrocatalytic material to generate hydrogens, Winther-Jensen et al. first produced PEDOT-PEG by vapor phase polymerization of PEDOT in the presence of PEG. Later on, this method was applied to make more biocompatible conducting polymers (Jimison et al. 2012) (Mueller et al. 2012). Recently, the PEG or PEO chains have been copolymerized with PEDOT to make the conducting polymers more ductile (Li et al. 2015). With the improved processability, the PEDOT-PEG has been fabricated to wires and implanted *in vivo*. It was shown that the biocompatibility was improved compared to the hard neural electrodes, due to the smaller mechanical gap between the electrode and tissues (Kolarcik et al. 2015).

Crosslinkers with non-conjugated, flexible chains were developed by Perepichka et al. They designed oligo(oxyetylene) chains with 2 EDOT ends

(Perepichka et al. 2002), as shown in Fig 3.1b. It was reported that the consequent polymer networks were strongly adherent on Pt electrodes, and could only be removed by polishing the electrode. Also the electrochemical stability of the polymer was improved. The polymer network retained at least 94% of its initial electroactivity, after 12000 cycles of CV scan. A quite interesting conclusion was made that even though the crosslinking might interrupted the effective conjugation, the interactions between water molecules and oligo(oxyethylene) stabilized the π-conjugated backbone into a privileged conformation corresponding to a considerable enhancement of the effective conjugation length and hence reduction of the band gap. However, none information about the cohesive strength was mentioned.

Recently, the Reynolds group have successfully introduced polar ester groups to the side of ProDOT, and obtained soluable PProDOT-PEDOT copolymers (Österholm et al. 2016) (Ponder et al. 2016). The increase of solubility does not only make the conjugated polymers more processable, but also improves their electrochemical stability by increasing the endurance of redox switching.

Desipite these developments in synthesis and processing, there is still relatively little information about stiffness, strength, ductility of conjugated polymers. This is evidently due to the lack of reliable and accurate mechanical characterization methods for non-free-standing coatings.

3.3 Overcoming delamination

For any type of coating, adhesion to the solid substrate is always a critical property of concern. In the current case, there are two major reasons for the low adhesion. One is that there are generally no specific chemical interactions (including

ionic, covalent, or hydrogen bonding) between the CPs and the metallic or semiconducting substrates. The other is the flat surface geometry of the substrate. Several approaches, either physical or chemical surface modification, have been attempted to improve the adhesion of CPs on substrates.

3.3.1 Physical modification of substrate surface

It was found that the roughened surface provided a mechanical interlock between the substrate and coating (Lee & Qu 2003). Cui roughened the smooth gold substrate by plating a fuzzy gold layer, and greatly improved the adhesion of subsequently deposited polypyrrole films. The improved adhesion was demonstrated through water rinsing, CV scan and insertion tests into agar gel (Cui & Martin 2003). Later on, Green et al reported that the stability of PEDOT coatings was improved with depositions on laser roughened platinum substrates (Green et al. 2012). However no quantitative information about the adhesion was provided in any of these studies.

3.3.2 Changing the surface chemistry of the substrate

Creating chemical bonds by changing the surface chemistry of substrates can be quite an effective strategy to improve the adhesion.

3.3.2.1 Creating hydrogen bonds

The modification of the substrate surface with self-assembled monolayers (SAMs) could be effective to create hydrogen bonds, when matching the hydrophilia of the coating. Huang *et al* found that the relatively hydrophilic CPs such as polypyrrole would adhere to hydrophilic substrates strongly (Huang et al. 1997).

3.3.2.2 Creating covalent or ionic bonds

To create the covalent or ionic bonds, typically, one end of the intermediate molecules (adhesion promoters) is designed to have specific interactions with the substrate while the other end forms chemical bonds with the conducting polymer during polymerization. There are several routes to form chemical bonding between CPs and substrates, depending on the substrate materials. The corresponding agents to different substrate materials are listed in Table 3.1.

3.3.2.2.1 Silanes

Silane coupling agents are widely used because of their unique ability to bond polymers with dissimilar materials such as inorganic oxides (Plueddemann 1991).

The Wrighton group initially anchored pyrrole functionalized silane to the Pt and n-type Si to improve the adhesion of PPy film on the substrate. The effectiveness was demonstrated with a Scotch tape test (Simon et al. 1982). The Locklin group have made considerable efforts in developing the silane functionalized Grignard reagents, to chemically graft CPs to multiple types of substrates (Sontag, Marshall, & Locklin, 2009) (Marshall, Sontag, & Locklin, 2010) (Marshall et al. 2010) (Yang et al., 2012). Carli *et al* synthesized the aminopropyl-triethoxysilane (APTES) substituted EDOT, and bound it the FTO electrodes. The PEDOT coating was then electrochemically deposited to APTES-EDOT. Scotch tape test and sonication test were conducted to confirm the improved adhesion. However, no quantitative values of adhesion were presented in the paper (Carli et al. 2014).

In our group, a silane functionalized adhesion promoter was investigated. The commercialized phenyltriethoxysilane was chosen, purchased from Sigma-Aldrich and

used without further purification. The proposed mechanism for grafting PEDOT (Fig. 3.4) was inspired by the Friedel-Craft reaction which was used to attach substituents to an aromatic ring (Wang et al. 2008). This mechanism has also been previously used in the oxidative chemical vapor deposition to graft PEDOT on substrates (Im et al. 2007).

A sonication test was conducted to confirm the enhanced adhesion. After 5 minutes of sonication, the unmodified PEDOT film lost around 70% percent of the film, while the phenyltriethoxysilane modified PEDOT film only lost around 10% (Figure 3.3).

Other than the electrochemical deposition, the silane agent has also been applied to spin coated PEDOT films to improve their adhesion and stability. Khodagholy et al. described the use of 3-glycidoxypropyltrimethoxysilane (GOPS) to crosslink films of solution cast PEDOT:PSS suspensions. With the crosslinking and adhesion promoting from GOPS, the spun-coated PEDOT:PSS coatings were stable during the short term *in vivo* recordings of brain activity (Khodagholy et al. 2011) (Khodagholy et al. 2013).

3.3.2.2.2 Thiols

The formation of self-assembled monolayers (SAMs) of thiols on inorganic surfaces such as gold and platinum is well known (Bain et al. 1989). The semi-covalent interaction between conjugated monomer functionalized thiol and substrate could be applied to enhance the adhesion of CPs.

Rubinstein *et al* found that polyaniline films electrochemically deposited on SAMs of p-aminothiophenol were denser than those grown on bare gold (Rubinstein et al. 1990). However, no mechanical or adhesion characterization of efficacy was

given. Mekhalif *et al* electrochemically deposited polybithiophene onto platinum through aromatic and aliphatic thiol monolayers (Mekhalif, Lang, & Gamier, 1995), and found that the adhesion of polybithiophene on aromatic thiol modified platinum is much better that that of aliphatic thiol modified one, according to the scotch tape test results. Around the same time, Willicut and McCarley synthesized a series of ω-(*N*-pyrrolyl)alkanethiol monomers as the adhesion promoter. They found that the SAMs would enhance the nucleation, and adhesion of PPy (Willicut & Mccarley 1994) (Willicut & McCarley 1995).

Smela synthesized 1-(2-thiolethyl)pyrrole as an adhesion promoter layer to solve the delamination problem of electrochemically deposited polypyrrole on gold substrates (Smela et al. 1998). However, the electrochemical characterization showed that the adhesion promotion monolayer was not stable during CV scan, irreversible oxidation peaks were observed during the first anodic potential excursion (Smela et al. 1998).

The Locklin group used a thiol functionalized Grignard monomer as the both the adhesion promoter and the initiator of a surface-initiated Kumada-type polycondensation reaction to yield polythiophene and polyphenylene films with thicknesses up to 42 nm on the gold substrate (Sontag et al. 2009). However, no discussion of mechanical properties or adhesion characterization was presented in the paper.

3.3.2.2.3 Acids

Acid groups have long been studied and used to tune the surface properties of metals and metal oxides via chemisorption. Armstrong *et al* has applied ferrocene

dicarboxylic acid and 3-thiophene acetic acid to improve the adhesion of PEDOT film onto ITO electrodes (Armstrong et al. 2003). However, no adhesion characterization was reported in their study. The application of phosphonic acids were carefully studied by Paniagua *et al* to modify the surface of transparent conductive oxides, such as ITO (Paniagua et al. 2008). In their study, the characterization was mainly focused on the device performance, however, no specific information of electrochemical stability or adhesion properties of the films was reported.

Wei *et al* promoted the adhesion between electrochemically deposited PEDOT and ITO substrate (Wei et al., 2015) with an EDOT derivative—EDOT acid, which was designed in our group (Povlich et al., 2013) (Kim et al., 2010).

The EIS results (Fig 3.7.) showed that the electrical properties were not affected much by the first EDOT acid layer modification. The performance of the PEDOT coated electrodes with EDOT acid modification was much better than the bare SS electrodes, and with stronger attachment of PEDOT coating compared to the previous PEDOT coated electrodes. The EDOT-acid only caused a slight increase in the impedance as compared to the pure PEDOT electrode coating. The slight change of impedance spectrum was likely related to the modestly limited charge transport between first layer conducting polymer and SS surface.

The sonication result showed that the PEDOT films on unmodified ITO electrodes could only sustain up to 5 s of sonication, while the EDOT-acid modified PEDOT remained intact after 2 min of sonication. However, while sonication is indeed an aggressive test, it doesn’t really provide detailed insight about the absolute strength of the adhesion. It also doesn’t let you focus on specific failure mechanisms, since the film could fail either by cracking or delamination or both.

3.3.2.2.4 Amines

Electrografting has recently emerged as an effective way to create chemical bonds between organic molecules and conducting solid substrates through electrochemical reactions. Adsorption of amines on metals in order to prevent their corrosion has been developed broadly, but the covalent electrografting that takes place by oxidation can only be observed on materials that withstand oxidative conditions. It was first described on carbon materials and then on Au, Pt, and p-Si (Bélanger & Pinson 2011).

In our group, Ouyang *et al* developed EDOT amine as the adhesion promoter, and expanded the adhesion promotion to inert metallic substrates, such as Au electrodes (Ouyang, 2014). The improvement in adhesion was measured by extended sonication.

3.3.2.2.5 Other agents

Alcohols can be electrografted to carbon under oxidative conditions (Bélanger & Pinson 2011). The electrografting in an acidic (0.1 M H_2SO_4) and also an aqueous LiClO4 solution of 1-octanol was indirectly demonstrated by the observation of reversible anodic peaks during CV scanning. Electrografting vinylics is another way to form strongly adhesive polymer films from anhydrous solutions of vinylic monomers such as acrylonitrile and methyl methacrylate (Palacin et al. 2004).

3.4 Conclusions and future work

All those research and development were inspiring, and have paved the way of further improvement of CPs. However, the durability of CPs is still not enough to break the barriers in the applications. Without the quantitative information of mechanical properties, adhesion, and durability, it is difficult to systematically compare the improvement made by those methods mentioned above, and select the superior ones.

In the following chapters, characterization methods of mechanical properties, adhesion and durability will be established and described in detail.

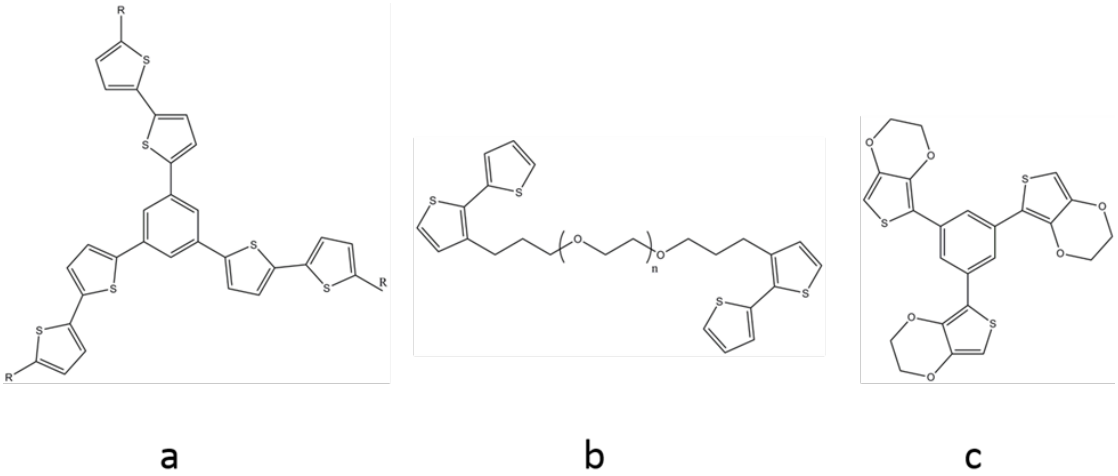

Figure 3.1 The chemical structures of potential crosslinkers: (a) 1,3,5-tris[5- (2,2A-bithienyl)] benzene (Cherioux et al. 1998), (b) bithiophene-oligo(oxyethylene)-bithiophene (Perepichka et al. 2002), (c) 1,3,5-tris[2-(3,4-ethylenedioxy-thienyl)]-benzene (Ouyang et al. 2015)

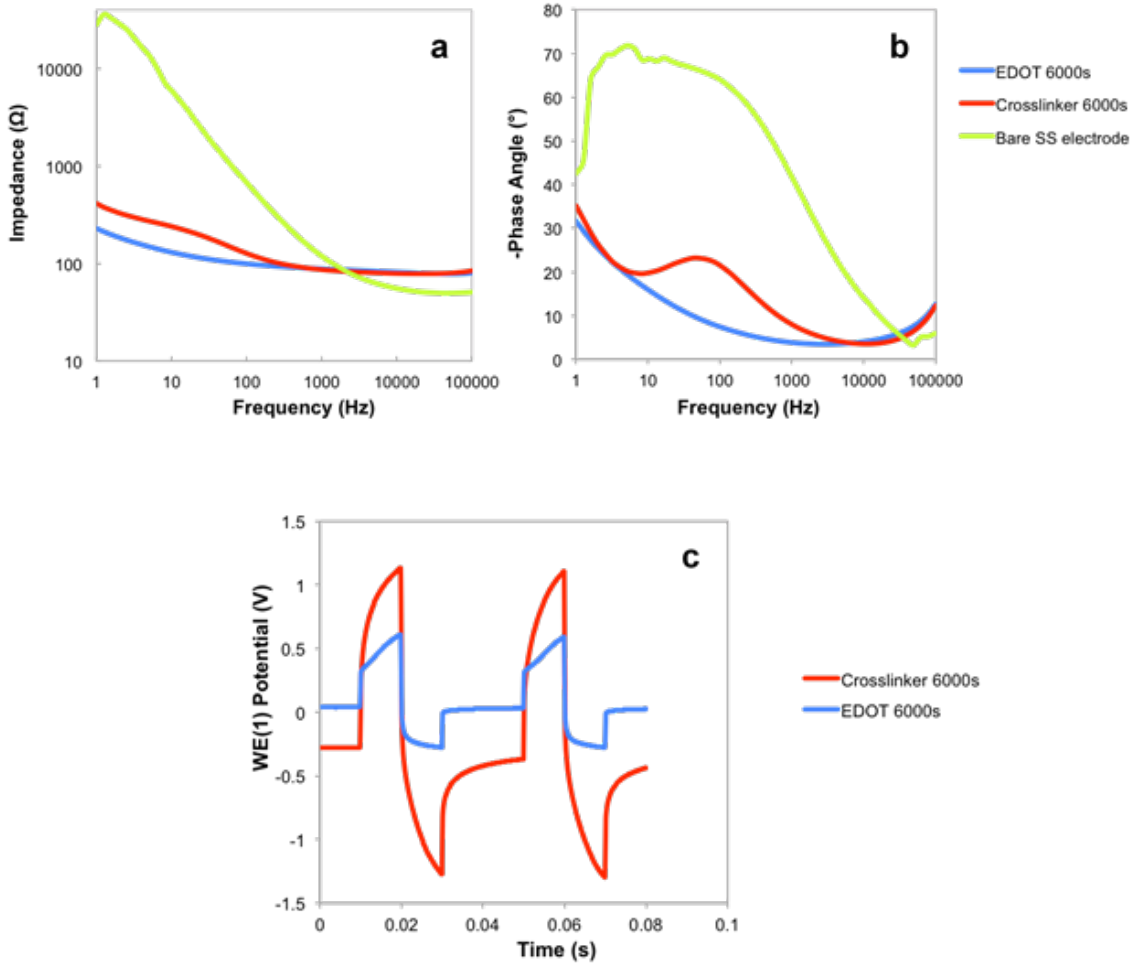

Figure 3.2 (A, B) Impedance and phase angle, (C) biphasic stimulation of PEDOT and 1% EPh crosslinked PEDOT coated electrodes (Ouyang et al, 2015).

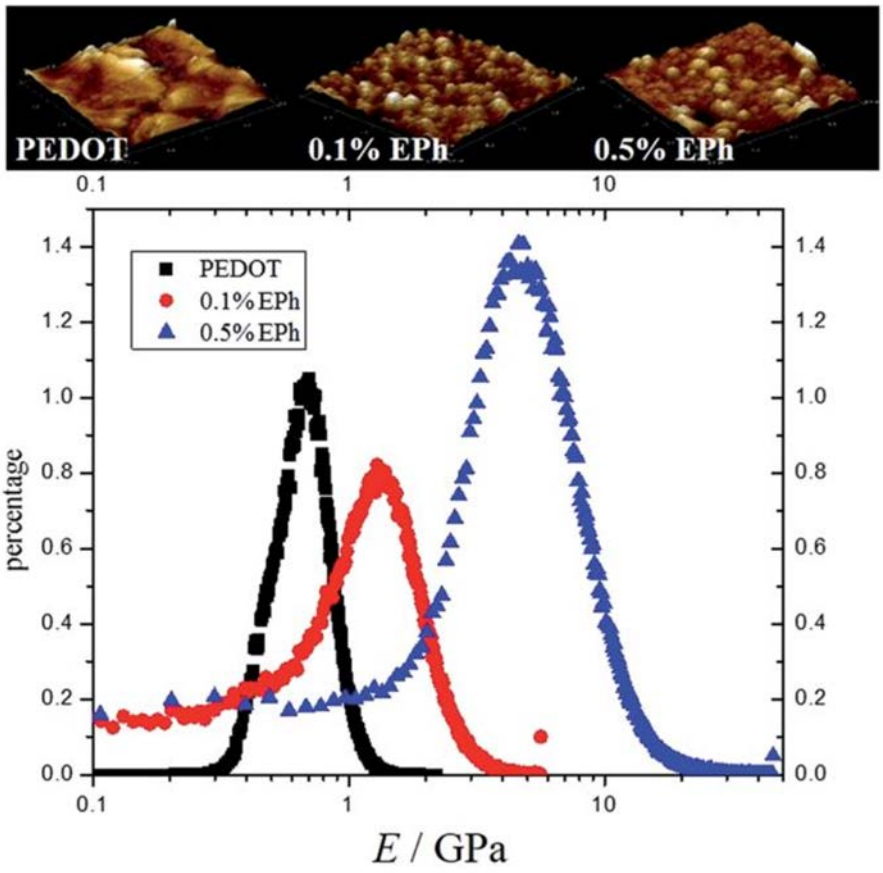

Figure 3.3. AFM QNM modulus distribution. (a) AFM image of the polymer films (2 μm by 2 μm); (b) AFM QNM modulus distribution of PEDOT, 0.1% EPh and 0.5% EPh (Ouyang et al. 2015).

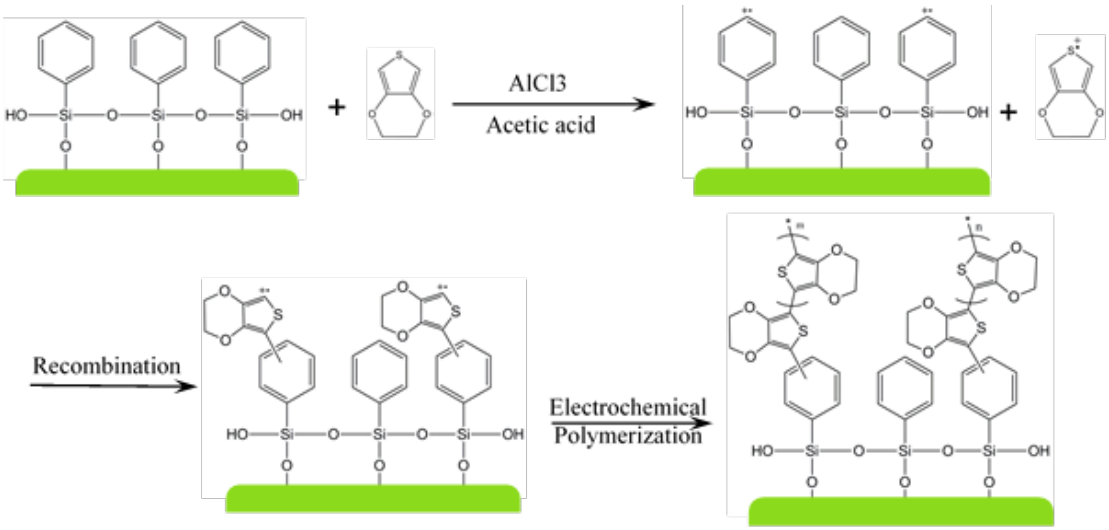

Figure 3.4. Schematic reaction mechanism involved in coupling PEDOT on stainless steel substrate through phenyltriethoxysilane.

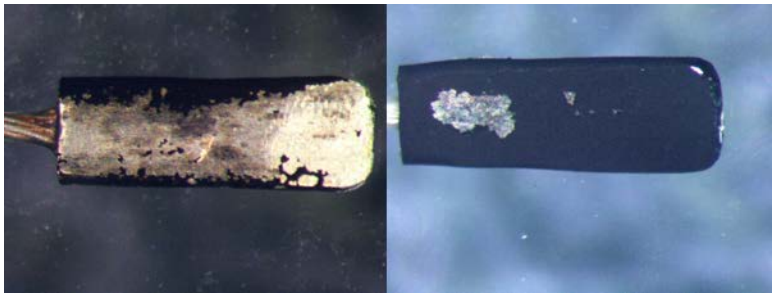

Figure 3.5. (A) PEDOT coated electrode after 5 min sonication, (B) Phenyltriethoxysilane + PEDOT coated electrode after 5min sonication.

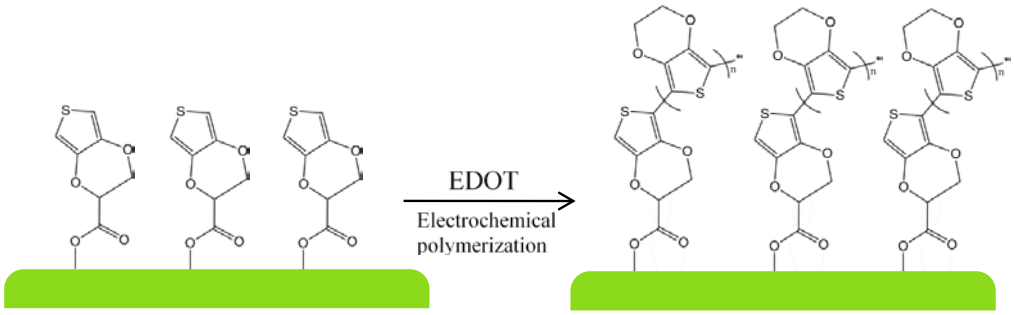

Figure 3.6. Schematic reaction mechanism of bonding EDOT carboxylic acid as the first layer and coat PEDOT on stainless steel substrate.

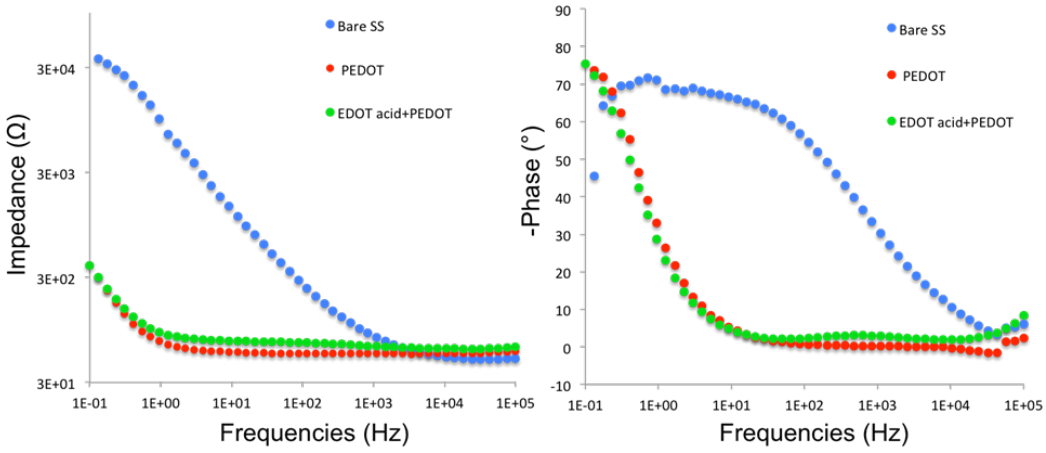

Figure 3.7. Impedance and phase angle spectrum among 0.1Hz-106 Hz frequency range.

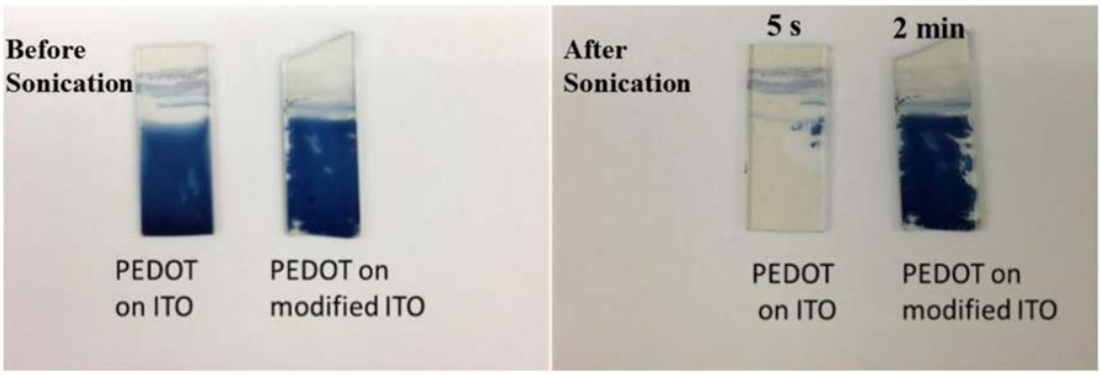

Figure 3.8 Optical images of PEDOT films on ITO and modified ITO before and after ultrasonication adhesion test. PEDOT on ITO was tested for 5 s and PEDOT on modified ITO was tested for 2 min (Wei et al. 2015).

Table 3.1 Effective adhesion promoters on different inorganic substrates

	ITO/IFO	SS	Si	Carbon	Pt	Au
Silanes	●	●	●		●	
Thiols					●	●
Acids	●	●	●			
Amines	●		●		●	●
Alcohols				●		
Vinylics		●	●	●	●	●

REFERENCES

Abidian, M. et al., 2010. Conducting-polymer nanotubes improve electrical properties, mechanical adhesion, neural attachment, and neurite outgrowth of neural electrodes. *Small*, 6(3), pp.421–9.

Alvi, F. et al., 2011. Graphene–polyethylenedioxythiophene conducting polymer nanocomposite based supercapacitor. *Electrochimica Acta*, 56(25), pp.9406–9412.

Armstrong, N.R. et al., 2003. Interface modification of ITO thin films: Organic photovoltaic cells. *Thin Solid Films*, 445(2), pp.342–352.

Asplund, M. et al., 2009. Toxicity evaluation of PEDOT/biomolecular composites intended for neural communication electrodes. *Biomedical materials (Bristol, England)*, 4(4), p.45009.

Baek, S., Green, R.A. & Poole-Warren, L.A., 2014. Effects of dopants on the biomechanical properties of conducting polymer films on platinum electrodes. *Journal of Biomedical Materials Research Part A*, 102(8), pp.2743–2754.

Bain, C.D. et al., 1989. Formation of Monolayer Films By the Spontaneous Assembly of Organic Thiols From Solution Onto Gold. *Journal Of The American Chemical Society*, 111(1), pp.321–335.

Bélanger, D. & Pinson, J., 2011. Electrografting: A powerful method for surface modification. *Chemical Society Reviews*, 40(7), pp.3995–4048.

Carli, S. et al., 2014. Conductive PEDOT Covalently Bound to Transparent FTO Electrodes. *The Journal of Physical Chemistry C*, 118(30), pp.16782–16790.

Castagnola, E. et al., 2014. PEDOT-CNT-coated low-impedance, ultra-flexible, and brain-conformable micro-ECoG arrays. *IEEE Trans Neural Syst Rehabil Eng*, 23(3), pp.342–350.

Chen, G.Z. et al., 2000. Carbon nanotube and polypyrrole composites: coating and doping. *Advanced Materials*, 12(7), pp.522–526.

Chen, H. et al., 2011. Multilayered polypyrrole-coated carbon nanotubes to improve functional stability and electrical properties of neural electrodes. *Journal of Physical Chemistry C*, 115(13), pp.5492–5499.

Chen, S. et al., 2013. PEDOT/MWCNT composite film coated microelectrode arrays for neural interface improvement. *Sensors and Actuators, A: Physical*, 193, pp.141–148.

Cherioux, F., Guyard, L. & Audebert, P., 1998. Synthesis and electrochemical properties of new star-shaped thiophene oligomers and their polymers. *Chemical Communications*, (20), pp.2225–2226.

Cui, X. & Martin, D.C., 2003. Fuzzy gold electrodes for lowering impedance and improving adhesion with electrodeposited conducting polymer films. *Sensors and Actuators, A: Physical*, 103(3), pp.384–394.

Cui, X. & Zhou, D., 2007. Poly (3,4-Ethylenedioxythiophene) for Chronic Neural Stimulation. *IEEE Transactions on Neural Systems and Rehabilitation Engineering*, 15(4), pp.502–508.

Gerwig, R. et al., 2012. PEDOT–CNT Composite Microelectrodes for Recording and Electrostimulation Applications: Fabrication, Morphology, and Electrical Properties. *Frontiers in Neuroengineering*, 5, p.8.

Ghosh, S. & Inganäs, O., 1999a. Conducting Polymer Haydrogels as 3D electrodes: Application for Supercapacitors. *Advanced Materials Communications*, 11(14), pp.1214–1218.

Ghosh, S. & Inganäs, O., 1999b. Self-assembly of a conducting polymer nanostructure by physical crosslinking: applications to conducting blends and modified electrodes. *Synthetic Metals*, 101, pp.413–416.

Green, R. et al., 2008. Conducting polymers for neural interfaces: challenges in developing an effective long-term implant. *Biomaterials*, 29(24–25), pp.3393–9.

Green, R. et al., 2013. Performance of conducting polymer electrodes for stimulating neuroprosthetics. *Journal of neural engineering*, 10, p.16009.

Green, R.A. et al., 2008. Novel neural interface for implant electrodes: improving electroactivity of polypyrrole through MWNT incorporation. *Journal of Materials Science: Materials in Medicine*, 19(4), pp.1625–1629.

Green, R. a. et al., 2012. Substrate dependent stability of conducting polymer coatings on medical electrodes. *Biomaterials*, 33(25), pp.5875–5886. Available at: http://dx.doi.org/10.1016/j.biomaterials.2012.05.017.

Huang, Z. et al., 1997. Selective Deposition of Conducting Polymers on Hydroxyl-Terminated Surfaces with Printed Monolayers of Alkylsiloxanes as Templates. *Langmuir*, 7463(12), pp.6480–6484. Available at: http://pubs.acs.org/doi/abs/10.1021/la970537z [Accessed August 1, 2016].

Idzik, K. et al., 2010. Electrochemical and spectral properties of meta-linked 1,3,5-tris(aryl)benzenes and 2,4,6-tris(aryl)-1-phenoles, and their polymers. *Electrochimica Acta*, 55(24), pp.7419–7426.

Im, S.G. et al., 2007. Grafted Conducting Polymer Films for Nano-patterning onto Various Organic and Inorganic Substrates by Oxidative Chemical Vapor Deposition. *Advanced Materials*, 19(19), pp.2863–2867.

Jimison, L.H. et al., 2012. PEDOT:TOS with PEG: a biofunctional surface with improved electronic characteristics. *Journal of Materials Chemistry*, 22(37), p.19498.

Khodagholy, D. et al., 2011. Highly conformable conducting polymer electrodes for in vivo recordings. *Advanced Materials*, 23(36), pp.268–272.

Khodagholy, D. et al., 2013. In vivo recordings of brain activity using organic transistors. *Nature Communications*, 4, p.1575.

Kolarcik, C.L. et al., 2015. Elastomeric and soft conducting microwires for implantable neural interfaces. *Soft Matter*.

Köse, M. & Mitchell, W., 2007. Theoretical studies on conjugated phenyl-cored thiophene dendrimers for photovoltaic applications. *Journal of the American Chemical Society*, (9), pp.14257–14270.

Kozai, T.D.Y. et al., 2015. Mechanical failure modes of chronically implanted planar silicon-based neural probes for laminar recording. *Biomaterials*, 37, pp.25–39.

Kung, T. et al., 2014. Regenerative peripheral nerve interface viability and signal transduction with an implanted electrode. *Plastic and reconstructive surgery*, 133(6), pp.1380–94.

Kung, T.A. et al., 2013. Implanted electrode with conductive polymer augments signal transduction from the regenerative neuregulin-1 / erbb2 signaling regulates early axonal regeneration. *Plastic and Reconstructive Surgery*, 131(5), p.58.

Lang, U., Naujoks, N. & Dual, J., 2009. Mechanical characterization of PEDOT:PSS thin films. *Synthetic Metals*, 159(5–6), pp.473–479.

Lee, H. et al., 2011. Fabrication of polypyrrole (PPy)/carbon nanotube (CNT) composite electrode on ceramic fabric for supercapacitor applications. *Electrochimica Acta*, 56(22), pp.7460–7466.

Lee, H.-Y. & Qu, J., 2003. Microstructure, adhesion strength and failure path at a polymer /roughened metal interface. *Journal of Adhesion Science and Technology J. Adhesion Sci. Technol*, 17(2), pp.195–215.

Li, P., Sun, K. & Ouyang, J., 2015. Stretchable and Conductive Polymer Films Prepared by Solution Blending. *ACS Applied Materials and Interfaces*, 7(33), pp.18415–18423.

Lu, Y. et al., 2010. Electrodeposited polypyrrole/carbon nanotubes composite films electrodes for neural interfaces. *Biomaterials*, 31(19), pp.5169–81.

Luo, X. et al., 2011. Highly stable carbon nanotube doped poly(3,4-ethylenedioxythiophene) for chronic neural stimulation. *Biomaterials*, 32(24), pp.5551–5557.

Marshall, N., Sontag, S.K. & Locklin, J., 2010. Substituted poly(p-phenylene) thin films via Surface-Initiated Kumada-Type catalyst transfer polycondensation. *Macromolecules*, 43(5), pp.2137–2144.

Mousavi, Z. et al., 2009. Poly(3,4-ethylenedioxythiophene) (PEDOT) doped with carbon nanotubes as ion-to-electron transducer in polymer membrane-based potassium ion-selective electrodes. *Journal of Electroanalytical Chemistry*, 633(1), pp.246–252.

Mueller, M. et al., 2012. Vacuum vapour phase polymerization of high conductivity PEDOT: Role of PEG-PPG-PEG, the origin of water, and choice of oxidant. *Polymer*, 53(11), pp.2146–2151.

Österholm, A.M. et al., 2016. Solution Processed PEDOT Analogues in Electrochemical Supercapacitors. *ACS Applied Materials & Interfaces*, 8(21), pp.13492–13498..

Ouyang, L., Kuo, C., Farrell, B., Pathak, S., Wei, B., Qu, J. & Martin, D., 2015. Poly[3,4-ethylene dioxythiophene (EDOT)-co-1,3,5-tri[2-(3,4-ethylene dioxythienyl)]-benzene (EPh)] copolymers (PEDOT-co-EPh): optical, electrochemical and mechanical properties. *J. Mater. Chem. B*, 0, pp.1–11.

Ouyang, L., Kuo, C., Farrell, B., Pathak, S., Wei, B., Qu, J. & Martin, D.C., 2015. Poly[3,4-ethylene dioxythiophene (EDOT)-co-1,3,5-tri[2-(3,4-ethylene dioxythienyl)]-benzene (EPh)] copolymers (PEDOT-co-EPh): optical, electrochemical and mechanical properties. *J. Mater. Chem. B*, 0, pp.1–11.

Palacin, S. et al., 2004. Molecule-to-metal bonds: Electrografting polymers on conducting surfaces. *ChemPhysChem*, 5(10), pp.1468–1481.

Paniagua, S.A. et al., 2008. Phosphonic Acid Modification of Indium-Tin Oxide Electrodes: Combined XPS/UPS/Contact Angle Studies. *J. Phys. Chem. C*, 112(21), pp.7809–7817.

Perepichka, I.F. et al., 2002. Hydrophilic Oligo (oxyethylene) -Derivatized Optoelectroelectrochemical Properties and Solid-State Chromism. *Chemistry of Materials*, 14(15), pp.449–457.

Plueddemann, E.P., 1991. Nature of Adhesion Through Silane Coupling Agents. In *Silane Coupling Agents*. Boston, MA: Springer US, pp. 115–152.

Ponder, J.F., Österholm, A.M. & Reynolds, J.R., 2016. Designing a Soluble PEDOT Analogue without Surfactants or Dispersants. *Macromolecules*, 49(6), pp.2106–2111.

Qu, J. et al., 2015. Stiffness, strength and adhesion characterization of electrochemically deposited conjugated polymer films. *Acta Biomaterialia*.

Rubinstein, I. et al., 1990. Morphology Control in Electrochemically Grown Conducting Polymer-Films .1. Precoating the Metal-Substrate with an Organic Monolayer. *Journal of the American Chemical Society*, 112(16), pp.6135–6136.

Samba, R., Herrmann, T. & Zeck, G., 2015. PEDOT-CNT coated electrodes stimulate retinal neurons at low voltage amplitudes and low charge densities. *Journal of neural engineering*, 12(1), p.16014.

Simon, R., Ricco, A. & Wrighton, M.S., 1982. Synthesis and Characterization of a New Surface Derivatizing Reagent To Promote the Adhesion of Polypyrrole Films to n-Type Silicon Photoanodes: N-(3-(Trimethoxysiyl))pyrrole. *Journal of the American Chemical Society*, 104(c), pp.2031–2034.

Smela, E., Zuccarello, G., et al., 1998. Thiol-Modified Pyrrole Monomers : 1 . Synthesis , Characterization , and Polymerization of 1- (2-Thioethyl) pyrrole and 3- (2-Thioethyl) pyrrole. *American chemical society*, 7463(13), pp.2970–2975.

Smela, E., Kariis, H. & Yang, Z., 1998. Thiol-modified pyrrole monomers: 3. Electrochemistry of 1-(2-thioethyl) pyrrole and 3-(2-thioethyl) pyrrole monolayers in propylene carbonate. *Langmuir*, 7463(20), pp.2984–2995.

Sontag, S.K., Marshall, N. & Locklin, J., 2009. Formation of conjugated polymer brushes by surface-initiated catalyst-transfer polycondensation. *Chemical communications (Cambridge, England)*, (23), pp.3354–6.

Wang, X.-S. et al., 2008. Organocatalyzed Friedel–Craft-type reaction of 2-naphthol with β,γ-unsaturated α-keto ester to form novel optically active naphthopyran derivatives. *Tetrahedron: Asymmetry*, 19(23), pp.2699–2704.

Wei, B. et al., 2015. Significant Enhancement of PEDOT Thin Film Adhesion to Inorganic Solid Substrates with EDOT-Acid. *ACS applied materials & interfaces*, 7(28), pp.15388–94.

Willicut, R. & McCarley, R., 1995. Electrochemically polymerizable self-□assembled monolayers. *Advanced Materials*, 7(8), pp.759–762.

Willicut, R.J. & Mccarley, R.L., 1994. Electrochemical polymerization of pyrrole containing self-assembled alkanethiol monolayers on Au. *Journal of the American Chemical Society*, 116(1 1), pp.10823–10824.

Xu, Y. et al., 2009. A hybrid material of graphene and poly (3,4-ethyldioxythiophene) with high conductivity, flexibility, and transparency. *Nano Research*, 2(4), pp.343–348.

Zhang, J. & Zhao, X.S., 2012. Conducting polymers directly coated on reduced graphene oxide sheets as high-performance supercapacitor electrodes. *Journal of Physical Chemistry C*, 116(9), pp.5420–5426.

Zhang, X. et al., 2004. Surfactant-directed polypyrrole/CNT nanocables: Synthesis, characterization, and enhanced electrical properties. *ChemPhysChem*, 5(7), pp.998–1002.

Zhu, S. & Swager, T., 1997. Conducting polymetallorotaxanes: metal ion mediated enhancements in conductivity and charge localization. *Journal of the American Chemical Society*, 7863(C), pp.12568–12577.

Chapter 4

STIFFNESS, STRENGTH AND ADHESION CHARACTERIZATION OF ELECTROCHEMICALLY DEPOSITED PEDOT FILMS

This chapter is adapted from the following publication: J. Qu, L. Ouyang, C. Kuo, D. Martin. "Stiffness, Strength and Adhesion Characterization of Electrochemically Deposited Conjugated Polymer Films". *Acta Biomaterialia*, 2016. 31, 114-121.

4.1 Introduction

Conjugated polymers (CPs) such as poly(3,4-ethylenedioxythiophene) (PEDOT) are both ionic and electronic conductors, and are of particular interest for applications such as organic electronics, biosensors, and biointerfacing materials (Cui et al. 2001)(Cui & Martin 2003)(Abidian & Martin 2008)(Green et al. 2008)(Abidian et al. 2009)(Lee et al. 2010)(Rivnay et al. 2014)(Lanzani 2014). CP coatings create high surface area, low impedance interfaces between neural tissue and metal electrodes (Cogan 2008). CP-coated neural electrodes have been shown to be more effective than bare metal electrodes in both short term and long-term animal studies (Kung et al. 2013) (Kung et al. 2014). These organic materials can also be chemically modified to realize specific biological functions (Zhu et al. 2014). However, the internal cracking of CP coatings deposited on metallic electrodes has been observed (Cui & Zhou 2007) (Green et al. 2013)(Zhou et al. 2010). Failures due to delamination and cracking of PEDOT coated onto stainless steel pad electrodes were also observed in animal tests after extended implantations in-vivo (Kung et al. 2014).

4.1.1 Mechanical properties and failure of CP coatings in neural interface applications

Although the stiffness of spun-cast (Okuzaki & Ishihara 2003) (Lang et al. 2009) and electrochemically deposited (Baek et al. 2014) (Yang & Martin 2006) PEDOT films have been previously examined, there is little information available about their intrinsic strength and adhesion to solid substrates. There is a therefore a need to design testing platforms and methods to reliably and accurately measure the mechanical properties and estimate the durability of CP coatings. PEDOT failures were observed after 14 days of pulse stimulation(Zhou et al. 2010). CP coating failures were also discovered just after the ethylene oxide (ETO) sterilization, even before any neural stimulation. In a recent study of a Regenerative Peripheral Nerve Interface (RPNI), PEDOT-coated stainless steel electrodes were examined after 7-months of *in-vivo* testing (Kung et al. 2014) with both optical and scanning electron microscopy. The PEDOT films showed evidence for both delamination from the metal substrate and internal cracking (Fig. 4.1). These results show that there is a need to improve both the adhesion of PEDOT to the solid substrates, as well as its intrinsic strength and ductility. It also demonstrates the need for better information about the mechanical properties of these coatings for optimizing the durability of candidate materials for long-term *in-vivo* applications.

4.1.2 Mechanical characterization methods for CPs

Previously, the mechanical properties of PEDOT:PSS solution cast films have been explored. The Young's modulus of different PEDOT:PSS forms have been

reported to be between 0.8 to 2.4 GPa (Okuzaki & Ishihara 2003) (Lang et al. 2009). The mechanical properties of electrochemically polymerized PEDOT have rarely been reported, due to the limitations of analytical techniques applicable to such thin films (typically a few microns or less) deposited onto relatively stiff metal electrodes. Commercially available PEDOT (Baytron ® P or Clevios™) is an aqueous dispersion of a PEDOT: poly(styrene sulfonate) (PSS) polyelectrolyte complex. In order to get good dispersions, the polymeric dopant PSS is provided in excess (typically at a 2.5:1 to 6:1 weight ratio versus PEDOT) (Lövenich 2014). The doping of electrochemically polymerized PEDOT, on the other hand, is often done with small molecules (such as $LiClO_4$) and at lower effective doping concentrations (Baek et al. 2014). The mechanical properties of electrochemically polymerized PEDOT and solution cast chemically polymerized PEDOT (Baytron® P) are thus expected to be different (Martin et al. 2010).

The experimental difficulty in obtaining large, free-standing electrochemically polymerized PEDOT films makes their mechanical characterization a challenge. Nanoindentation and PeakForce QNM (quantitative nanomechanical property mapping) AFM have both been used to estimate the modulus of electrochemically deposited PEDOT (Baek et al. 2014) (Yang & Martin 2006). The Young's modulus of PEDOT:$LiClO_4$ was reported to be 1.39 ± 0.79 GPa when measured with QNM AFM mode (Baek et al., 2014). However, in this study the reference used to calibrate the tip spring constant was quite soft when compared to the CPs, which may result in an underestimation of the Young's modulus. The fuzzy and porous structure of the PEDOT surface also brings limitations to nanoindentation methods, including irreproducible indentation patterns and large surface noise. Also nanoindentation

methods only provide information about the relatively small-strain elastic response (modulus), whereas the tensile strength, strain to failure, and adhesion to the substrate are also of interest, particularly for long-term durability studies.

Here, we describe methods for measuring the elastic modulus and interfacial shear strength of electrochemically deposited CP coatings on gold-coated soft substrates. PEDOT was electrochemically deposited on gold/palladium-coated hydrocarbon film (Parafilm M®). The thin metallic coating was used to create a conductive surface in order to electrochemically deposit the PEDOT from solution. During the stretching/tensile tests, the cracking behavior of PEDOT and a chemically crosslinked PEDOT derivative (PEDOT-co-EPH) were observed *in-situ* by optical microscopy, providing information about the tensile strength and the interfacial shear strength of PEDOT on the substrate. The cracking phenomena observed in this test are analogous to previous observations of brittle coatings on ductile substrates (Chen et al. 1999)(Chen et al. 2000)(Tang et al. 2001).

The advantages and disadvantages of the applicable mechanical characterization methods are listed in Table 1. Compared to the normal tensile test and indentation methods, our method provides information about crack propagation, cracking density, and interfacial shear strength. Our methods also avoid potential errors induced by the tip selection and characterization in nanoindentation and QNM AFM methods.

4.2 Theory

Since the PEDOT coated hydrocarbon film is a laminar composite, the Voigt model was used to estimate the in-plane Young's modulus (Voigt 1889) (Lim 2009).

This model is based on the assumption that the strain of reinforced layers and the matrix are the same:

$$\in_c = \frac{\sigma_c}{E_c} = \in_s = \frac{\sigma_s}{E_s} = \in_{f1} = \frac{\sigma_{f1}}{E_{f1}} = \in_{f2} = \frac{\sigma_{f2}}{E_{f2}} = \cdots$$

where σ_f, $\in_f$, σ_s, $\in_s$, σ_c, $\in_c$ are the stress and strain of the reinforced layers, the substrate and the whole composite, respectively. As the stress is the force per unit area, a force balance gives:

$$\sigma_c = \sigma_s f_s + \sigma_{f1} f_{f1} + \sigma_{f2} f_{f2} + \sigma_{f3} f_{f3} + \cdots$$

Hence the Young's modulus of the whole composite can be calculated as:

$$E_c = \frac{\sigma_c}{\in_c} = \frac{\sigma_s f_s + \sigma_{f1} f_{f1} + \sigma_{f2} f_{f2} + \sigma_{f3} f_{f3} + \cdots}{\in_c}$$

$$E_c = E_s f_s + E_{f1} f_{f1} + E_{f2} f_{f2} + E_{f3} f_{f3} + \cdots$$

where *f* is the volume fraction of each component, which we assume is equal to the fractional thickness.

According to the Voigt model, we obtain the Young's modulus of the gold coated hydrocarbon film

$$E_{c1} = E_s f_{s1} + E_g f_{g1}$$

and,

$$f_{s1} = \frac{\delta_s}{\delta_s + \delta_g}, \; f_{g1} = \frac{\delta_g}{\delta_s + \delta_g}$$

The Young's modulus of PEDOT coated hydrocarbon film is,

$$E_{c2} = E_s f_{s2} + E_g f_{g2} + E_p f_{p2}$$

The volume fractions of each layer are given by,

$$f_{s2} = \frac{\delta_s}{\delta_s + \delta_g + \delta_p}, f_{g2} = \frac{\delta_g}{\delta_s + \delta_g + \delta_p}, f_{p2} = \frac{\delta_p}{\delta_s + \delta_g + \delta_p}$$

Hence,

$$E_{c2} = E_s \frac{\delta_s}{\delta_s + \delta_g + \delta_p} + E_g \frac{\delta_g}{\delta_s + \delta_g + \delta_p} + E_p \frac{\delta_p}{\delta_s + \delta_g + \delta_p}$$

$$E_{c2} = E_s \frac{\delta_s}{\delta_s + \delta_g} \frac{\delta_s + \delta_g}{\delta_s + \delta_g + \delta_p} + E_g \frac{\delta_g}{\delta_s + \delta_g} \frac{\delta_s + \delta_g}{\delta_s + \delta_g + \delta_p} + E_p \frac{\delta_p}{\delta_s + \delta_g + \delta_p}$$

$$E_{c2} = E_{c1} \left(1 - f_{p2}\right) + E_p f_{p2}$$

where $\delta_s, \delta_g, \delta_p$ are the thickness of the hydrocarbon substrate (~127 microns), gold/palladium thin layer (~10 nm) and CP coating (~500 nm), respectively.

The stress environment (brittle coating on ductile substrate) of the materials examined in this test is analogous to other hard coatings in tribological applications (Bentzon et al. 1995)(Tang et al. 2001). According to the Agrawal and Raj (A-R) model(Agrawal & Raj 1989)(Agrawal & Raj 1990), the maximum interfacial shear stress, τ, that can develop at the interface between the PEDOT coating and the substrate is related to the tensile strength of the PEDOT film, σ, by the following equation:

$$\tau = (\pi \delta \sigma)/\hat{\lambda}$$

where $\sigma = E\varepsilon_f$, ε_f is the strain corresponding to the onset of cracking in the coating; and E and δ are the Young's modulus and thickness of the coating, respectively. $\hat{\lambda}$ is the characteristic crack spacing at the stage where the number of transverse cracks becomes saturated with increasing tensile strain. The value of $\hat{\lambda}$ is determined by the interfacial shear stress between the brittle coating and the more ductile substrate. This model has been previously used to evaluate the adhesion strength of several brittle inorganic (Chen et al. 1999)(Chen et al. 2000) (Nekkanty et al. 2007) and organic (Tang et al. 2001) hard coatings on relatively ductile substrates.

4.3 Experimental procedures

4.3.1 Sample preparation

Soft hydrocarbon films (Parafilm M®, 127 μm thick) were used as the ductile substrate. A gold/palladium (70/30) alloy was sputtered for 4 min on the substrate before the PEDOT deposition. The metal layer was kept as thin as possible so that the films could be electrochemically deposited into uniform films, but the influence of the metal on the overall mechanics could be minimized. The thickness of the gold/palladium ultrathin film was estimated to be only 50 nm by FIB-SEM (Zeiss Auriga™ 60 Crossbeam FIB-SEM) and 35.3 nm by X-ray Reflectivity (Rigaku Ultima IV XRD) (Fig. 4.3, 4.4 and Table 4.1). We therefore assumed that the loads in this layer were negligible relative to the much thicker PEDOT film (300-700 nm) and the hydrocarbon film substrate (127 um). The gold/palladium-coated hydrocarbon film was cut into rectangular shapes with a nominal width of 7 mm. PEDOT and crosslinked PEDOT were electrochemically deposited onto the metal-coated hydrocarbon film.

EDOT monomer, $LiClO_4$ and propylene carbonate (PPC) were used as received from Sigma Aldrich. EPh was synthesized in our lab (Ouyang et al. 2015), based on previously published methods (Idzik et al. 2010). PEDOT and EPh-crosslinked PEDOT were deposited galvanostatically on gold-coated hydrocarbon film (for tensile test) and gold-coated silicon wafers (for QNM AFM test, the gold coating was ~35 nm thick). An electrochemical cell with 1 cm diameter was used for the electrochemical deposition of PEDOT/$LiClO_4$. The gold/palladium coated hydrocarbon film or gold/palladium coated silicon wafer acted as the working electrode and a platinum wire soldered at the bottom of the cell was the counter

electrode. The stock monomer solution contained 0.1 M EDOT and 0.1 M $LiClO_4$ in propylene carbonate (PPC). The monomer solutions for 0.1%, 0.5%, 1%, 5% crosslinked PEDOT respectively contained an additional 0.0001M, 0.0005M, 0.001M, and 0.005M of EPh in PPC.

A constant current of 10 μA was provided by a Metrohm Autolab system, corresponding to a current density of 0.14 $\mu A/mm^2$ (0.014 mA/cm^2). Different deposition times of 2000 s, 3000 s, 4000 s, 5000 s, and 6000 s corresponding to the charge densities of 28.6 mC/cm^2, 42.9 mC/cm^2, 57.1 mC/cm^2, 71.4 mC/cm^2, 85.7 mC/cm^2 were applied to deposit PEDOT films with a range of thicknesses corresponding to ~300 nm to ~700 nm. The thicknesses of the hydrocarbon filmPEDOT and crosslinked PEDOT films were measured by optical microscopy (Nikon) and by scanning electron microscopy (Zeiss Auriga™ 60 Crossbeam FIB-SEM). A current of 10 μA (current density of 64.3 mC/cm^2) was applied to the EPh-crosslinked PEDOT layer deposition, corresponding to a nominal thickness of 500 nm.

4.3.2 Thin film cracking

The PEDOT and EPh-crosslinked PEDOT coated hydrocarbon film tensile specimens were loaded on a Tytron™ 250 mechanical testing apparatus. The specimens were deformed at a strain rate of 0.02 mm/s. The transverse cracking generated in the PEDOT film were recorded during the experiment as a function of sample elongation. These in-situ video observations were acquired using a Nikon stereomicroscope and DinoCapture software. The characteristic crack spacing data was obtained by averaging out the numbers of the cracks counted on 15 separate fields on different samples. All of the tensile tests were conducted at 25°C.

4.3.3 AFM indentation

The Young's modulus was obtained by PeakForce QNM® (quantitative nanomechanical property mapping) mode with Nanoscope Dimension 3100 software on a Bioscope Catalyst (Bruker Nano/ Veeco) AFM, and was calculated following the Derjaguin, Muller and Toporov (DMT) model (Derjaguin et al. 1994). All samples were measured at room temperature in the dry state. A TAP150A probe (with a force constant of ~5 N/m) was used to indent the sample surface to a depth of about 1-2 nm.

4.3.4 Statistical analysis

Data were analyzed and plotted with the Origin 9.1 software. All data points were expressed as the mean ± standard deviation (SD).

4.4 Results and discussion

Firstly, to eliminate the effect of the Au/Pd layer to the test, we observed the morphology of sputtered Au/Pd under FIB-SEM. It was shown that the Au/Pd layer is porous (Fig. 4.3b). The loose stacking of Au/Pd particles and the porous structure resulted the low strength. The low density and lower thickness (compared to the FIB-SEM data) estimated from XRR (Table 4.2, and Fig 4.4) confirms the porous structure of Au/Pd layer. Without the adhesion promoting layer, the adhesion of Au/Pd layer on smooth silicon wafer was weak. The gentle wiping with Kimwipes® took most of the Au/Pd coating away, only tiny islands of gold layer were left on the silicon wafer (Fig. 4.3c), which indicated both weak cohesion and weak adhesion.

Since the Au/Pd layer is so thin and amorphous, it was assumed that the shared stress load in this layer could be neglected. It was further confirmed by the stress-strain curve (Fig 4.5.). It was shown that the yield strain of gold coated Parafilm is around 4%, which is close to bare parafilm (gold layer is too thin and weak to affect the stress-strain curve). The tensile strain of PEDOT is around 2%. That means the rule of mixtures is valid to extract the mechanical properties of PEDOT from the assembly. Since the PEDOT is brittle, the tensile strain is close to yield strain, all the tensile strength of PEDOT and crosslinked PEDOT were calculated following $\sigma = E\,\varepsilon$.

During the early stage of tensile testing, cracks formed in the PEDOT perpendicular to the direction of the applied deformation (Fig 4.6. a, b, c). As the assembly was stretched further, the PEDOT cracking increased. Eventually, the crack density saturated, reaching a maximum value characteristic of a particular sample (Fig 4.6. d, e). The characteristic crack spacing $\hat{\lambda}$ was obtained by measuring the total number of PEDOT cracks along the stretching direction, and dividing this value by the unstretched dimensions of the sample over the field of view.

4.4.1 Validation of thin film cracking

To validate the method, PEDOT coatings of several different thicknesses were tested. The crack spacing of each thickness of PEDOT were counted at least 300 times for each sample (Fig 4.7).

As was the cracking strain, the local strain when the crack saturated was also measured. The crack saturation strain is around 10% -15% (Table 4.3). Each sample was stretched to around 300% strain, which means the cracking was fully saturated

during the stretch process. As shown in Fig. 4.7b, the distributions of the measured PEDOT crack spacings were broader in the thicker PEDOT films. This is consistent with the rougher surface morphology as the deposition times become longer and films become thicker (Fig. 4.7a). If the value of PEDOT film tensile strength and film adhesion are the same for different film thicknesses, then the thickness of PEDOT film and the characteristic crack spacing should have a linear relationship. We extracted the characteristic crack spacing values from the peaks, and plotted them as a function of film thickness (Fig. 4.7b). The data indeed show the anticipated linear relationship between the crack spacing and the thickness (Agrawal & Raj 1989).

The mechanical property values we determined are compiled in Table 4.3. The Young's modulus of electrochemically deposited PEDOT was 2.6 ± 1.4 GPa, the tensile strength was 56 ± 27 MPa, and the interfacial shear strength was 0.7 ± 0.3 MPa. The values of these properties were found to be essentially independent of the film thickness. Our results are in the similar range with the values of the Young's modulus (2.8 ± 0.5 GPa, at 23% relative humidity), tensile strain (~2.5%, at 23% relative humidity) and the tensile strength (53.2 ± 9.5 MPa, at 23% relative humidity) of pipetted Baytron® P film measured by Lang (Lang et al. 2009).

The linear relationship between crack spacing and film thickness of the PEDOT was shown in Fig 4.8. The Young's modulus of films of PEDOT with different thicknesses (Fig 4.8) shows that there was no significant dependence on thickness.

4.4.2 Characterization of enhanced mechanical properties of crosslinked PEDOT

Given the apparent success of our approach, we then used these same techniques to evaluate the mechanical properties of EPh-crosslinked PEDOT.

As shown in Fig. 4.9b, the distribution of 0.1% crosslinked PEDOT crack spacing was the most narrow, which is consistent with the smoother surface morphology seen with 0.1% EPh (Fig. 4.9a). Adding a small amount of EPh crosslinker made the film surface smoother, but above 0.5% the morphology of the film became rougher. The morphology of the films was consistent with the crack spacing distribution, with the smooth films having a more narrow distribution, and the rougher films showing a larger distribution. The mechanical properties of PEDOT and crosslinked PEDOT films extracted from our testing were compiled and are listed in Table 4.4.

The addition of crosslinker didn't affect the cracking strain or the crack saturation strain that much. The tensile strength and interfacial shear strength values as a function of EPh composition are shown graphically in Fig. 4.10. The results show that the Young's modulus, tensile strength and adhesion to the substrate were all significantly improved by adding the EPh crosslinker to the PEDOT. Specifically, the tensile strength of the 5% EPh crosslinked PEDOT increased to around 300 MPa, whereas the non-crosslinked PEDOT had a strength of ~30 MPa. The interfacial shear strength increased from ~0.5 MPa to ~2.5 MPa with the addition of 5% EPh crosslinker.

4.4.3 Comparison with AFM indentation

To corroborate the Young's modulus of PEDOT and crosslinked PEDOT obtained from our method, we also conducted quantitative nanomechanical (QNM) AFM experiments. This test provides estimates of the modulus distribution across the surface of the film over the region examined. The data are shown in Fig. 4.11. We found the average QNM modulus of PEDOT and 0.5% crosslinked PEDOT were around 1.6 GPa and 2.2 GPa respectively. It should be noted that the QNM histograms show reasonably broad distributions that seem to be slightly assymetric toward the higher modulus direction. The values of the modulus are somewhat smaller than the results obtained (2.6 ± 1.4 GPa and 5.1 ± 2.6 GPa) from our method, but are still in a similar range.

4.5 Conclusions

The measurement of the interfacial shear strength of PEDOT films with different thicknesses shows a linear relationship between crack spacing and thickness. The Young's modulus results are similar to those measured with the nanoindentation and QNM AFM mode and the values of solution cast PEDOT:PSS film. The crosslinking of PEDOT with EPh significantly increased the strength, stiffness, and adhesion of the PEDOT films to the underlying substrates. These results support that contention that EPh is a promising component to enhance the durability of PEDOT coating on neural electrodes. Our methods provide a convenient means for evaluating the stiffness, strength, and adhesion of CP films on solid substrates. Information about the failure strength and adhesion of CP coatings to substrates are essential for

estimating their durability in applications, but cannot be obtained by nanoindentation and AFM.

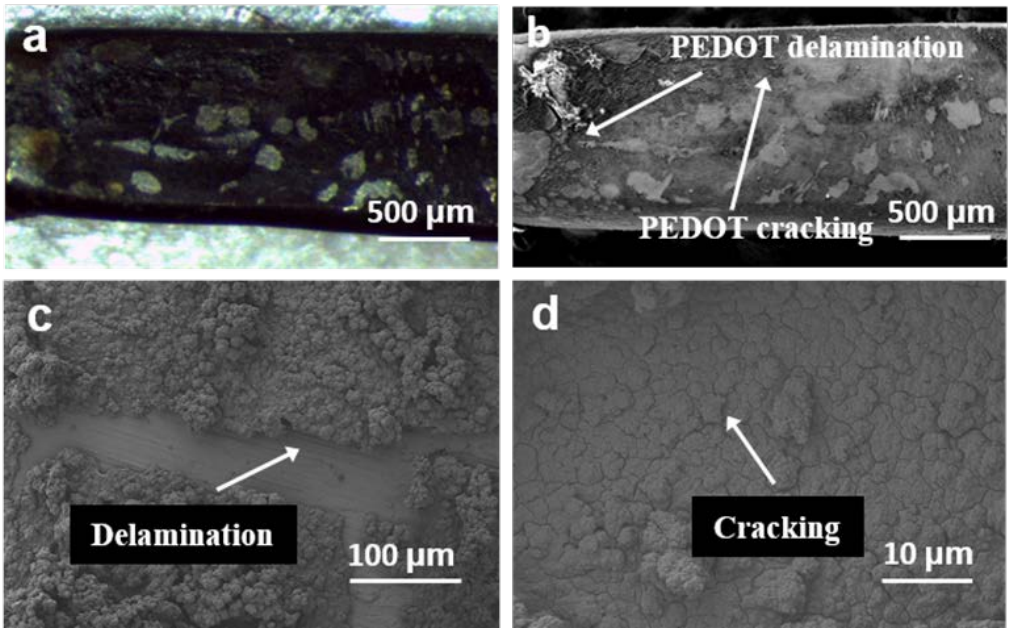

Figure 4.1. Failure modes of CP coatings: (a, b) correlated reflective light optical microscopic and scanning electron microscopic (SEM) images of PEDOT coated neural electrode after 7-month in-vivo test; (c, d) SEM images of PEDOT coated stainless steel RPNI electrode after 7-month in-vivo test.

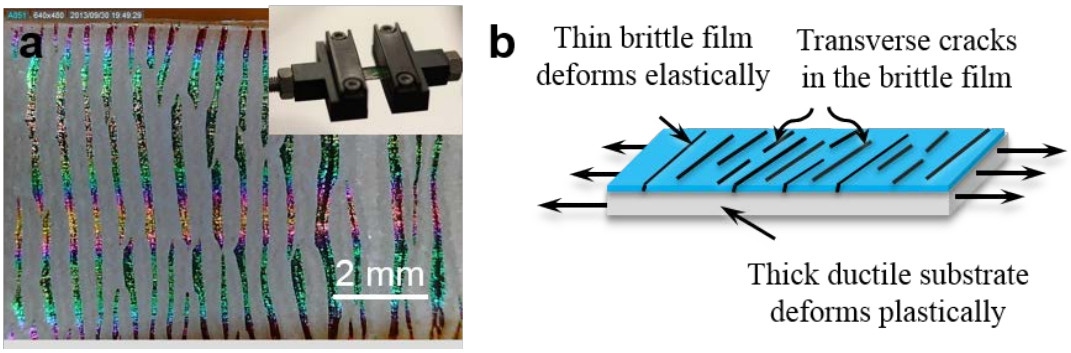

Figure 4.2. (A) Saturated conducting polymer film cracking on hydrocarbon substrate (Parafilm M® with the experiment setup, (B) mechanism of brittle film cracking on ductile substrate.

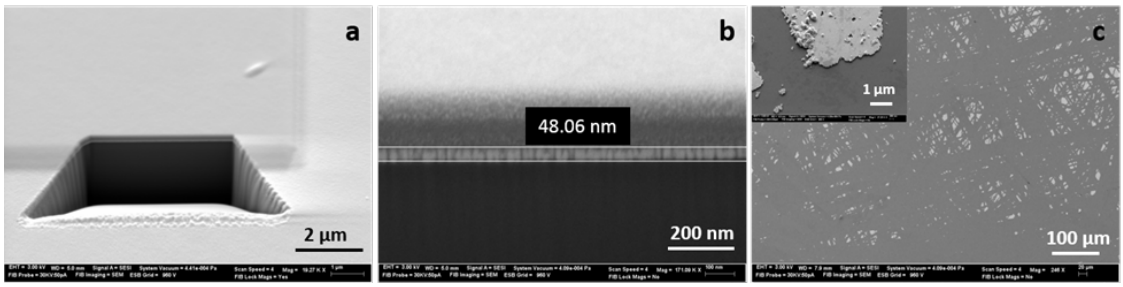

Figure 4.3. (a) Cross-section cut by focused ion beam (FIB) in SEM, (b) cross-section observation and thickness of Au/Pd measurement, (c) surface observation after gentle wiping the sputtered silicon wafer with Kimwipes®.

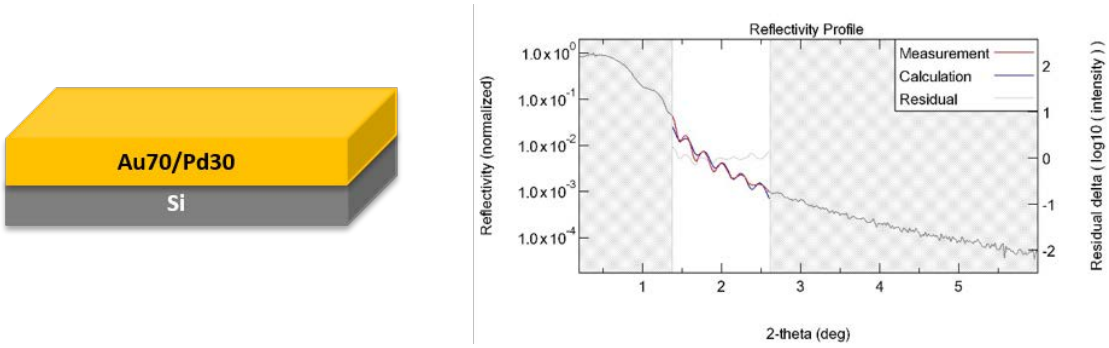

Figure 4.4. X-ray reflectivity (XRR) for 4-min sputtering of gold/palladium.

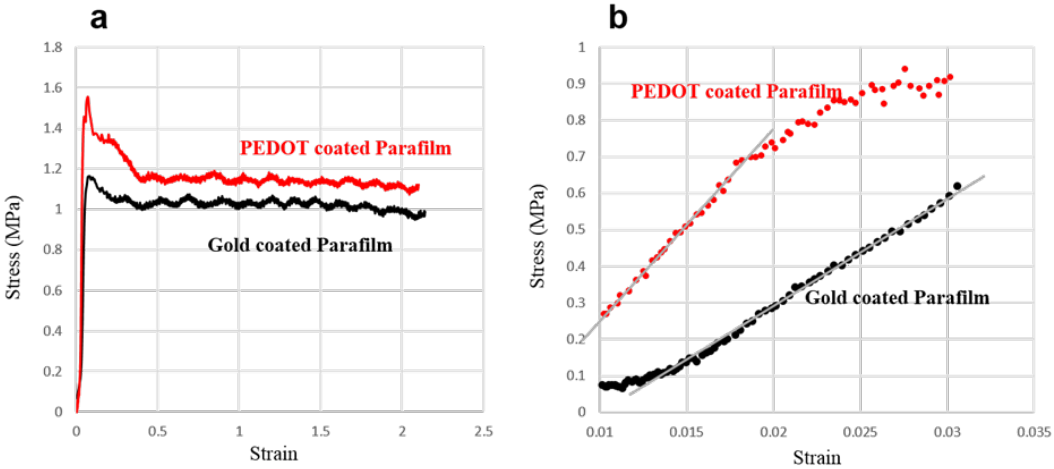

Figure 4.5. (a) Stress-strain curve of PEDOT coated and gold coated Parafilm M®, (b) elastic deformation part of stress strain curve.

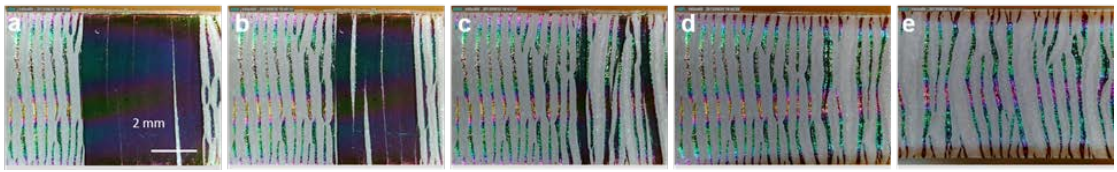

Figure 4.6. In-situ observation of PEDOT cracking behavior.

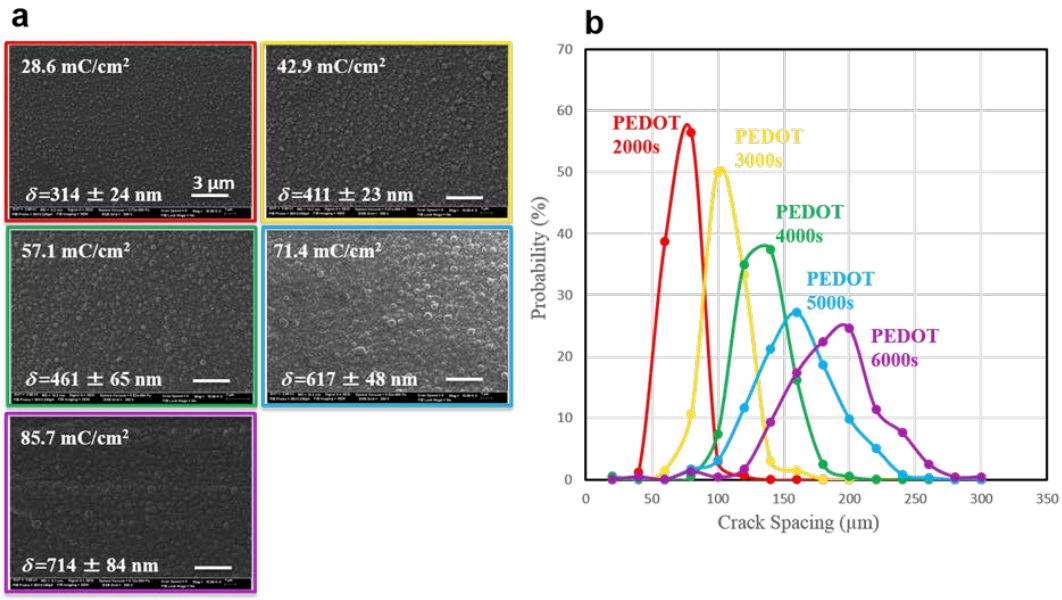

Figure 4.7. (a) PEDOT surface morphology with different deposition times: 2000 s (28.6 mC/cm^2), 3000 s (42.9 mC/cm^2), 4000 s (57.1 mC/cm^2), 5000 s (71.4 mC/cm^2), and 6000 s (85.7 mC/cm^2) (scale bar=3 μm); (b) Statistics of crack spacing of PEDOT with different thickness.

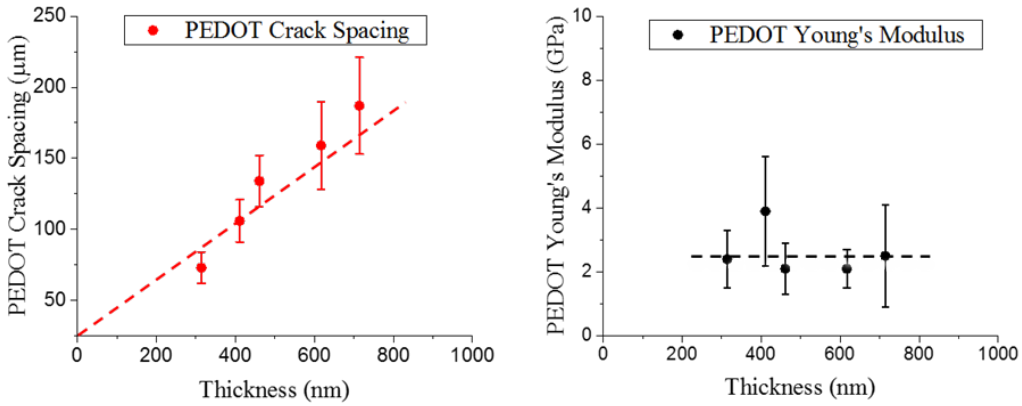

Figure 4.8. Young's modulus and cracking spacing as a function of average film thickness.

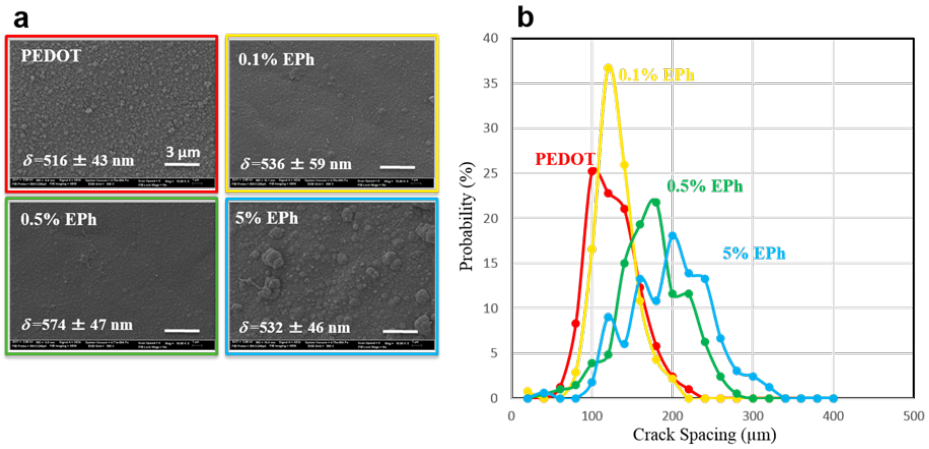

Figure 4.9. (a) The surface morphology of PEDOT and crosslniked PEDOT; (b) Statistics of crack spacing of PEDOT and crosslinked PEDOT.

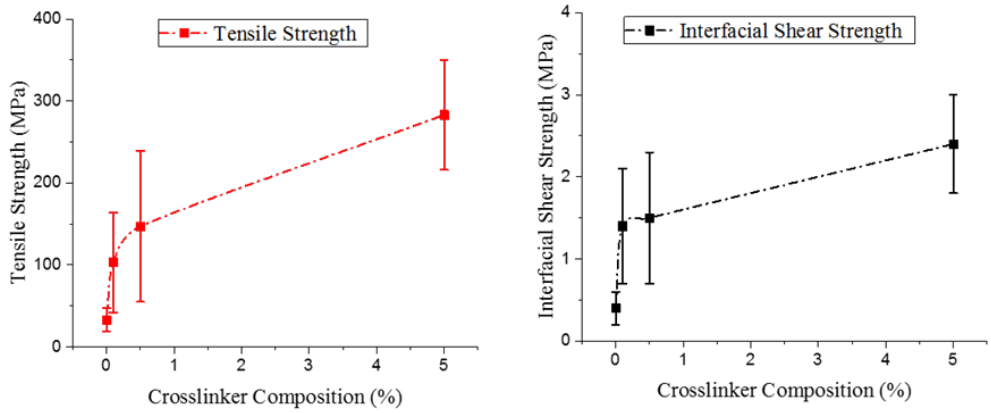

Figure 4.10. The relationship of tensile strength and interfacial shear strength with crosslinker composition.

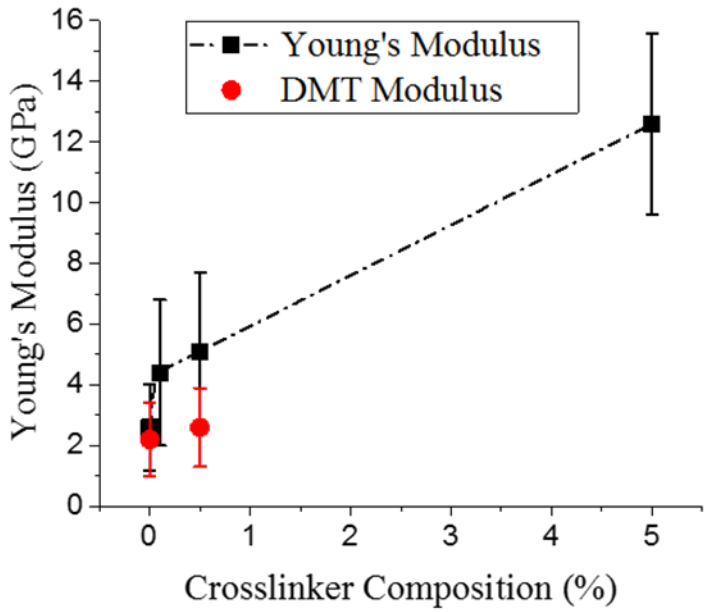

Figure 4.11. The DMT modulus of PEDOT and 0.5% crosslinked PEDOT obtained from AFM comparison with the Young's modulus from our method.

Table 4.1. Comparison of different mechanical characterization methods.

	Tensile Test	**Nanoindentation**	**QNM AFM**	**Thin Film Cracking**
Film type	Chemically polymerized	Chemically & electrochemically polymerized	Chemically & electrochemically polymerized	Chemically & electrochemically polymerized
Mechanical properties	Young's modulus, Tensile strength Tensile strain	Modulus	Modulus	Modulus Tensile strength Tensile strain Interfacial shear strength
Limitations	Not applicable for electrochemically polymerized PEDOT	Value dependency on tip's geometry Irreproducible indentation pattern, Large surface noise	Value dependency on tip's spring constant, Value dependency on calibration method, High cost for AFM tip	Subtler to the electrochemical deposition conditions

Table 4.2. XRR fitting results of Au/Pd coating parameters

Material	Thickness (nm)	Top Density (g/cm^3)	Bottom Density (g/cm^3)
Au/Pd (70/30)	35.3	12.1	5.4

Table 4.3. Mechanical properties of PEDOT with different thickness

Charge density (mC/cm^2)	Crack spacing (μm)	Film thickness (nm)	Cracking strain (%)	Young's Modulus (GPa)	Tensile Strength (MPa)	Effective Interfacial Shear Strength (MPa)
28.6	73 ± 11	314 ± 24	2.4 ± 0.4	2.4 ± 0.9	51 ± 14	0.7 ± 0.2
42.9	106 ± 15	411 ± 23	1.9 ± 0.2	3.9 ± 1.7	76 ± 28	0.9 ± 0.3
57.1	134 ± 18	461 ± 65	2.2 ± 0.1	2.1 ± 0.8	43 ± 16	0.5 ± 0.2
64.3	126 ± 31	516 ± 43	2.1 ± 0.3	2.6 ± 1.4	56 ± 27	0.7 ± 0.3
71.4	159 ± 31	617 ± 48	2.1 ± 0.4	2.1 ± 0.6	40 ± 7	0.5 ± 0.1
85.7	187 ± 34	714 ± 84	2.3 ± 0.5	2.5 ± 1.6	64 ± 38	0.8 ± 0.5

REFERENCES

Abidian, M.R. et al., 2009. Interfacing Conducting Polymer Nanotubes with the Central Nervous System: Chronic Neural Recording using Poly(3,4-ethylenedioxythiophene) Nanotubes. *Advanced Materials*, 21(37), pp.3764–3770.

Abidian, M.R. & Martin, D.C., 2008. Experimental and theoretical characterization of implantable neural microelectrodes modified with conducting polymer nanotubes. *Biomaterials*, 29(9), pp.1273–83.

Agrawal, D. & Raj, R., 1989. Measurement of the ultimate shear strength of a metal-ceramic interface. *Acta Metallurgica*, 37(4), pp.1265–1270.

Agrawal, D. & Raj, R., 1990. Ultimate shear strengths of copper-silica and nickel-silica interfaces. *Materials Science and Engineering: A*, 126, pp.125–131.

Baek, S., Green, R.A. & Poole-Warren, L.A., 2014. Effects of dopants on the biomechanical properties of conducting polymer films on platinum electrodes. *Journal of Biomedical Materials Research Part A*, 102(8), pp.2743–2754.

Bentzon, M., Barholm-Hansen, C. & Hansen, J., 1995. Interfacial shear strength of diamond-like metals carbon coatings deposited on. *Diamond and Related Materials*, 4, pp.787–790.

Chen, B. et al., 2000. A tensile-film-cracking model for evaluating interfacial shear strength of elastic film on ductile substrate. *Surface and Coatings Technology*, 126, pp.91–95.

Chen, B. et al., 1999. In situ observation of the cracking behavior of TiN coating on 304 stainless steel subjected to tensile strain. *Thin Solid Films*, 352, pp.173–178.

Cogan, S.F., 2008. Neural stimulation and recording electrodes. *Annual Review of Biomedical Engineering*, 10, pp.275–309.

Cui, X. et al., 2001. Electrochemical deposition and characterization of conducting polymer polypyrrole/PSS on multichannel neural probes. *Sensors and Actuators A: Physical*, 93(1), pp.8–18.

Cui, X. & Martin, D.C., 2003. Electrochemical deposition and characterization of poly(3,4-ethylenedioxythiophene) on neural microelectrode arrays. *Sensors and Actuators B: Chemical*, 89(1-2), pp.92–102.

Cui, X. & Zhou, D., 2007. Poly (3,4-Ethylenedioxythiophene) for Chronic Neural Stimulation. *IEEE Transactions on Neural Systems and Rehabilitation Engineering*, 15(4), pp.502–508.

Derjaguin, B., Muller, V. & Toporov, Y., 1994. Effect of contact deformations on the adhesion of particles. *Progress in Surface Science*, 45(2), pp.131–143.

Green, R. et al., 2008. Conducting polymers for neural interfaces: challenges in developing an effective long-term implant. *Biomaterials*, 29(24-25), pp.3393–9.

Green, R. et al., 2013. Performance of conducting polymer electrodes for stimulating neuroprosthetics. *Journal of neural engineering*, 10, p.016009.

Idzik, K. et al., 2010. Electrochemical and spectral properties of meta-linked 1,3,5-tris(aryl)benzenes and 2,4,6-tris(aryl)-1-phenoles, and their polymers. *Electrochimica Acta*, 55(24), pp.7419–7426.

Kung, T. et al., 2014. Regenerative peripheral nerve interface viability and signal transduction with an implanted electrode. *Plastic and reconstructive surgery*, 133(6), pp.1380–94.

Kung, T.A. et al., 2013. Implanted electrode with conductive polymer augments signal transduction from the regenerative neuregulin-1 / erbb2 signaling regulates early axonal regeneration. *Plastic and Reconstructive Surgery*, 131(5), p.58.

Lang, U., Naujoks, N. & Dual, J., 2009. Mechanical characterization of PEDOT:PSS thin films. *Synthetic Metals*, 159(5-6), pp.473–479.

Lanzani, G., 2014. Materials for bioelectronics: Organic electronics meets biology. *Nature materials*, 13(8), pp.775–776.

Lee, K., Povlich, L. & Kim, J., 2010. Recent advances in fluorescent and colorimetric conjugated polymer-based biosensors. *The Analyst*, 135(9), pp.2179–89.

Lim, T., 2009. Out-of-plane modulus of semi-auxetic laminates. *European Journal of Mechanics, A/Solids*, 28(4), pp.752–756. Available at: http://dx.doi.org/10.1016/j.euromechsol.2009.02.001.

Lövenich, W., 2014. PEDOT-properties and applications. *Polymer Science Series C*, 56(1), pp.135–143.

Martin, D.C. et al., 2010. The Morphology of Poly(3,4-Ethylenedioxythiophene). *Polymer Reviews*, 50, pp.340–384.

Nekkanty, S., Walter, M. & Shivpuri, R., 2007. A cohesive zone finite element approach to model tensile cracks in thin film coatings. *Journal of Mechanics of Materials and Structure*, 2(7), pp.1231–1247.

Okuzaki, H. & Ishihara, M., 2003. Spinning and Characterization of Conducting Microfibers. *Macromolecular Rapid Communications*, 24(3), pp.261–264.

Ouyang, L. et al., 2015. Poly[3,4-ethylene dioxythiophene (EDOT)-co-1,3,5-tri[2-(3,4-ethylene dioxythienyl)]-benzene (EPh)] copolymers (PEDOT-co-EPh): optical, electrochemical and mechanical properties. *J. Mater. Chem. B*, 00, pp.1–11.

Rivnay, J., Owens, R.M. & Malliaras, G.G., 2014. The rise of organic bioelectronics. *Chemistry of Materials*, 26, pp.679–685.

Tang, H., Foran, B. & Martin, D., 2001. Quantitative measurement of adhesion between polypropylene blends and paints by tensile mechanical testing. *Polymer Engineering & Science*, 41(3), pp.440–448.

Voigt, W., 1889. Ueber die Beziehung zwischen den beiden Elasticitätsconstanten isotroper Körper. *Annalen der Physik*, 274(12), pp.573–587.

Yang, J. & Martin, D., 2006. Impedance spectroscopy and nanoindentation of conducting poly (3, 4-ethylenedioxythiophene) coatings on microfabricated neural prosthetic devices. *Journal of Materials Research*, 21(5), pp.1124–1132.

Zhou, D.D. et al., 2010. *Implantable neural prostheses 2* D. Zhou & E. Greenbaum, eds., New York, NY: Springer New York.

Zhu, B. et al., 2014. Large enhancement in neurite outgrowth on a cell membrane-mimicking conducting polymer. *Nature communications*, 5(May), p.4523.

Chapter 5

ESTABLISHING SYSTEMATIC DURABILITY TESTS FOR CONJUGATED POLYMER THIN FILMS AS BIOMEDICAL INTERFACING MATERIALS

5.1 Introduction

Biomedical electrodes, such as neural electrodes (Cui et al. 2003) (Luo et al. 2011)(Kung et al. 2014), cardiac electrodes (Xu et al. 2015), and epidermal electrodes (Lipomi et al. 2011)(Ying et al. 2012), have become powerful tools for the investigation and treatment of target tissues and organs (Cogan 2008)(Donoghue 2008)(Viventi et al. 2011)(Viventi et al. 2010). They have great potential for permanently improving the quality of life for patients. However, there remain problems with the long-term performance of biomedical electrodes implanted in soft tissues. The signals recorded by these electrodes typically degrade over time, which eventually leads to electrode failure (Barrese et al. 2013)(Kozai et al. 2015).

Biomedical electrode failures normally take place in one of three stages: defects in the electrode at the pre-implantation stage; biological injury and electrode damage during the surgical period; and finally immune response, biological tissue degradation, and electrode materials failure at the post-implantation stage (Barrese et al. 2013)(Barrese et al. 2016). The failure mechanisms of implanted electrodes are thought to be related to a complex combination of the biological reactive tissue responses and material failures of the device (Kozai et al. 2015). The factors leading to failure can themselves be considered in three categories: electrode (material

properties, manufacture techniques), animal (health condition, immune response), and operation (transportation, surgical techniques, injuries) factors. It is thought that material properties dominate the electrode failure, affect the immune response of animals, and determine whether the transportation and surgery go on smoothly.

Hard, inorganic, metallic and semiconducting neural electrodes have been developed by the neuroscience pioneers since the late 19th century. However, the insulating scar and cell degradation caused by the immune response are closely related to the huge mechanical mismatch between the hard materials and soft tissues (Lee et al. 2005)(Subbaroyan et al. 2005). At the same time, as electron or hole conductors, metallic and semiconducting materials are not efficient and capacitive enough for biosignal transfer. The search for more biocompatible, conductive, and durable electrode materials is therefore a topic of continuing interest. In recent years, conjugated polymers with stable backbones, such as poly (3,4-ethylenedioxythiophene) (PEDOT) have emerged, which quickly became of interest as an electrode coating. Taking PEDOT as an example, the impedances at biologically significant frequencies (1-1000 Hz) are substantially lower, and charge storage capacities are larger than ITO (Nyberg et al. 2007), IrOx (Wilks et al. 2009), gold (Leleux et al. 2014), or Pt (Venkatraman et al. 2011). This means conjugated polymer coated biomedical electrodes are more sensitive, accurate and safer. With lower stiffness (Lang et al. 2009)(Qu et al. 2015) and non-cytotoxicity (del Valle et al. 2007)(Kim et al. 2007), conjugated polymer coatings are regarded as a promising material for interfacing hard, inorganic materials with soft, organic tissues.

Despite the extent of current interest, perhaps the weakest aspect of conjugated polymer coatings during applications is their relatively poor durability. The durability

of the interfacing materials is affected by the external environment and internal material properties. In our case, the external shear stress, repeated charge injection, and corrosion from the electrolytes are the prime environmental factors. Material failures may happen when the mechanical properties, adhesion to the substrate, electrochemical and chemical stability are not enough.

Most previous failure analysis studies have focused on the biological reactive tissue response during *in vivo* tests, which has provided valuable information of the interaction between materials and tissues (Barrese et al. 2013)(Prasad et al. 2012)(Gilgunn et al. 2013)(Sridharan et al. 2013)(Prasad et al. 2014). A few studies have applied finite-element analysis (FEA) to simulate the shear stress and help predict the material failure (Subbaroyan et al. 2005) (Lee et al. 2005) (Kozai et al. 2015). However, relatively few investigations have examined the gap between modeling and *in vivo* testing, let alone critically correlate the adhesion, mechanical and electrochemical properties with the durability of materials. Testing at the pre-implantation stage would likely save much time and money before starting detailed animal studies. However, this requires methods that provide quantitative information about performance, and accurate simulation aspects of the environment that will occur in vivo.

In this chapter, we measured the adhesion of PEDOT coating on metallic substrates, and correlated film durability with the adhesion by introducing a tribology test. It was found that these tests could provide useful information for systematically comparing the performance of and selecting the premium materials.

5.2 Experimental procedures

5.2.1 Materials

3,4- ethylenedioxythiophene (EDOT), tetrabutyl ammonium perchlorate (TBAP), and 2,3-dihydrothieno-(3,4-b)(1,4)- dioxine-2-carboxylic acid (EDOT-acid) were purchased from Tractus Chemicals. All other chemicals were of analytical grade. Deionized water was from a Millipore Q water purification system. All reagents and solvents were used without further purification, unless otherwise noted. ITO-coated glass slides were purchased from Delta Technologies. Soft tempered stainless steel (SS) wires and sheets were purchased from McMaster-Carr.

5.2.2 Cleaning, activation, and surface treatment of substrates

The SS wires, SS sheets, ITO-coated (with 0.15−0.20 μm thick ITO coatings on 0.7 mm thick glass substrates) and gold coated (with 0.075−0.15 μm thick gold coatings on 0.7 mm thick glass substrates) glass slides were ultrasonically cleaned (Kendal HB-23, 220 W) in acetone, 2-propanol, and deionized water, respectively for 10 min. After drying in a stream of N_2, the SS wires and sheets, and the ITO glass slides were treated in UV Ozone (Novascan PSD UV Ozone cleaner) for 60 min for further cleaning and activation. Some of the substrates were dipped into a 10 mM ethanol solution of EDOT-acid at room temperature for 24 h. The substrates were then rinsed with acetonitrile to remove any residual EDOT-acid molecules and finally dried in the air for the electrochemical deposition (Wei et al. 2015).

5.2.3 Fabrication of PEDOT coatings for interfacial strength tests

Electrochemical polymerization was performed with a Gamry Reference 600 Potentiostat/Galvanostat/ZRA and Gamry instruments framework software in a three-electrode cell. PEDOT was polymerized on either unmodified or EDOT-acid modified SS wires (0.005 cm diameter, 20 mm length), under galvanostatic conditions (50 μA) from an acetonitrile solution containing 0.02 M EDOT, and 0.1 M TBAP for 700 s, 1000 s and 1300 s respectively.

5.2.4 Fabrication of PEDOT coatings for wear tests

The electrochemical polymerization was performed with the same instrument and software mentioned above. PEDOT was polymerized respectively on unmodified ITO glass slides, SS sheets, gold coated glass slides and modified ITO glass slide under galvanostatic conditions (0.1 mA) from an acetonitrile solution containing 0.02 M EDOT, 0.1 M TBAP for 1000 seconds. The SS sheets were 7 mm × 30 mm. In each case, at least 3 samples were evaluated.

5.2.5 Thin film cracking test

The stress environment of brittle film on a ductile substrate during a tensile strip test is analogous to that of inorganic coatings in tribological applications. According to the Agrawal and Raj (A–R) model (Agrawal & Raj 1989)(Agrawal & Raj 1990), the interfacial shear strength, τ, between the more brittle PEDOT coating and the ductile substrate is related to the tensile strength of the PEDOT film, σ. After rewriting with the Tresca failure criterion, the relationship between cohesive strength τ, and adhesive strength τ_a follows this equation:

$$\frac{\tau_a}{\tau_c} = \frac{2 \cdot \pi \cdot t}{\lambda}$$

where t is thickness of the coating, and λ is the characteristic crack spacing at the stage where the number of transverse cracks becomes saturated with increasing tensile strain.

The untreated and treated PEDOT coated SS wires were pulled in tension till a stable transverse cracking pattern formed. The average crack spacing, λ, and average thickness of PEDOT coatings, t, were measured with a Zeiss Auriga 60 Focused Ion Beam-Scanning Electron Microscope (FIB-SEM) operating at 3 kV.

5.2.6 Wear test and impedance characterization

To mimic the friction behavior between the coated electrodes and the targeted soft tissue, a custom *in-situ* linear reciprocating tribometer (illustrated in Fig 5.2) was used. Pork loin was chosen to mimic the fraction and tissues, and was attached to the beam head with super glue. The normal forces were measured with a 6-channel ATI Nano-17 load cell. The normal load was 20 mN, the measured contact radius was between 2-2.5 mm, and the mean contact pressure was 1.02-1.59 kPa, which is at the upper limit of lower limbs tissue fluid pressure (range -1 to 10 mmHg)(Olszewski et al. 2010). The sliding speed was limited to 5 mm/s, and the reciprocating length was 1 mm.

In-situ optical microscopy measurements were made after N cycles of sliding, with N = 0, 1, 2, 5, 10, 20, 50, 100, and 200. ImageJ was used to estimate the residual surface area remaining of the PEDOT coatings after various amounts of testing. A threshold halfway was manually chosen to detect the boundary of remaining coating. The fraction of remaining surface area ratio was determined by A_r/A_0,where Ar is the remaining surface area, and A_0 is the original surface area.

5.2.7 Electrochemical characterization

The electrochemical characterization was performed with a Gamry Reference 600 Potentiostat/Galvanostat/ZRA and Gamry instruments framework software as mentioned above. Cyclic voltammetry (CV) tests were performed in 1x monomer-free phosphate buffered saline (PBS) solution with an Ag/AgCl glass body electrode (Fisher Scientific) as the reference. The scan rate was 100 mV/s.

Electrochemical impedance spectroscopy (EIS) was performed in an electrochemical cell with a platinum foil as the counter electrode. Monomer free PBS was used as the electrolyte. For EIS measurements, 0.01 V bias versus Ag/AgCl was applied. The frequency range between 0.1~100k Hz was scanned. The PEDOT films were scanned between −0.9 V and +0.5 V in a phosphate buffered saline (PBS) buffer solution free of monomer. The sample acted as the working electrode, a platinum plate was the counter electrode, a saturated Ag/AgCl electrode was the reference electrode.

5.3 Results and discussion

5.3.1 Thin film cracking test

A series of tests were conducted with PEDOT coated SS wires. The fracture strain of these soft tempered SS wires can reach 90%, which makes them excellent substrates for the measurement of interfacial shear strength of PEDOT, since the characteristic fracture strains for PEDOT are only around 2% (Qu et al. 2015). The crack spacings of PEDOT films on treated SS surfaces were uniformly smaller than those of similar thicknesses on untreated surfaces. In Fig 4, the thicknesses of PEDOT on two substrates were about 2 μm, and the average crack spacing of PEDOT on untreated SS was around 60 μm, while that of PEDOT on treated SS was around 20

μm, about 1/3 of the untreated ones. That means the PEDOT adhesion on treated SS wires was significantly improved.

The corresponding crack spacing of PEDOT with different thicknesses were measured as shown in Fig. 5. There was a linear relationship between the thickness of the PEDOT film and the average crack spacing. The crack spacings on the treated SS substrates were systematically lower than those on the untreated substrates. The slope of the untreated SS curve was 30.6; while the slope of treated SS was 10.8. So, for the PEDOT on untreated SS, $\tau_{a/}\ \tau_c = 0.21$; and for the PEDOT on treated PEDOT coatings, $\tau_{a/}\ \tau_c = 0.58$. If the tensile strength of both treated and untreated PEDOT films are assumed to be the same, $\tau_c = 56$ MPa (Qu et al. 2015), then the interfacial shear strength of the PEDOT coating on the untreated SS substrate, τ_{a1}, was around 11.8 MPa, and that of the PEDOT coating on the treated SS substrate, τ_{a2}, was around 32.5 MPa. These results indicate that treating the surface of the SS with EDOT-acid caused an increase of the interfacial shear strength by approximately a factor of 3 times.

5.3.2 Wear test and impedance characterization

The failures of interfacing materials in the biomedical electronics typically follow two modes: cracking or delamination (Cui & Zhou 2007)(Campbell et al. 2011)(Gilgunn et al. 2013). When the coatings are not mechanically robust or adhesive enough, several loads of external stress can cause the failure. In our case, the most common external stress is the shear stress generated from the friction between the electrodes and tissues. To simulate the conditions after implantation, a tribological wear test was introduced as the durability test for biomedical electrodes for the first time.

The results of the wear test are shown in Figure 6, where the amount of coating remaining is plotted as a function of the number of cycles (N). These results showed that the stability of the PEDOT films on the untreated ITO substrate was the worst. Around 35% of the film was lost only after 10 cycles of wear testing. The stability of the PEDOT coatings on the EDOT-acid treated ITO and SS substrates was significantly enhanced compared to the untreated ones (Fig. 6). However, we also found that the stability of PEDOT on gold coated glass was the best, even much better than the EDOT-acid modified ITO and SS. Since there was no PEDOT loss after 200 cycles of wear test, we even extended the test to N = 500 cycles for these samples. Again, no PEDOT loss was apparent even after 500 cycles of wear testing.

Based on Fig. 5 & 6, and assuming the tensile strength/cohesion of PEDOT coatings is the same on different substrates, the cycle numbers needed to cause 10% PEDOT area loss and the adhesion/cohesion ratio were determined and are listed in Table 1.

In order to determine how materials failure affected electrical properties of the interfacing material, impedance tests were conducted before and after the wear testing. The impedance of PEDOT on treated ITO after the wear test at 10 Hz dramatically increased from ~50 Ω to ~320 Ω, which was the largest change compared to the other types of electrodes. This was associated with the larger amounts of PEDOT film lost after the wear test. The performance of PEDOT coated Au was the most stable, with no change and the lowest impedance at the biologically significant frequency range (1-1000 Hz).

The wear test results indicated that only PEDOT coatings deposited on gold from acetonitrile, passed this test, with both the cohesive and adhesive strength high

enough to survive under the lasting stress environment. The results from impedance test confirmed that with large cohesive and adhesive strength, the durability of PEDOT on gold was much better.

5.3.3 Electrochemical stability

The results of prior tests indicated that PEDOT coated gold electrodes were superior under extended shear stress. SEM images confirmed that the electrochemical stability of gold coated PEDOT was also superior. Before the CV test, the morphology of all the five groups of PEDOT coatings looked quite similar (Fig 8a). After 3000 cycles of CV scanning, many wrinkles emerged on the untreated SS and ITO substrates (Fig 8b&e). When compared to SS, the size of the wrinkles on ITO were larger. The wrinkles were evidently caused by the repeated swelling and shrinking of PEDOT coatings during the redox switching, when the adhesion was not strong enough. With the EDOT-acid treatment, the improved adhesion reduced the amount of wrinkles on SS and ITO substrates (Fig 8c&f). PEDOT on Au showed the best electrochemical stability again. No wrinkles were observed after the CV scan. The superior electrochemical stability was apparently mainly due to the stronger adhesion of PEDOT on Au.

Both the external stress and charge injection simulation tests showed that PEDOT coatings on Au were superior, even when compared to chemically modified SS or ITO substrates. It evidently means that stronger bonds formed between the PEDOT and Au. To verify this hypothesis, X-ray photoelectron spectroscopy (XPS) was conducted.

5.3.4 Confirmation of the interactions at the interface

For the S 2p core level, the S 2p1/2 peak at 163.5 eV, and the S 2p3/2 peak at 164.8 eV are ascribed to thiophene species (Fig. 10). Another two doublets at lower binding energy provide evidence of sulfur in EDOT derivatives. These peaks can be ascribed to thiols or sulfide. In addition, the two doublets shown respectively in the Au 4f 5/2 peak at 83.6 eV, and the Au 4f 7/2 peak at 87.3 eV, also confirmed that some certain chemical interactions happened between the sulfur in thiophene and the Au. This evidence for chemical interations between the gold surface and sulfur groups in the thiophene units may explain the strong tenacity of PEDOT film on Au surfaces.

5.4 Conclusions

The thin film cracking and wear test established in this chapter, correlated the adhesion, mechanical properties and electrochemical stability with the durability of the interfacing materials in the biomedical electronics. It made a critical difference in systematically comparing different materials, and provided valuable information for materials development and selection. The superior durability of PEDOT coatings which were electrochemically deposited on Au was observed, in contrast with the other substrates. The interaction between thiophenes and Au may provide clues for the further development and optimization of biomedical interfacing materials.

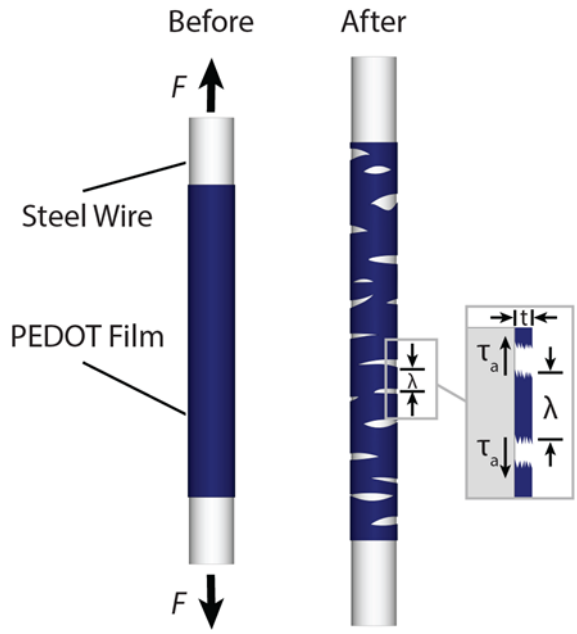

Figure 5.1 The tensile strip test used to characterize the interfacial shear strength of PEDOT coatings on the steel wire.

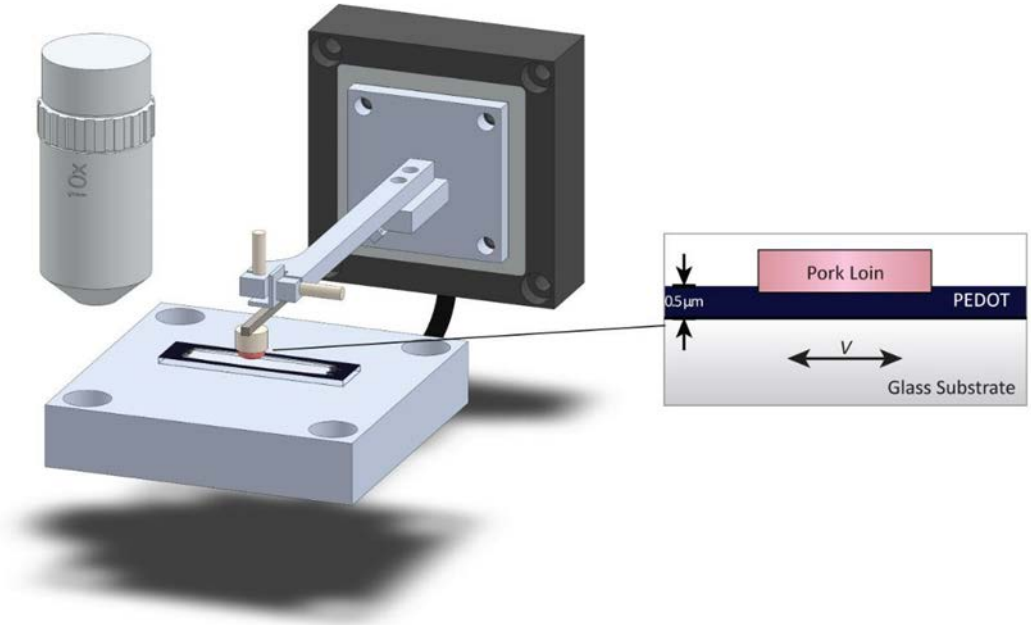

Figure 5.2 The setup of tribometer for the wear test.

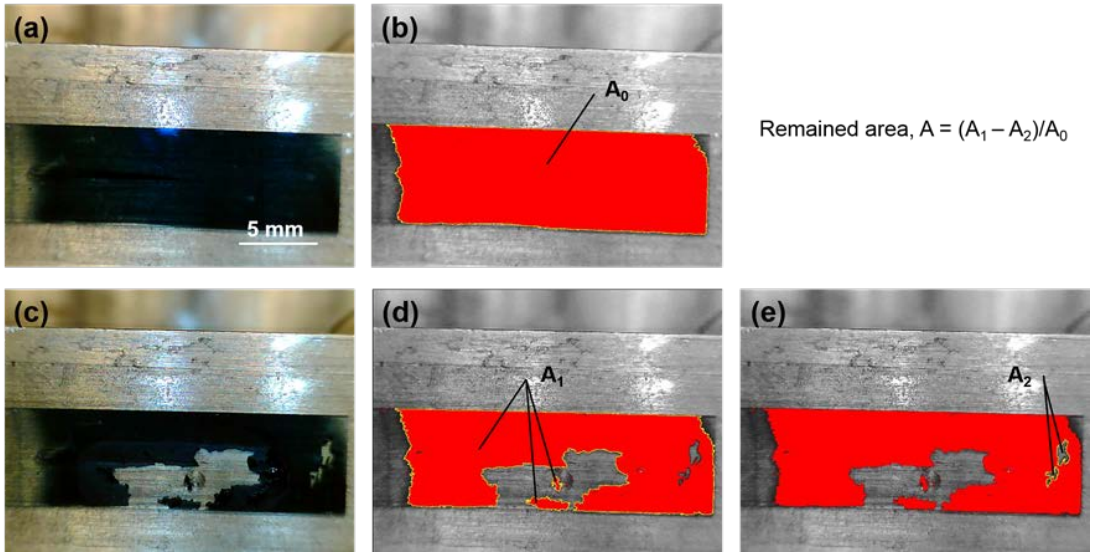

Figure 5.3 (a, b) Optical microscope image of PEDOT film on treated ITO glass slide before wear tests, and (c, d, e) the PEDOT film after 50 cycles of wear testing. Figure 3b, 3d, 3e was the red channel of the original images. A_0, A_1, A_2 were selected around the edge of film automatically with the wand tool in ImageJ.

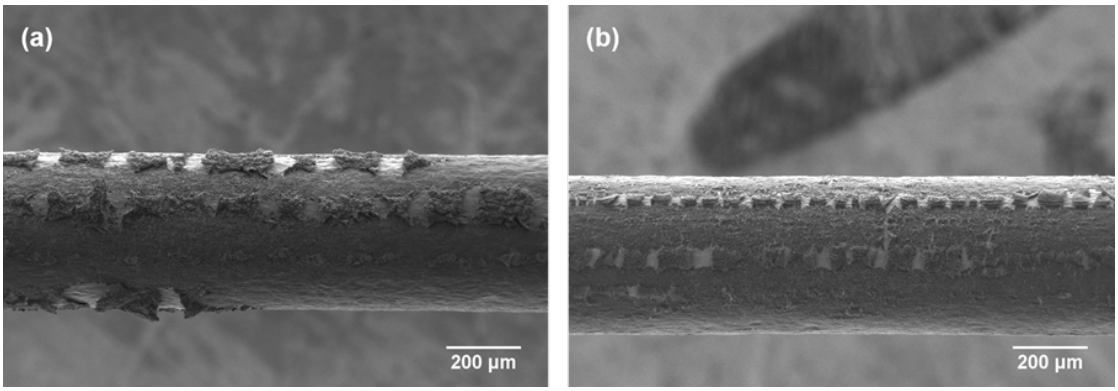

Figure 5.4 The SEM images of PEDOT cracking on untreated SS wire (a), and on treated SS wire (b).

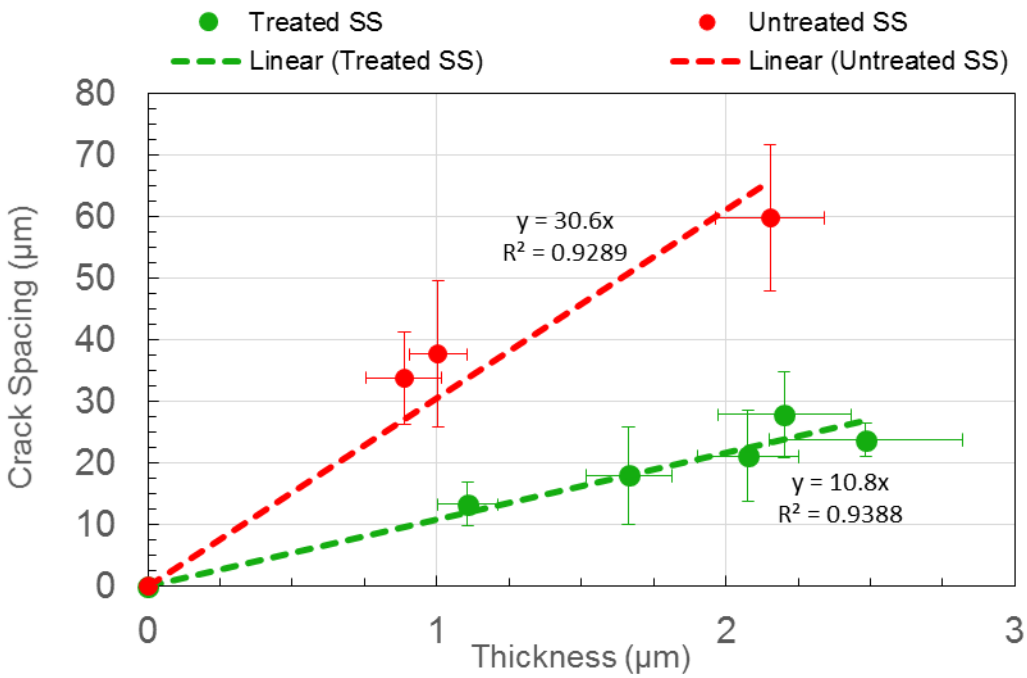

Figure 5.5 Untreated and treated PEDOT film crack spacing versus the thickness of PEDOT films. Each data point represents 10-30 repeat measurements

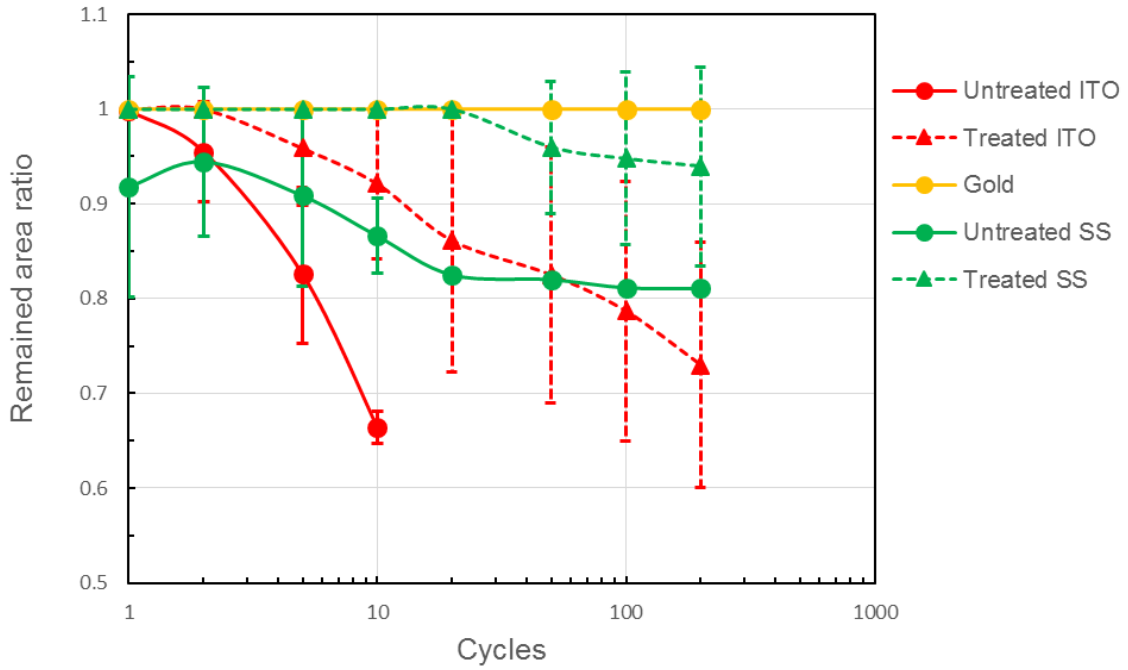

Figure 5.6 The remained area ratio of PEDOT films versus the cycles of wear testing.

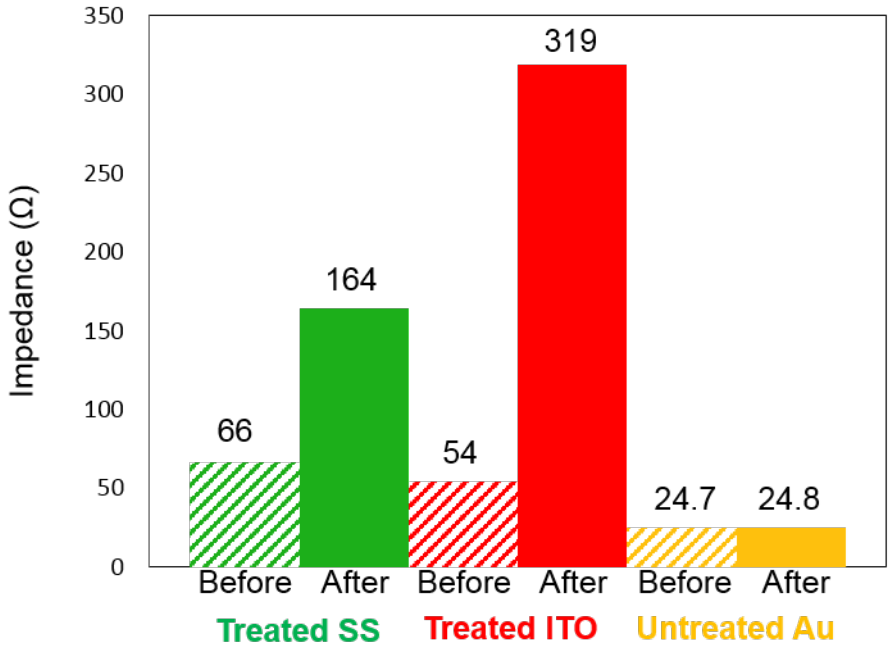

Figure 5.7 The impedance of PEDOT coated electrodes at 10 Hz, before and after 200 cycles of wear test.

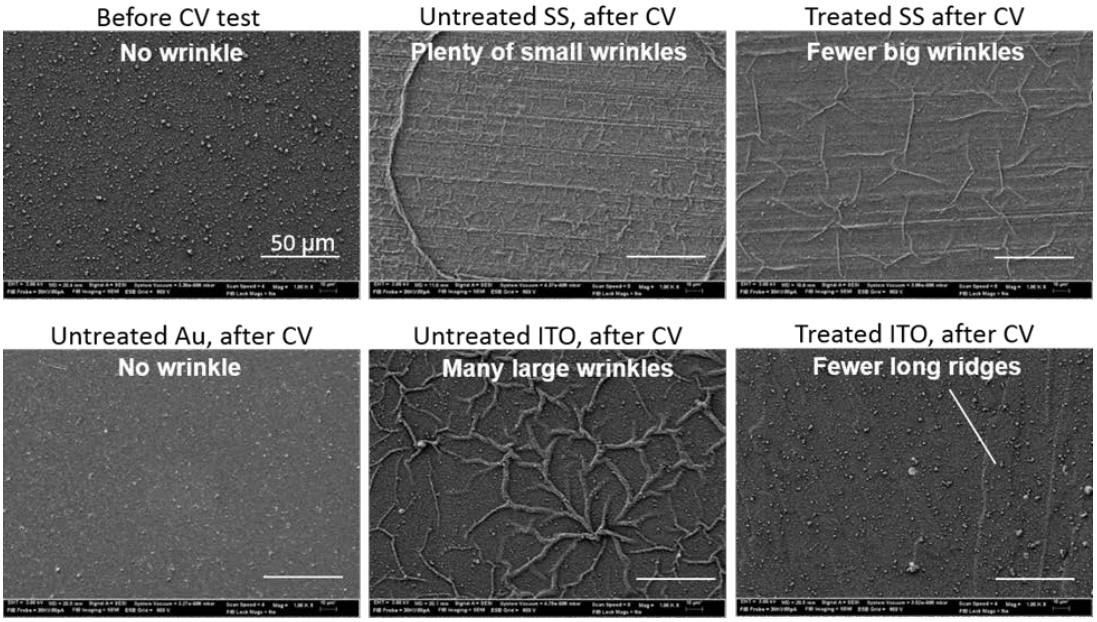

Figure 5.8 The SEM of PEDOT films after 3000 cycles of CV scanning.

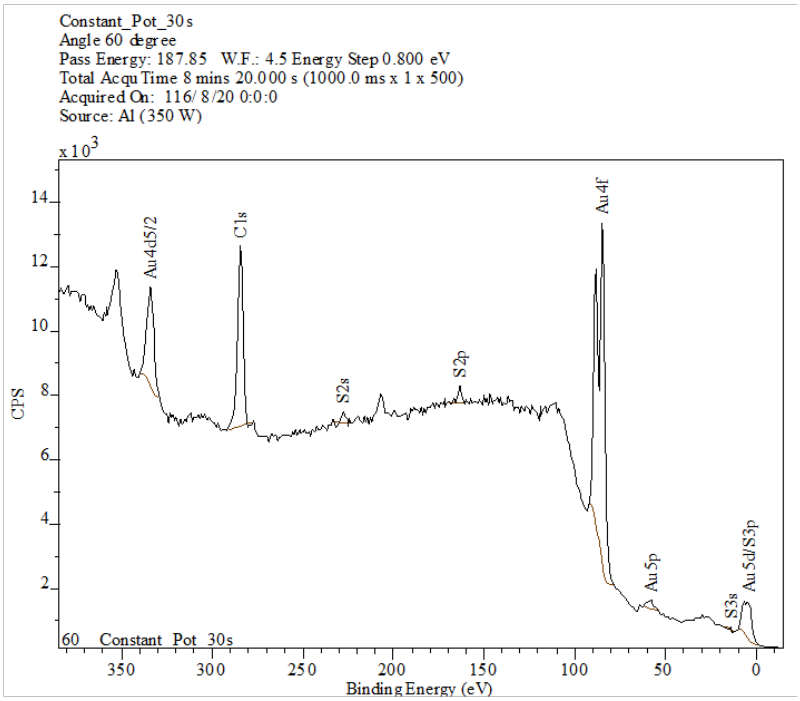

CasaXPS (K. Jones)

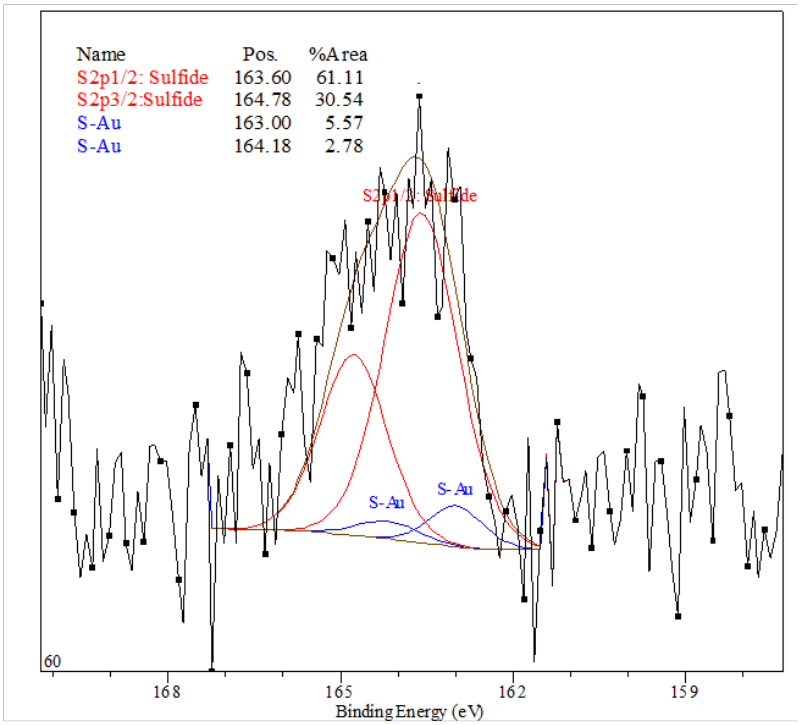

CasaXPS (K. Jones)

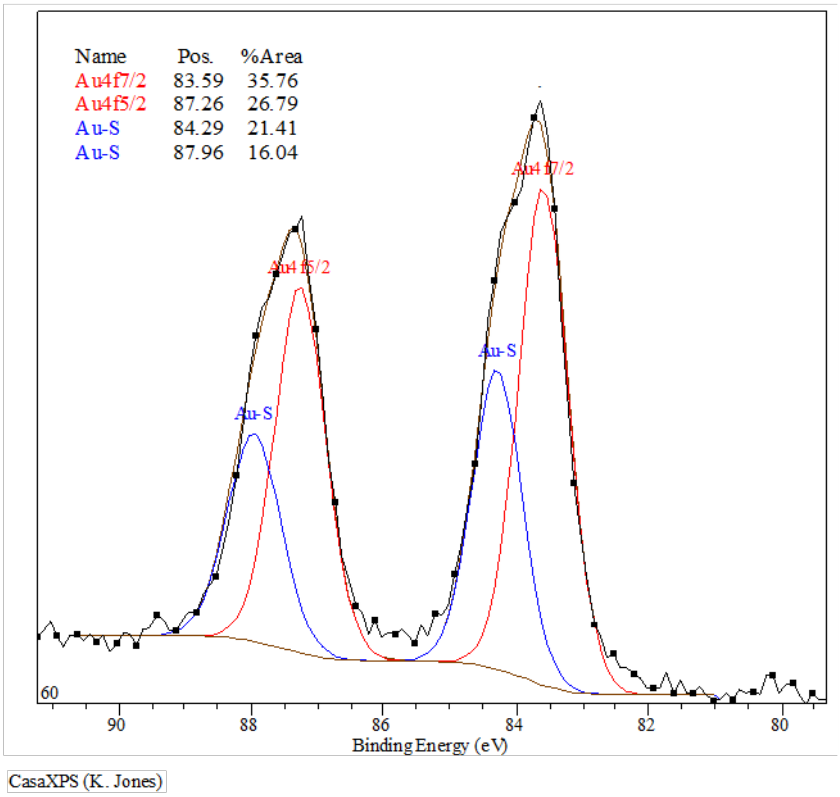

Figure 5.9 The X-ray photoemission spectrum of PEDOT coated Au.

Table 5.1. The relationship of reliability and adhesion/cohesion ratio

	Failure cycles (10% area loss)	Adhesion/cohesion ratio
Untreated SS	7-9	0.21
Treated SS	80-200	0.58
Untreated ITO	2-4	<0.21
Treated ITO	10-20	$0.21<\tau_a/\tau_c<0.58$
Untreated Au	> 500	>0.58

REFERENCES

Agrawal, D. & Raj, R., 1989. Measurement of the ultimate shear strength of a metal-ceramic interface. *Acta Metallurgica*, 37(4), pp.1265–1270.

Agrawal, D. & Raj, R., 1990. Ultimate shear strengths of copper-silica and nickel-silica interfaces. *Materials Science and Engineering: A*, 126, pp.125–131.

Barrese, J.C. et al., 2013. Failure mode analysis of silicon-based intracortical microelectrode arrays in non-human primates. *Journal of Neural Engineering*, 10(6), p.66014.

Barrese, J.C., Aceros, J. & Donoghue, J.P., 2016. Scanning electron microscopy of chronically implanted intracortical microelectrode arrays in non-human primates. *Journal of Neural Engineering*, 13(2), p.26003.

Campbell, A. et al., 2011. A preliminary study of vapour-phase polymerized poly(3,4-ethylenedioxythiophene) as a transparent neural electrode. In *Proceedings of IEEE Sensors*. IEEE, pp. 1575–1578.

Cogan, S.F., 2008. Neural stimulation and recording electrodes. *Annual Review of Biomedical Engineering*, 10, pp.275–309.

Cui, X. et al., 2003. In vivo studies of polypyrrole/peptide coated neural probes. *Biomaterials*, 24(5), pp.777–787.

Cui, X.T. & Zhou, D.D., 2007. Poly (3,4-ethylenedioxythiophene) for chronic neural stimulation. *IEEE Transactions on Neural Systems and Rehabilitation Engineering*, 15(1), pp.502–508.

Donoghue, J.P., 2008. Bridging the brain to the world: a perspective on neural interface systems. *Neuron*, 60(3), pp.511–21.

Gilgunn, P.J. et al., 2013. Structural analysis of explanted microelectrode arrays. In *International IEEE/EMBS Conference on Neural Engineering, NER*. pp. 719–722.

Kim, D.-H. et al., 2007. Effect of Immobilized Nerve Growth Factor on Conductive Polymers: Electrical Properties and Cellular Response. *Advanced Functional Materials*, 17(1), pp.79–86.

Kozai, T.D.Y. et al., 2015. Mechanical failure modes of chronically implanted planar silicon-based neural probes for laminar recording. *Biomaterials*, 37, pp.25–39.

Kung, T. et al., 2014. Regenerative peripheral nerve interface viability and signal transduction with an implanted electrode. *Plastic and reconstructive surgery*, 133(6), pp.1380–94.

Lang, U., Naujoks, N. & Dual, J., 2009. Mechanical characterization of PEDOT:PSS thin films. *Synthetic Metals*, 159(5–6), pp.473–479.

Lee, H. et al., 2005. Biomechanical analysis of silicon microelectrode-induced strain in the brain. *Journal of neural engineering*, 2(4), pp.81–9.

Leleux, P. et al., 2014. Ionic liquid gel-assisted electrodes for long-term cutaneous recordings. *Advanced healthcare materials*, 3(9), pp.1377–80.

Lipomi, D.J. et al., 2011. Skin-like pressure and strain sensors based on transparent elastic films of carbon nanotubes. *Nature nanotechnology*, 6(12), pp.788–92.

Luo, X. et al., 2011. Highly stable carbon nanotube doped poly(3,4-ethylenedioxythiophene) for chronic neural stimulation. *Biomaterials*, 32(24), pp.5551–5557.

Nyberg, T., Shimada, A. & Torimitsu, K., 2007. Ion conducting polymer microelectrodes for interfacing with neural networks. *Journal of Neuroscience Methods*, 160(1), pp.16–25.

Olszewski, W.L. et al., 2010. Tissue fluid pressure and flow in the subcutaneous tissue in lymphedema - hints for manual and pneumatic compression therapy. *Phlebolymphology*, 17(3), pp.144–150.

Prasad, A. et al., 2014. Abiotic-biotic characterization of Pt/Ir microelectrode arrays in chronic implants. *Frontiers in neuroengineering*, 7(February), p.2.

Prasad, A. et al., 2012. Comprehensive characterization and failure modes of tungsten microwire arrays in chronic neural implants. *Journal of Neural Engineering*, 9(5), p.56015.

Qu, J. et al., 2015. Stiffness, strength and adhesion characterization of electrochemically deposited conjugated polymer films. *Acta Biomaterialia*.

Sridharan, A., Rajan, S.D. & Muthuswamy, J., 2013. Long-term changes in the material properties of brain tissue at the implant-tissue interface. *Journal of neural engineering*, 10(6), p.66001.

Subbaroyan, J., Martin, D.C. & Kipke, D.R., 2005. A finite-element model of the mechanical effects of implantable microelectrodes in the cerebral cortex. *Journal of neural engineering*, 2(4), pp.103–113.

del Valle, L.J. et al., 2007. Cellular adhesion and proliferation on poly(3,4-ethylenedioxythiophene): Benefits in the electroactivity of the conducting polymer. *European Polymer Journal*, 43(6), pp.2342–2349.

Venkatraman, S. et al., 2011. In vitro and in vivo evaluation of PEDOT microelectrodes for neural stimulation and recording. *IEEE Transactions on Neural Systems and Rehabilitation Engineering*, 19(3), pp.307–316.

Viventi, J. et al., 2010. A conformal, bio-interfaced class of silicon electronics for mapping cardiac electrophysiology. *Science translational medicine*, 2(24), p.24ra22.

Viventi, J. et al., 2011. Flexible, foldable, actively multiplexed, high-density electrode array for mapping brain activity in vivo. *Nature neuroscience*, 14(12), pp.1599–605.

Wei, B. et al., 2015. Significant Enhancement of PEDOT Thin Film Adhesion to Inorganic Solid Substrates with EDOT-Acid. *ACS applied materials & interfaces*, 7(28), pp.15388–94.

Wilks, S.J. et al., 2009. Poly(3,4-ethylenedioxythiophene) as a Micro-Neural Interface Material for Electrostimulation. *Frontiers in neuroengineering*, 2(June), p.7.

Xu, L. et al., 2015. Materials and fractal designs for 3D multifunctional integumentary membranes with capabilities in cardiac electrotherapy. *Advanced Materials*, 27(10), pp.1731–1737.

Ying, M. et al., 2012. Silicon nanomembranes for fingertip electronics. *Nanotechnology*, 23(34), p.344004.

Chapter 6

CONCLUSIONS AND SUGGESTIONS FOR FUTURE WORK

6.1 Conclusions

It is a challenge for biomedical interfacing materials to be highly efficient in signal transfer, biocompatible, and durable at the same time. With the emergence of conjugated polymers, the biocompatibility and signal transfer performance have been successfully improved. However, for all the current interfacing materials, the durability still needs considerable improvement. To improve the durability of PEDOT, an iterative cycle of chemistry and formulation development, materials characterization, and in vitro and in vivo tests should be conducted. For many years, considerable attention was put into developing strategies for new chemistry for conjugated polymers and dopants. However, little information has been presented surrounding formulation development or the characterization of adhesion, mechanical properties and durability. This thesis has covered several of these aspects that have not been so carefully examined in previous studies of conjugated polymers. The approaches to improve and characterize the durability of conjugated polymers, especially PEDOT, as biomedical interfacing materials, have been discussed.

Through the formulation optimization, the PEDOT coatings were prepared from alternative solvents that were more conductive and durable compared to the PEDOT coating deposited from aqueous solution. The 7-month *in vivo* tests demonstrated the improved performance brought by the PEDOT coating during the neural signal recording procedure. During the recording process, the amplitude of the

signal of PEDOT coated electrode was around twice of that of bare SS electrodes. However, some impairment of PEDOT coatings was still observed after the in vivo testing, with around 30% of the polymer coating area lost.

To further improve the durability of conjugated polymer coatings, the existing methods to improve the electrochemical stability, strength, and adhesion were reviewed. A silane functionalized adhesion promoter (phenyltriethoxysilane) and a crosslinker (EPh) were applied to improve the adhesion and strength of PEDOT respectively. Sonication tests showed that with the adhesion promoter modification, PEDOT coatings survived longer. An AFM nano-indentation test showed that the effective Young's modulus of PEDOT was increased from 1.6 GPa to 2.2 GPa with 0.5% addition of crosslinker. However, further improvements are still desired, particularly for long-term performance. Without the quantitative information of ultimate mechanical properties, adhesion and durability, it is difficult to systematically compare the improvements made by variations in synthesis and processing, and select superior materials. To tackle this problem, this thesis explored several characterization methods that provided quantitative information of material properties and indicated the long-term performance of biomedical electrodes.

Based on the Agrawal-Raj model (Agrawal & Raj 1989) (Agrawal & Raj 1990), a thin film cracking method was established to measure the stiffness, strength and interfacial shear strength of PEDOT and crosslinked PEDOT coatings. The Young's modulus of electrochemically deposited PEDOT:$LiClO_4$ was found to be similar to those measured with the nano-indentation and QNM AFM mode (Baek et al. 2014) (Hassarati et al. 2014), and the values of solution cast PEDOT:PSS film (Lang et al. 2009). The thin film cracking method also confirmed the effectiveness of the

crosslinking agent EPh. The stiffness of PEDOT was increased from 2.6 GPa to 12.6 GPa, and the strength was improved from 0.7 MPa to 2.4 MPa with 5% addition of EPh. With a similar conjugated structure as EDOT, EPh didn't affect the fracture strain much, as the resulting polymers were still relatively brittle. With their improved strength however, crosslinking PEDOT with EPh is still a promising route for enhancing the durability of PEDOT coatings on biomedical electrodes. The thin film cracking method established in Chapter 4 provided a convenient means for evaluating the stiffness, strength, and adhesion of CP films on solid substrates, which are all essential for estimating their durability in applications, but cannot be obtained by previous nanoindentation and AFM methods.

Further, the thin film cracking successfully provided the interfacial shear strength of PEDOT coatings on stainless steel substrates. The effectiveness of an adhesion promoter—EDOT-acid was confirmed. With the EDOT-acid modification to the stainless steel surface, the adhesion of PEDOT coating, as measured by the effective interfacial shear strength, was improved by about 3 times. To simulate the external shear stress of implanted biomedical electrodes, a tribology test was introduced as a wear test. Then, the adhesion and mechanical properties were correlated with the durability of the interfacing materials for biomedical electronics for the first time. It made a critical difference in systematically comparing different materials, and provided valuable information for materials development and selection. With those tests, the superior durability of PEDOT on Au was observed, in contrast with the other substrates. The interaction between thiophenes and Au may provide clues for the further development and optimization of biomedical interfacing materials.

6.2 Future work

Chemistry developments for achieving durable and processable conducting polymers will make them stand out from traditional semiconductors and metallic conductors, and expand their applications in the organic solar cells and biomedical electronics. Through the Chapter 2, it is seen that introducing flexible chains to conjugated polymers is promising to improve the durability in the repeated redox switching process. Recently, the Reynolds group successfully synthesized soluble ProDOT-EDOT copolymers by introducing alkoxy groups, and measured the molecular weight of PEDOT/PProDOT derivatives for the first time (Österholm et al. 2016)(Ponder et al. 2016). More work needs to be done to develop the chemistry of designing conjugated polymers with additional desired properties, such as improved ductility or elasticity, and the capability of drug delivery.

The characterization of molecular structure of conjugated polymers is another useful direction. So far, little information about the polymer physics has been dig out about conjugated polymers. With the characterization methods established in previous chapters, the adhesion and mechanical properties of newly emerging conjugated polymers, such as the soluble ones, will be provided. Possible molecular structures, such as intramolecular folding and intermolecular stacking, can be simulated with software, such as Materials Studio. By comparing the experimental data with the simulated conductivity, adhesion and mechanical properties, a more accurate structure of conjugated polymers could be defined. This will provide valuable insight for chemistry development to achieve the desired properties. It is also feasible to combine the molecular simulation with the *in-situ* TEM, and high resolution TEM techniques to analyze the growth mechanism of conjugated polymers.

REFERENCES

Agrawal, D. & Raj, R., 1989. Measurement of the ultimate shear strength of a metal-ceramic interface. *Acta Metallurgica*, 37(4), pp.1265–1270.

Agrawal, D. & Raj, R., 1990. Ultimate shear strengths of copper-silica and nickel-silica interfaces. *Materials Science and Engineering: A*, 126, pp.125–131.

Baek, S., Green, R.A. & Poole-Warren, L.A., 2014. Effects of dopants on the biomechanical properties of conducting polymer films on platinum electrodes. *Journal of Biomedical Materials Research Part A*, 102(8), pp.2743–2754.

Hassarati, R.T. et al., 2014. Stiffness quantification of conductive polymers for bioelectrodes. *Journal of Polymer Science, Part B: Polymer Physics*, 52(9), pp.666–675.

Lang, U., Naujoks, N. & Dual, J., 2009. Mechanical characterization of PEDOT:PSS thin films. *Synthetic Metals*, 159(5–6), pp.473–479.

Österholm, A.M. et al., 2016. Solution Processed PEDOT Analogues in Electrochemical Supercapacitors. *ACS Applied Materials & Interfaces*, 8(21), pp.13492–13498. Available at: http://pubs.acs.org/doi/abs/10.1021/acsami.6b02434 [Accessed December 16, 2016].

Ponder, J.F., Österholm, A.M. & Reynolds, J.R., 2016. Designing a Soluble PEDOT Analogue without Surfactants or Dispersants. *Macromolecules*, 49(6), pp.2106–2111.

Appendix

COPYRIGHT PERMISSIONS

Permission for utilization of one publication in the Chapter 3.

Copyright Clearance Center RightsLink®

Home | Account Info | Help

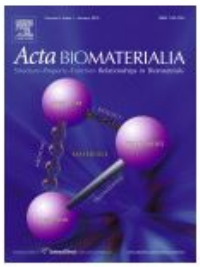

Title: Stiffness, strength and adhesion characterization of electrochemically deposited conjugated polymer films

Author: Jing Qu,Liangqi Ouyang,Chin-chen Kuo,David C. Martin

Publication: Acta Biomaterialia

Publisher: Elsevier

Date: February 2016

Logged in as:
Jing Qu
LOGOUT

Order Completed

Thank you for your order.

This Agreement between Jing Qu ("You") and Elsevier ("Elsevier") consists of your license details and the terms and conditions provided by Elsevier and Copyright Clearance Center.

Your confirmation email will contain your order number for future reference.

License Number	4040870873166
License date	Feb 02, 2017
Licensed Content Publisher	Elsevier
Licensed Content Publication	Acta Biomaterialia
Licensed Content Title	Stiffness, strength and adhesion characterization of electrochemically deposited conjugated polymer films
Licensed Content Author	Jing Qu,Liangqi Ouyang,Chin-chen Kuo,David C. Martin
Licensed Content Date	February 2016
Licensed Content Volume	31
Licensed Content Issue	n/a
Licensed Content Pages	8
Type of Use	reuse in a thesis/dissertation
Portion	full article
Format	both print and electronic
Are you the author of this Elsevier article?	Yes
Will you be translating?	No
Order reference number	
Title of your thesis/dissertation	Electrochemically Deposited Conducting Polymers for Reliable Biomedical Interfacing Materials: Formulation, Mechanical Characterization, and Failure Analysis
Expected completion date	Feb 2017
Estimated size (number of pages)	140
Elsevier VAT number	GB 494 6272 12
Requestor Location	Jing Qu 70 Munro Road NEWARK, DE 19711 United States Attn: Jing Qu
Total	0.00 USD